Non-Viral Gene Delivery Systems: Studies on HER2-Targeted PEG-PEI Co-polymers and Modified Chitosans

Dissertation

zur Erlangung des Doktorgrades der Naturwissenschaften (Dr. rer. nat.)

dem

Fachbereich Pharmazie der Philipps-Universität Marburg

vorgelegt von

Oliver Germershaus

aus Erfurt

Marburg/Lahn 2008

Vom Fachbereich Pharmazie der Philipps-Universität Marburg als Dissertation am 20.05.2008 angenommen.

Erstgutachter: Prof. Dr. Thomas Kissel

Zweitgutachter: Prof. Dr. Udo Bakowsky

Drittgutachter: Prof. Dr. Rolf Schubert

Die vorliegende Arbeit entstand auf Anregung und unter Leitung von

Herrn Prof. Dr. Thomas Kissel

am Institut für Pharmazeutische Technologie und Biopharmazie
der Phillips-Universität Marburg.

Gewidmet meinen Eltern
in Liebe und großer Dankbarkeit

Table of Contents

1 Introduction ____ *1*

1.1 Gene Therapy – Concept ____ 2

1.2 Targeted Non-Viral Gene Therapy using Polyethylenimine ____ 4

1.3 Non-Viral Gene Delivery using Chitosan ____ 13

1.4 References ____ 17

2 Trastuzumab-Polyethylenimine-Polyethyleneglycol Conjugates for Targeting HER2 Expressing Tumors ____ *26*

2.1 Abstract ____ 27

2.2 Introduction ____ 28

2.3 Materials and Methods ____ 30

2.4 Results ____ 35

2.5 Discussion ____ 44

2.6 Conclusion ____ 49

2.7 Acknowledgments ____ 49

2.8 References ____ 50

3 HER2 Targeted Polyplexes: The Effect of Polyplex Composition and Conjugation Chemistry on in vitro and in vivo Characteristics ____ *55*

3.1 Abstract ____ 56

3.2 Introduction ____ 56

3.3 Materials and Methods ____ 58

3.4 Results ____ 63

3.5 Discussion ____ 74

3.6 Acknowledgments ____ 80

3.7 References ____ 81

4 Establishment and Characterization of a HER2 Tumor Model in SCID Mice and In Vivo Gene Delivery using PEI- and PEI-PEG-Trastuzumab Polyplexes ____ *86*

4.1 Abstract ____ 87

4.2 Introduction 88

4.3 Materials and Methods 89

4.4 Results and Discussion 91

4.5 Conclusion 98

4.6 Acknowledgments 98

4.7 References 99

5 Gene Delivery using Chitosan, Trimethyl Chitosan or Polyethylenglycol-graft-Trimethyl Chitosan Block Copolymers: Establishment of Structure-Activity Relationships in Vitro *102*

5.1 Abstract 103

5.2 Introduction 103

5.3 Materials and Methods 105

5.4 Results and Discussion 109

5.5 Conclusion 122

5.6 Acknowledgments 123

5.7 References 124

6 Kinetics and Mechanism of Uptake of Chitosan, Trimethyl Chitosan and PEG-Trimethyl Chitosan Polyplexes in L929 mouse fibroblasts and A549 human alveolar epithelial cells *129*

6.1 Abstract 130

6.2 Introduction 131

6.3 Materials and Methods 133

6.4 Results and Discussion 136

6.5 Acknowledgments 148

6.6 References 149

7 Summary and Perspectives *156*

7.1 Summary 157

7.2 Perspectives 160

7.3 Zusammenfassung 163

7.4 Ausblick 167

8 Appendices *170*

8.1 Abbreviations 171

8.2 List of Publications 172

8.3 Curriculum Vitae 175

8.4 Danksagung 176

1 Introduction

1.1 Gene Therapy – Concept

Growing understanding of genes involved in diseases and the knowledge of the sequence of the human genome gave rise to hopes about treatments for until then incurable diseases (*1, 2*). Practical use of this knowledge however, depends on efficient methods to manipulate or replace defective genes.

Basically, genes can be delivered using an in vivo or an ex vivo approach. The latter utilizes cells cultured in vitro, which are transfected, selected and expanded outside patients body and are later implanted. Usually, cells used for this procedure are obtained from the same patient to avoid rejection of the implant. The in vivo approach tries to directly administer the genes of interest into the (target-)cells of a patient. This approach, being technically far more challenging, is often the only viable option if ex vivo cultivation of cells is not possible or cells can not be re-implanted.

Direct delivery of nucleic acids in the absence of a carrier is only feasible in rare cases such as intramuscular injection of naked DNA or topical gene therapy using electroporation (for review see (*3*)). Therefore, carriers are widely used in gene therapy be it ex vivo or in vivo. These can be divided into two major classes: viral and non-viral vectors. Viral vectors include different viruses such as retrovirus, adenovirus and vaccinia virus. These systems impress by their high efficiency but on the other hand also suffer from serious drawbacks such as high immunogenicity after repeated administration, potential oncogenicity due to insertional mutagenesis and limited cargo capacity. Furthermore, viral vectors are less attractive from a technological point of view: large-scale production and subsequent modification (e.g. with a targeting moiety) is technically challenging.

Given these hurdles in developing safe and efficient viral vectors, non-viral vectors more and more emerge as a viable alternative. Especially with regard to new therapeutics like oligonucleotides and siRNA, which do not depend on translocation into the cell nucleus but are effective in the cytosol, these vectors are attractive alternatives. Non-viral vectors again fall into two main classes. Liposomal formulations, and cationic polymers.

Liposomal formulations usually consist of cationic lipids with a positively charged head group and a hydrophobic moiety (e.g. 1,2-dioleoyl-3-tetramethylammonium propane, DOTAP or N-[1-(2,3-dioleyloxy)propyl]-N,N,N trimethylammonium chloride, DOTMA). These characteristics cause the cationic lipids to assemble into liposomes when dispersed in aqueous solution (*4*). By mixing with nucleic acid the liposome structure collapses and nanoplexes are formed. Morphology, size and surface charge of these complexes is usually controlled by mixing ratio between cationic charges from lipids and negative charges from nucleic acids. Often helper lipids such as dioleoylphosphatidylethanolamine (DOPE) or cholesterol are used to stabilize the system, increase endosomal escape and influence DNA binding (*5, 6*). Despite the success of cationic lipids in in vitro gene transfer, reflected in the broad use of commercial liposomal formulations such as Lipofectamin® in cell culture experiments, concerns were raised on both in vitro and in vivo toxicity and stability (*7-9*).

The class of cationic polymers on the other hand comprises very diverse structures ranging from synthetic polymers like polyethylenimine or polyamidoamine dendrimers to natural polymers like chitosan (for review see (*10*)). However, a common feature of these polymers is their ability to interact with nucleic acids and to spontaneously form nanosized complexes (polyplexes). The main advantage of these polymers is the ability to be synthesized or produced in a tailor-made fashion including subsequent functionalization with e.g. targeting- or shielding moieties. On the downside, these polymers, just like liposomal systems, suffer from significantly lower efficiencies compared to viral systems both in vitro and in vivo. Furthermore, toxicity is a major concern and a rough correlation between cytotoxicity and efficiency was stated (*11*).

As of July 2007, 7.6% of gene therapy clinical trials were based on lipofection (http://www.wiley.co.uk/genetherapy/clinical/) while gene transfer using polycations is still in its infancy (Figure 1). This fact is somehow paradoxical since polycations have been used for transfections long before liposomal formulations (*12, 13*). However, polycations suffered from very low efficiency and the progress in the field was marginal until Boussif et al. introduced polyethylenimine (PEI) in 1995 (*14*). Since than efficiency of polycations significantly increased and nowadays roughly matches efficiency of lipofection (*15*). However, gene delivery using polycations to humans was only rarely reported. One of the few reports deals with topical gene delivery of diphtheria A

toxin under H19 promotor using JetPEI® into the bladder of two patients with bladder cancer (*16*). In this study nearly complete ablation of the tumor was observed in patients by video imaging.

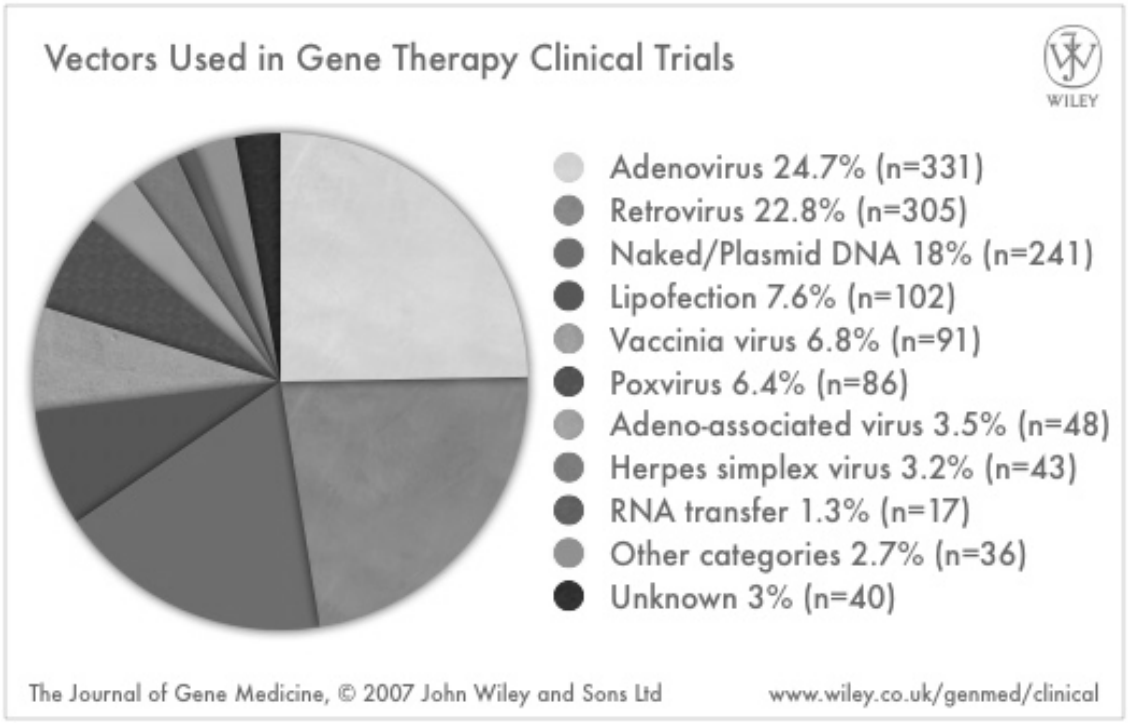

Figure 1: Vectors used in gene therapy clinical trials as of July 2007 (from http://www.wiley.co.uk/genetherapy/clinical)

1.2 Targeted Non-Viral Gene Therapy using Polyethylenimine

Branched PEI is a synthetic polymer obtained by acid catalyzed cationic polymerization of aziridine (Figure 2) (*17*). Due to its high charge density, PEI was found to be useful in a variety of industrial applications, e.g. as flocculation agent in the paper industry (*18*). The high charge density of PEI was found to also mediate efficient DNA binding and protection against nucleases (*14*). Furthermore, PEI mediates efficient endosomal release. During processing of endosomes, pH decreases to ~6 in early and ~5 in late endosomes. Finally, late endosomes fuse with lysosomes with a pH of 4.5 (*19*). During this process, the buffering capacity of PEI leads to increased influx of protons, chloride ions, and water, eventually causing rupture of the vesicle due to high osmotic pressure. This so-called ‘proton-sponge hypothesis’ was first proposed by Behr and colleagues

(*14, 20*) and was experimentally verified by several authors (*21-23*). These special characteristics rendered PEI one of the most efficient cationic polymers for gene delivery both in vitro and in vivo known at that time (*14, 24, 25*).

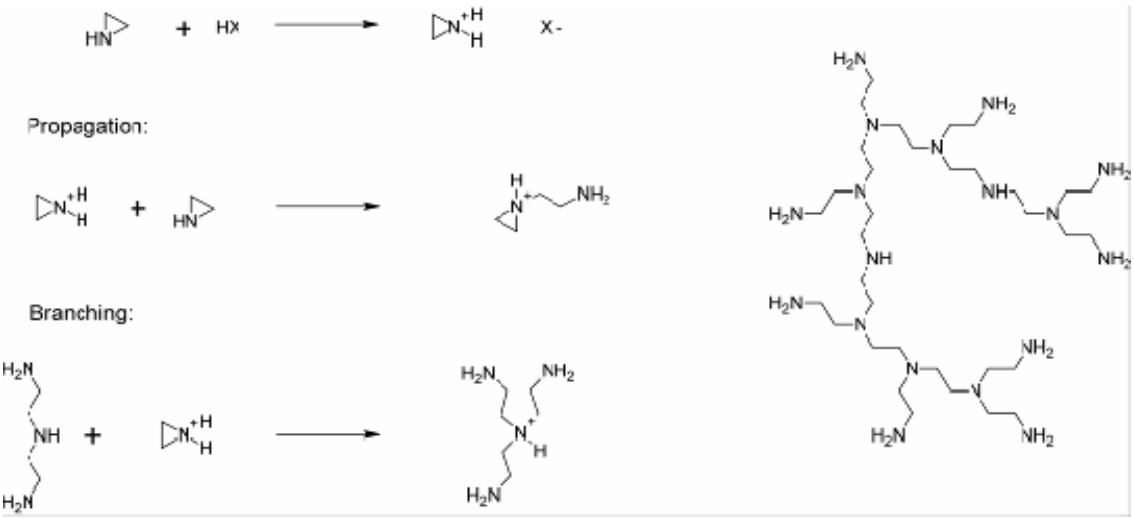

Figure 2: Mechanism of acid catalyzed polymerization of branched polyethylenimine and the resulting polymer structure (adapted from (26))

It was Kircheis et al. which, soon after PEI was introduced as non-viral vector, modified the polymer with cell binding ligands in an attempt to further improve transfection efficiency and specificity (*27*). In this study, transferrin or antiCD3 antibody were covalently linked to PEI of 800 kDa using cyanoborohydride or N-succinimidyl-3-(2-pyridyldithio)propionate (SPDP), respectively. With these second-generation PEIs, an up to 1000-fold increased transfection efficiency was found in vitro and it was shown, that transfection can be competitively inhibited by free ligand. Later Zanta et al. prepared galactose-modified PEI for hepatocyte targeting (*28*). In vitro transfections of human or murine hepatocyte-derived cell lines (HepG2 and BNL CL.2) were 1000- to 10000-fold more efficient than with murine fibroblasts (3T3). Again hepatocyte-specific targeting was verified by replacement of galactose with glucose, removal of galactose residues or excess asialofetuin, all of which resulted in suppression of transfection. Table 1 summarizes studies involving targeting ligands conjugated to PEI.

Target	Ligand	Polycation	Shielding	Reference
Liver	Galactose	PEI	-	(*28-30*)
		PEI	PEG	(*31, 32*)
	Linear tetragalactose	PEI	-	(*33*)
Dendritic cells	Mannose	PEI	-	(*34*)
Epithelial cells	RGD peptides	PEI	-	(*35*)
		PEI	PEG	(*36-39*)
Pulmonary endothelium	anti-platelet endothelial cell adhesion molecule (PECAM) antibody	PEI	-	(*40*)
T-cells	Anti-CD3 antibody	PEI	-	(*27, 41*)
Islet beta cells	Anti-glutamic acid decarboxylase (GAD) Fab'	PEI	PEG	(*42*)
Tumors (general)	Transferrin	PEI	w/ or w/o PEG	(*43-47*)
	Epithelial growth factor	PEI	w/ or w/o PEG	(*43, 45, 47, 48*)
	Folate	PEI	w/ or w/o PEG	(*49-51*)
		Crosslinked PEI	PEG-cholesterol	(*52*)
Tumors (specific)	Anti-human epidermal growth factor receptor-2 (HER2) antibody	PEI	-	(*53, 54*)
		PEI	PEG	(*55, 56*)
	Anti-OA3 Fab'	PEI	PEG	(*57*)
	Anti-prostate-specific membrane antigen (PSMA) antibody	PEI	PEG	(*58*)

Table 1: Studies on targeted non-viral gene delivery systems based on PEI.

Considering the in vivo situation, the vector system will in most cases be administered by intravenous injection. This administration route requires the vector to have special characteristics. The ideal polyplex should a) condense nucleic acids into neutral complexes thus avoiding toxicity and interactions with blood components such as erythrocytes or ionic macromolecules; b) form stable and small polyplexes to facilitate diffusion and extravasation; c) specifically bind to its target cells leaving non-targeted cells unaffected; and d) avoid degradation of the cargo (DNA, oligos, RNA). However, PEI polyplexes need to be prepared with an excess of polycation to yield small particles and to protect its cargo against degradation. These particles are positively charged and suspensions are stabilized by electrostatic repulsion. In contrast, neutral particles formed at lower ratios of positively charged nitrogens of the polymer to negatively charged phosphates in the nucleic acid backbone (N/P ratios) are prone to precipitation. The positive surface charge of PEI polyplexes also mediates non-specific interaction with proteoglycans on the cell surface enabling efficient cellular uptake and transfection (*59*). However, intravenous administration of positively charged particles leads to opsonization thus inducing polyplex clearance by the reticuloendothelial system (*60*). Grafting of hydrophilic polymers such as polyethylenglycol (PEG) or poly(*N*-(2-hydroxypropyl)methacrylamide) (pHPMA) (*61-64*) led to reduction of surface charge, decreased unspecific transfection (*63, 65*) and was reported to increase circulation times (*61, 62*). For illustration of the concept of targeted gene delivery see Figure 3.

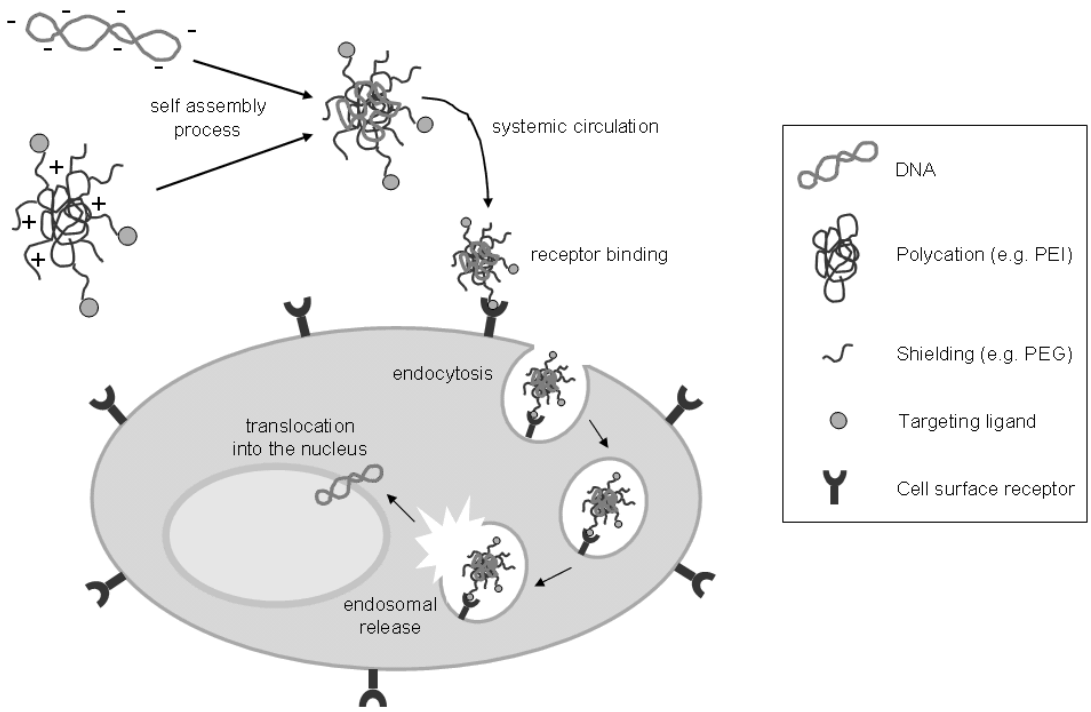

Figure 3: Schematic presentation of targeted gene delivery using non-viral vectors: Polycation (e.g. PEI) is modified with targeting ligands and shielding moieties. Polycation and DNA upon mixing spontaneously form polyplexes, which delivery the cargo DNA through systemic circulation to the target tissue (e.g. tumor). The targeted polyplexes bind to the cell surface via ligand-receptor interaction and are internalized. Later, complexes are release from the endosome and DNA is translocated into the nucleus. Translocation, transcription and translation finally result in protein expression.

Our group (*61, 66*) and others (*32, 63*) synthesized PEG-graft-PEIs and studied their biophysical and biological properties. Petersen et al. focused their attention on optimization of complexation and shielding properties of these copolymers by varying PEG molecular weight and grafting ratio (*66*). It was found that zetapotential of polyplexes decreased with increasing grafting ratio if PEG chains were larger or equal to 5 kDa. PEG with lower molecular weight (550 Da) was not able to efficiently shield positive surface charge and formed large and diffuse complexes with DNA. In contrast, PEG 5 kDa reduced the diameter of complexes prepared in 150 mM sodium chloride solution from 142 to 62 nm. If more than six PEG chains, irrespective of the molecular weight, were grafted per PEI molecule, DNA complexes of low cytotoxicity were formed.

Further studies with these copolymers were focused on in vivo biodistribution and pharmacokinetics of complexes with oligonucleotides or plasmid DNA (*61, 67*). Kunath et al. showed that using oligonucleotide/PEG-PEI polyplexes prepared with copolymers with short PEG chains and a high grafting ratio, area under the curve could be increased compared to PEI (*61*). However, in this study only kinetics and biodistribution of the polymer which was labeled with ^{125}I by the method of Bolton and Hunter (*68*) was determined. Merdan et al. in their study used both, radioactively labeled plasmid DNA (^{32}P) and labeled polymer (^{125}I), applying different DNA doses (*67*). A dose dependent stability of PEG-PEI/DNA complexes was found. If 1.5 µg pDNA were applied per mouse, fast separation of plasmid and polymer occurred resulting in diverging plasma level-time profiles. Furthermore, organ distributions were dissimilar as well. While 40% of the injected dose of copolymer was found in the liver, plasmid appeared at a significantly lower level. ^{32}P was found in the urine, probably being the result of pDNA degradation. At a higher pDNA dose of 25 µg per mouse, no significant separation of DNA from polymer was found but area under the curve of DNA applied using PEG-PEI was not enhanced compared to polyplexes prepared with unmodified PEI.

Due to the decreased surface charge of PEGylated PEI and thus decreased non-specific interaction, these copolymers are exceptionally suitable for targeted gene delivery both in vitro and in vivo (Figure 4).

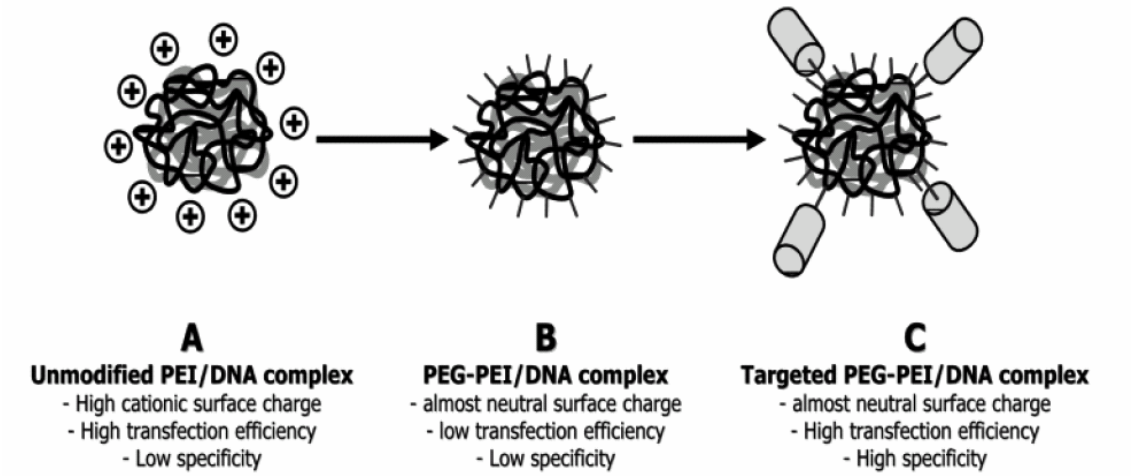

Figure 4: Rationale for polymer modification with PEG and targeting ligands. PEI/DNA polyplexes efficiently bind to the cell surface due to the high cationic surface charge. This leads to high transfection efficiency but poor specificity (A). PEGylation of PEI strongly reduced the

cationic charge of polyplexes, thus inhibiting unspecific binding. However, transfection efficiency of these polyplexes is strongly reduced as well (B). Conjugation of cell binding ligands improves binding and internalization only in target cells while leaving non-targeted cells virtually unaffected (C). (from (57))

Most studies on targeted PEG-PEI polyplexes focused on in vitro characterization. The first to describe PEG-PEI copolymers in combination with targeting ligands was Erbacher et al. in 1999 (*32*). In this study, PEG-PEI copolymer was synthesized and galactose was attached to the distal end of the PEG chains. However, no increase in transgene expression was found with targeted polyplexes in this early study. Blessing et al. and Woodle et al. in 2001 showed efficient gene transfer with EGF- or RGD-targeted, PEG shielded complexes in vitro, respectively. Different routes to prepare PEG shielded and targeted polyplexes were chosen in these studies. Similar to Erbacher, Woodle et al. first synthesized PEG grafted PEI and RGD-modified, amine reactive PEG which then was reacted with PEG-PEI. Subsequently, pDNA was condensed into polyplexes using the RGD-PEG-PEI conjugate. This so called pre-PEGylation approach has striking advantages: conjugate synthesis is straightforward and reproducible, product purification is easy, and conjugates can be stored over long term. On the other hand, the affinity of these copolymers to DNA tends to be reduced and polyplexes might be instable. In contrast, Blessing et al. applied the so called post-PEGylation approach. DNA is first condensed with PEI or EGF-PEI into polyplexes and is afterwards covalently modified with PEG (Figure 5). This technique produces very stable and small polyplexes but on the other hand involves several synthesis steps after formation of polyplexes. In terms of byproducts, sterility and storage-ability, this method is clearly disadvantageous.

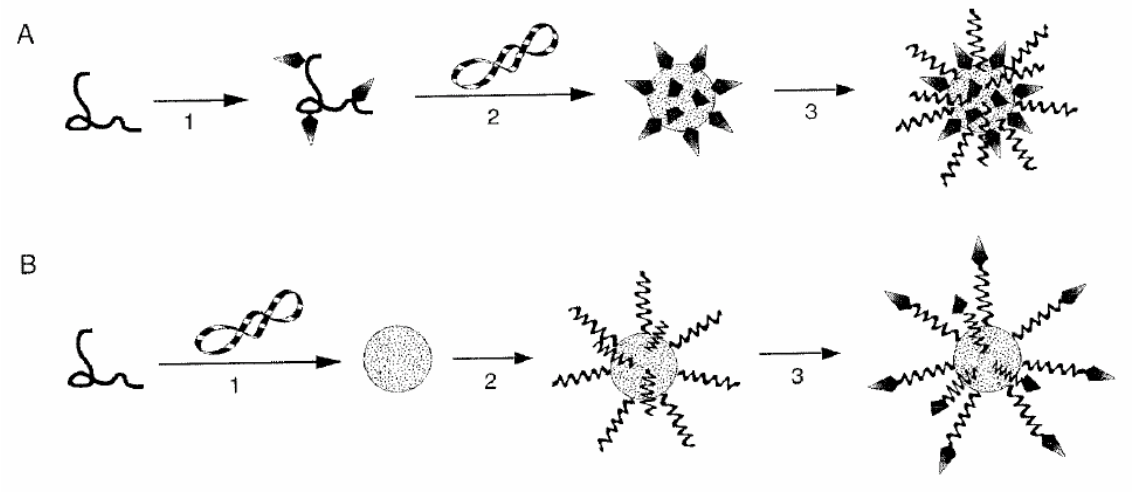

Figure 5: Schematic presentation of the formation of targeted PEGylated PEI/DNA polyplexes. Route A: Covalent conjugation of a ligand to PEI (1), condensation of DNA into polyplexes using this conjugate (2), PEGylation of the resulting polyplexes by an amine-reactive PEG derivative. Route B: Condensation of DNA unsing unmodified PEI (1), modification of the free amino groups on polyplex surface with a heterobifunctional PEG derivative (2), covalent conjugation of the ligand to the distal end of PEG (3) (from (48))

Besides several in vitro studies published so far (see Table 1) only few reports on successful systemic in vivo gene delivery using targeted and shielded PEI can be found. Kursa et al. described a modular vector system consisting of linear PEI as main condensing agent, PEG-PEI for surface shielding and transferrin-PEG-PEI for cell-specific targeting (*44*). Using this construction kit, characteristics of polyplexes can easily be varied. After freeze thawing of polyplexes containing PEG-PEI, physicochemical characteristics were not significantly changed and transfection efficiency was not altered. Moreover, systemic application of freeze thawed polyplexes showed in vivo tumor targeting. An optimized formulation was used for in vivo delivery of DNA encoding for tumor necrosis factor alpha to different tumor models. Significant tumor growth inhibition was found in all tumor models after repetitive application of freeze thawed polyplexes.

Moffatt et al. used an elegant post-PEGylation approach with salicylhydroxamic acid (SHA)-reactive PEG covalently modified with anti-PSMA antibody and SHA-modified PEI to condense DNA (Figure 6) (*58*). These vectors were shown to transfect PSMA positive cells with high efficiency in vitro resulting in significant growth inhibition

when DNA-p53 was used. Specificity of transfection was verified by competitive inhibition with free antibody. A murine orthotopic prostate cancer model was used to study targeting in vivo and it was found that gene delivery increased 20-fold over untargeted vectors.

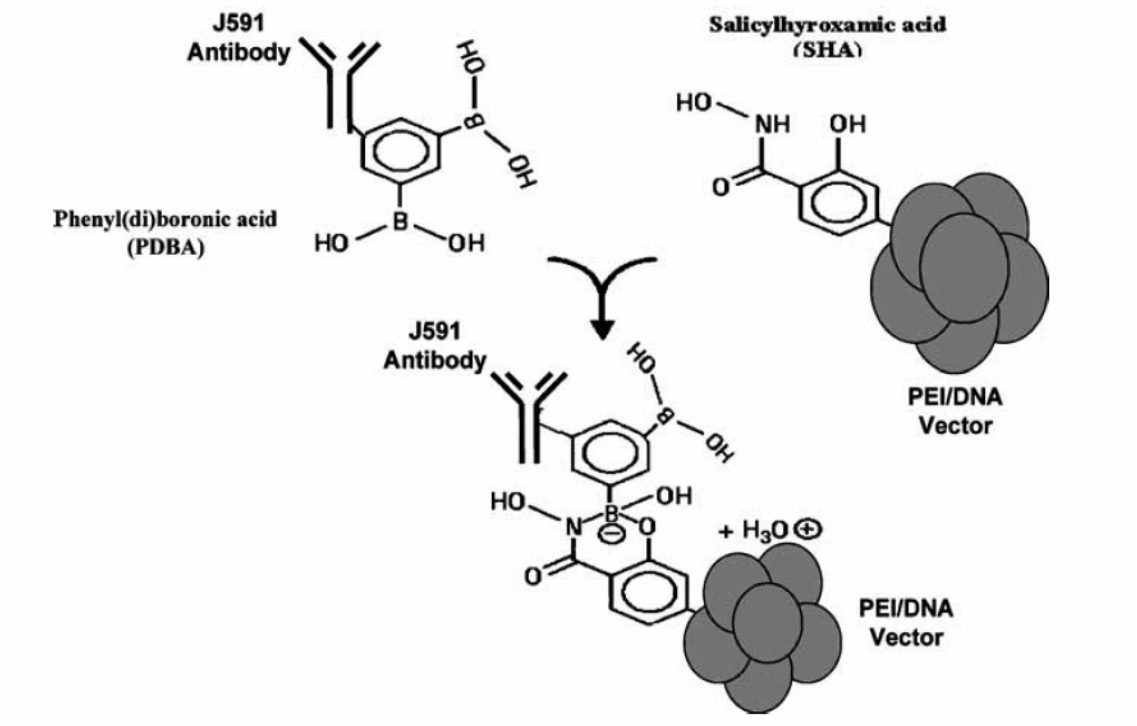

Figure 6: Phenyl(di)boronic acid–salicylhydroxamic acid conjugation. PDBA was coupled to anti-PSMA (J591) antibody via a hydrolysable PEG linker. SHA modified PEI was used to complex β-gal DNA and subsequently modified with antibody by self-assembly of PDBA and SHA. (from (58))

In this work, PEG-PEI copolymers were used for targeted in vitro gene delivery. In chapter 2, a proof-of-concept study is presented establishing PEG-PEI for targeting using HER2 directed monoclonal antibody Trastuzumab. An in vitro model consisting of HER2 positive and -negative cells was established to study targeting in vitro. Physicochemical and biological properties of the resulting targeted polyplexes were characterized and it was shown that this non-viral vector system can be used for specific transfection of HER2 overexpressing cell lines in vitro.

In chapter 3, we studied different conjugates, varying PEG-PEI copolymers used for synthesis, the linker chemistry and the degree of substitution with Trastuzumab. These

conjugates were characterized concerning their physicochemical characteristics, targeting-ability in vitro and pharmakokinteics and biodistribution in vivo in mice.

Chapter 4 describes the development of a HER2 overexpressing tumor model in vivo in SCID mice. Tumors were characterized with respect to macroscopy, histology, vascularization and HER2 expression. Finally, Trastuzumab-PEG-PEI conjugates identified in chapter 3 were used to evaluate in vivo targeting-ability by systemic and intratumoral application.

1.3 Non-Viral Gene Delivery using Chitosan

Chitosan, a biopolymer derived from crustacean shells, is one of the most reported non-viral naturally occurring gene carriers. It has a strong affinity to DNA and spontaneously forms polyplexes. However, due to its apparent pK_a of 6.5 it is only soluble at pH 1-6 where most of the amino groups are protonated.

Chitosan already found wide application in the pharmaceutical field before researchers started to use it as a gene delivery agent. For example, chitosan was used as an excipient in oral dosage forms (*69*), as absorption enhancer (*70*), for dermal applications (*71*), and for preparation of micro- (*72*) and nanoparticles (*73*).

Mumper in 1995 was the first to propose chitosan as a non-viral vector for gene delivery (*74*). Polyplexes with DNA were formed at different mixing ratios and it was found that particle size depended on the molecular weight of chitosan used (108-540 kDa). Besides molecular weight, degree of deacetylation, DNA concentration, pH of buffer, charge ratio and temperature were found to influence size and transfection efficiency of chitosan/DNA polyplexes (*75-80*). Chitosan/DNA nanoparticles were found to be globular-donut or rod-shaped by transmission electron microscopy and atomic force microscopy (*81-83*).

However, the transfection efficiency of chitosan is several orders lower than that of PEI or lipofectamine, which both serve as a gold standard in the field (*80, 84*). To optimize gene transfer efficiency of chitosan, several modifications of chitosans have been published.

1.3.1 Hydrophobically modified Chitosan

Lee and Kim et al. modified chitosan with deoxycholic acid, a main component of bile salt (*85, 86*). Bile acid can self-assemble in water and therefore, deoxycholic acid modified chitosan formed micelles of about 160 nm in PBS at pH 7.2. DNA readily formed polyplexes with self-aggregates and retardation of DNA was inhibited at N/P ratio 4 in agarose gel electrophoresis. However, transfection results were less promising. Self-aggregates showed an increased efficiency compared to free DNA but were far less efficient than lipofectamine.

Liu et al. prepared alkylated chitosan by reaction of alkyl bromide with chitosan (*87*). It was found that these vectors mediate higher transgene expression than unmodified chitosan. Transfection efficiency increased with increasing alkyl blocks up to a length of 8 carbon atoms, then leveling off. The authors proposed that the enhancement of transfection is due to improved cell entry facilitated by hydrophobic interactions and easier unpacking of DNA.

In 2005 Yoo et al. showed that hydrophobically modified glycol chitosan enhances transfection efficiency compared to chitosan in vitro and after intra muscular injection in vivo (*88*). Increased transfection efficiency was also reported by Uchegbu et al. for hydrophobically modified glycol chitosan and quaternized glycol chitosan both in vitro and in vivo (*89*).

1.3.2 Chitosan-ligand conjugates

As with many other non-viral vectors, different cell-binding ligands were coupled to chitosan. Galactose is a well known ligand for hepatocyte targeting. It can bind to target cells via asialoglycoprotein receptor and is subsequently internalized. Park et al. Gao et al., Kim et al. and Satoh et al. successfully utilized this method to increase transfection efficiency of chitosan or chitosan derivatives (*90-93*). A similar approach was chosen by Hashimoto et al. using lactose as targeting ligand for asiologlycoprotein receptor (*94*).

The transferrin receptor was one of the first to be exploited for non-viral gene delivery. Modification of chitosan with transferrin resulted in up to fourfold increased transfection efficiency compared to unmodified chitosan (*95*). In this study a second ligand, C-terminal globular domain of the fiber protein (KNOB) was used for cell targeting and

resulted in 130-fold increased transfection in HeLa cells and several fold increase in HEK293 cells.

Folate is another classic ligand for tumor cell targeting. Mansouri and Chan et al. described the synthesis and characterization of folate receptor-targeted chitosan derivatives (*96, 97*). Lee et al. reported significantly enhanced transfection efficiencies in folate receptor overexpressing cells using a chitosan-folic acid conjugate (*98*). Furthermore, by competitive inhibition with free folic acid, specificity of transfection was proven.

1.3.3 Chitosan-polycation conjugates

The idea of a combination of chitosan and another cationic polymer already emerged in 2002 (*99*) and was revived by Kim et al. in 2005 (*100*). In this study, the authors combined PEI with water-soluble chitosan or galactosylated chitosan for hepatocyte targeting. Interestingly, a synergism between PEI and chitosan was revealed and the combination even outperformed PEI polyplexes in different cell lines. Jiang et al. further developed this system by synthesizing chitosan-graft-PEI (*101*). Consequently, galactosylated chitosan-graft-PEI was developed as well and it was shown to target hepatocytes both in vitro and in vivo (*102*). Similarly, chitosan-graft-poly-L-lysine was synthesized by Yu and found to improve transfection efficiency in HEK293 cells compared to unmodified chitosan (*103*).

1.3.4 Quaternized Chitosan

Quaternized modifications of chitosan were first published by Kotze et al. as absorption enhancers for large hydrophilic compounds across mucosal surfaces (*104*). N-trimethyl chitosan was found to immediately reduce the transepithelial electrical resistance of Caco-2 cells and to open tight junctions of intestinal epithelial cells. These properties resulted in a large increase in the transport of different hydrophilic molecules. Later Thanou and colleagues co-administered buserelin and trimethyl chitosan intraduodenally in rats and showed that the in vitro results hold also true for the situation in vivo (*105*).

In 2002, quaternized chitosan was introduced in the gene delivery field (*106*). Oligomeric chitosan (< 20 monomer units) was quaternized by a reductive methylation

procedure using methyl iodide in an alkaline environment. These trimethyl chitosan oligomers spontaneously formed 200 to 500 nm sized polyplexes with DNA. Transfection experiments in COS-1 and Caco-2 cells revealed up to 131-fold increased reporter gene expression compared to free DNA while unmodified chitosan only showed 2-4-fold increased transfection. The authors also studied the cytotoxicity of the polyplexes at 1 mg/ml in both cell lines. It was found that neither chitosan nor trimethyl chitosan oligomers decreased cell viability. In contrast, DOTAP which was used as a standard in the transfection experiments decreased cell viability to about 50%.

Studying the cytotoxicity of different trimethyl chitosans (TMC) Mao et al. discovered that cytotoxicity is a function of molecular weight (*107*). While TMC of 5 kDa was virtually non-toxic as found in the study of Thanou et al., a slight increase in molecular weight strongly increased cytotoxicity of the polymer (TMC 25 kDa: IC_{50} of 125 µg/ml). PEG grafted TMCs were synthesized and shown to decrease cytotoxicity and solubility of higher molecular weight TMC.

In chapter 5 of this thesis, PTMC was evaluated for in vitro gene delivery efficiency. A direct comparison between physicochemical properties such as complexation efficiency, size, zetapotential and polyplex stability of chitosan-, TMC- and PTMC/DNA polyplexes was made. Furthermore, cell interactions, cytotoxicity and transfection efficiency of the different polyplexes was studied.

In chapter 6, we evaluate important steps in the transfection process to find potential starting points for further improvements of the system. This chapter presents data on colloidal stability, uptake kinetics, route of uptake and route of transfection of chitosan, TMC and PTMC polyplexes was performed.

1.4 References

(1) Mulligan, R. C. (1993) The basic science of gene therapy. *Science 260*, 926-32.

(2) Venter, J. C., Adams, M. D., Myers, E. W., Li, P. W., Mural, R. J., Sutton, G. G., Smith, H. O., Yandell, M., Evans, C. A., Holt, R. A., et al. (2001) The sequence of the human genome. *Science 291*, 1304-51.

(3) Herweijer, H., and Wolff, J. A. (2003) Progress and prospects: naked DNA gene transfer and therapy. *Gene Ther 10*, 453-8.

(4) Mahato, R. I. (2005) Water insoluble and soluble lipids for gene delivery. *Adv Drug Deliv Rev 57*, 699-712.

(5) Smisterova, J., Wagenaar, A., Stuart, M. C., Polushkin, E., ten Brinke, G., Hulst, R., Engberts, J. B., and Hoekstra, D. (2001) Molecular shape of the cationic lipid controls the structure of cationic lipid/dioleylphosphatidylethanolamine-DNA complexes and the efficiency of gene delivery. *J Biol Chem 276*, 47615-22.

(6) Farhood, H., Serbina, N., and Huang, L. (1995) The role of dioleoyl phosphatidylethanolamine in cationic liposome mediated gene transfer. *Biochim Biophys Acta 1235*, 289-95.

(7) Lappalainen, K., Jaaskelainen, I., Syrjanen, K., Urtti, A., and Syrjanen, S. (1994) Comparison of cell proliferation and toxicity assays using two cationic liposomes. *Pharm Res 11*, 1127-31.

(8) Schiffelers, R. M., de Wolf, H. K., van Rooy, I., and Storm, G. (2007) Synthetic delivery systems for intravenous administration of nucleic acids. *Nanomed 2*, 169-81.

(9) De Smedt, S. C., Demeester, J., and Hennink, W. E. (2000) Cationic polymer based gene delivery systems. *Pharm Res 17*, 113-26.

(10) Merdan, T., Kopecek, J., and Kissel, T. (2002) Prospects for cationic polymers in gene and oligonucleotide therapy against cancer. *Adv Drug Deliv Rev 54*, 715-58.

(11) Godbey, W. T., Wu, K. K., and Mikos, A. G. (2001) Poly(ethylenimine)-mediated gene delivery affects endothelial cell function and viability. *Biomaterials 22*, 471-80.

(12) Ehrlich, M., Sarafyan, L. P., and Myers, D. J. (1976) Interaction of microbial DNA with cultured mammalian cells. Binding of the donor DNA to the cell surface. *Biochim Biophys Acta 454*, 397-409.

(13) Henner, W. D., Kleber, I., and Benzinger, R. (1973) Transfection of Escherichia coli spheroplasts. 3. Facilitation of transfection and stabilization of spheroplasts by different basic polymers. *J Virol 12*, 741-7.

(14) Boussif, O., Lezoualc'h, F., Zanta, M. A., Mergny, M. D., Scherman, D., Demeneix, B., and Behr, J. P. (1995) A versatile vector for gene and oligonucleotide transfer into cells in culture and in vivo: polyethylenimine. *Proc Natl Acad Sci U S A 92*, 7297-301.

(15) Gebhart, C. L., and Kabanov, A. V. (2001) Evaluation of polyplexes as gene transfer agents. *J Control Release 73*, 401-16.

(16) Ohana, P., Gofrit, O., Ayesh, S., Al-Sharef, W., Mizrahi, A., Birman, T., Schneider, T., Matouk, I., de Groot, N., Tavdy, E., et al. (2004) Regulatory sequences of the H19 gene in DNA based therapy of bladder cancer. *Gene Ther Mol Biol 8*, 181-192.

(17) Dick, C. R., and Ham, G. E. (1970) Characterization of polyethyleneimine. *J. Macromol. Sci. A 4*, 1301–1314.

(18) Horn, D., and Linhart, F. (1991) *Paper Chemistry*, Blackie, London.

(19) Brodsky, F. M., Chen, C. Y., Knuehl, C., Towler, M. C., and Wakeham, D. E. (2001) Biological basket weaving: formation and function of clathrin-coated vesicles. *Annu Rev Cell Dev Biol 17*, 517-68.

(20) Behr, J. P. (1997) The proton sponge: A trick to enter cells the viruses did not exploit. *Chimia 51*, 34-36.

(21) Merdan, T., Kunath, K., Fischer, D., Kopecek, J., and Kissel, T. (2002) Intracellular processing of poly(ethylene imine)/ribozyme complexes can be observed in living cells by using confocal laser scanning microscopy and inhibitor experiments. *Pharm Res 19*, 140-6.

(22) Sonawane, N. D., Szoka, F. C., Jr., and Verkman, A. S. (2003) Chloride accumulation and swelling in endosomes enhances DNA transfer by polyamine-DNA polyplexes. *J Biol Chem 278*, 44826-31.

(23) Akinc, A., Thomas, M., Klibanov, A. M., and Langer, R. (2005) Exploring polyethylenimine-mediated DNA transfection and the proton sponge hypothesis. *J Gene Med 7*, 657-63.

(24) Boussif, O., Zanta, M. A., and Behr, J. P. (1996) Optimized galenics improve in vitro gene transfer with cationic molecules up to 1000-fold. *Gene Ther 3*, 1074-80.

(25) Abdallah, B., Hassan, A., Benoist, C., Goula, D., Behr, J. P., and Demeneix, B. A. (1996) A powerful nonviral vector for in vivo gene transfer into the adult mammalian brain: polyethylenimine. *Hum Gene Ther 7*, 1947-54.

(26) von Harpe, A., Petersen, H., Li, Y., and Kissel, T. (2000) Characterization of commercially available and synthesized polyethylenimines for gene delivery. *J Control Release 69*, 309-22.

(27) Kircheis, R., Kichler, A., Wallner, G., Kursa, M., Ogris, M., Felzmann, T., Buchberger, M., and Wagner, E. (1997) Coupling of cell-binding ligands to polyethylenimine for targeted gene delivery. *Gene Ther 4*, 409-18.

(28) Zanta, M. A., Boussif, O., Adib, A., and Behr, J. P. (1997) In vitro gene delivery to hepatocytes with galactosylated polyethylenimine. *Bioconjug Chem 8*, 839-44.

(29) Morimoto, K., Nishikawa, M., Kawakami, S., Nakano, T., Hattori, Y., Fumoto, S., Yamashita, F., and Hashida, M. (2003) Molecular weight-dependent gene transfection activity of unmodified and galactosylated polyethyleneimine on hepatoma cells and mouse liver. *Mol Ther 7*, 254-61.

(30) Kunath, K., von Harpe, A., Fischer, D., and Kissel, T. (2003) Galactose-PEI-DNA complexes for targeted gene delivery: degree of substitution affects complex size and transfection efficiency. *J Control Release 88*, 159-72.

(31) Sagara, K., and Kim, S. W. (2002) A new synthesis of galactose-poly(ethylene glycol)-polyethylenimine for gene delivery to hepatocytes. *J Control Release 79*, 271-81.

(32) Erbacher, P., Bettinger, T., Belguise-Valladier, P., Zou, S., Coll, J. L., Behr, J. P., and Remy, J. S. (1999) Transfection and physical properties of various saccharide, poly(ethylene glycol), and antibody-derivatized polyethylenimines (PEI). *J Gene Med 1*, 210-22.

(33) Bettinger, T., Remy, J. S., and Erbacher, P. (1999) Size reduction of galactosylated PEI/DNA complexes improves lectin-mediated gene transfer into hepatocytes. *Bioconjug Chem 10*, 558-61.

(34) Diebold, S. S., Lehrmann, H., Kursa, M., Wagner, E., Cotten, M., and Zenke, M. (1999) Efficient gene delivery into human dendritic cells by adenovirus polyethylenimine and mannose polyethylenimine transfection. *Hum Gene Ther 10*, 775-86.

(35) Erbacher, P., Remy, J. S., and Behr, J. P. (1999) Gene transfer with synthetic virus-like particles via the integrin-mediated endocytosis pathway. *Gene Ther 6*, 138-45.

(36) Kunath, K., Merdan, T., Hegener, O., Haberlein, H., and Kissel, T. (2003) Integrin targeting using RGD-PEI conjugates for in vitro gene transfer. *J Gene Med 5*, 588-99.

(37) Woodle, M. C., Scaria, P., Ganesh, S., Subramanian, K., Titmas, R., Cheng, C., Yang, J., Pan, Y., Weng, K., Gu, C., et al. (2001) Sterically stabilized polyplex: ligand-mediated activity. *J Control Release 74*, 309-11.

(38) Schiffelers, R. M., Ansari, A., Xu, J., Zhou, Q., Tang, Q., Storm, G., Molema, G., Lu, P. Y., Scaria, P. V., and Woodle, M. C. (2004) Cancer siRNA therapy by tumor selective delivery with ligand-targeted sterically stabilized nanoparticle. *Nucleic Acids Res 32*, e149.

(39) gKim, W. J., Yockman, J. W., Lee, M., Jeong, J. H., Kim, Y. H., and Kim, S. W. (2005) Soluble Flt-1 gene delivery using PEI-g-PEG-RGD conjugate for anti-angiogenesis. *J Control Release 106*, 224-34.

(40) Li, S., Tan, Y., Viroonchatapan, E., Pitt, B. R., and Huang, L. (2000) Targeted gene delivery to pulmonary endothelium by anti-PECAM antibody. *Am J Physiol Lung Cell Mol Physiol 278*, L504-11.

(41) Guillem, V. M., Tormo, M., Revert, F., Benet, I., Garcia-Conde, J., Crespo, A., and Alino, S. F. (2002) Polyethyleneimine-based immunopolyplex for targeted gene transfer in human lymphoma cell lines. *J Gene Med 4*, 170-82.

(42) Jeong, J. H., Lee, M., Kim, W. J., Yockman, J. W., Park, T. G., Kim, Y. H., and Kim, S. W. (2005) Anti-GAD antibody targeted non-viral gene delivery to islet beta cells. *J Control Release 107*, 562-570.

(43) Ogris, M., Walker, G., Blessing, T., Kircheis, R., Wolschek, M., and Wagner, E. (2003) Tumor-targeted gene therapy: strategies for the preparation of ligand-polyethylene glycol-polyethylenimine/DNA complexes. *J Control Release 91*, 173-81.

(44) Kursa, M., Walker, G. F., Roessler, V., Ogris, M., Roedl, W., Kircheis, R., and Wagner, E. (2003) Novel shielded transferrin-polyethylene glycol-polyethylenimine/DNA complexes for systemic tumor-targeted gene transfer. *Bioconjug Chem 14*, 222-31.

(45) Kircheis, R., Blessing, T., Brunner, S., Wightman, L., and Wagner, E. (2001) Tumor targeting with surface-shielded ligand--polycation DNA complexes. *J Control Release 72*, 165-70.

(46) Hildebrandt, I. J., Iyer, M., Wagner, E., and Gambhir, S. S. (2003) Optical imaging of transferrin targeted PEI/DNA complexes in living subjects. *Gene Ther 10*, 758-64.

(47) Smrekar, B., Wightman, L., Wolschek, M. F., Lichtenberger, C., Ruzicka, R., Ogris, M., Rodl, W., Kursa, M., Wagner, E., and Kircheis, R. (2003) Tissue-dependent factors affect gene delivery to tumors in vivo. *Gene Ther 10*, 1079-88.

(48) Blessing, T., Kursa, M., Holzhauser, R., Kircheis, R., and Wagner, E. (2001) Different strategies for formation of pegylated EGF-conjugated PEI/DNA complexes for targeted gene delivery. *Bioconjug Chem 12*, 529-37.

(49) Guo, W., and Lee, R. L. (1999) Receptor-targeted gene delivery via folate-conjugated polyethylenimine. *AAPS PharmSci 1*, E19.

(50) Benns, J. M., Mahato, R. I., and Kim, S. W. (2002) Optimization of factors influencing the transfection efficiency of folate-PEG-folate-graft-polyethylenimine. *J Control Release 79*, 255-69.

(51) Hwa Kim, S., Hoon Jeong, J., Chul Cho, K., Wan Kim, S., and Gwan Park, T. (2005) Target-specific gene silencing by siRNA plasmid DNA complexed with folate-modified poly(ethylenimine). *J Control Release 104*, 223-32.

(52) Gosselin, M. A., Guo, W., and Lee, R. J. (2002) Incorporation of reversibly cross-linked polyplexes into LPDII vectors for gene delivery. *Bioconjug Chem 13*, 1044-53.

(53) Chiu, S. J., Ueno, N. T., and Lee, R. J. (2004) Tumor-targeted gene delivery via anti-HER2 antibody (trastuzumab, Herceptin(R)) conjugated polyethylenimine. *J Control Release 97*, 357-69.

(54) Strehblow, C., Schuster, M., Moritz, T., Kirch, H. C., Opalka, B., and Petri, J. B. (2005) Monoclonal antibody-polyethyleneimine conjugates targeting Her-2/neu or CD90 allow cell type-specific nonviral gene delivery. *J Control Release 102*, 737-47.

(55) Germershaus, O., Merdan, T., Bakowsky, U., Behe, M., and Kissel, T. (2006) Trastuzumab-polyethylenimine-polyethylene glycol conjugates for targeting Her2-expressing tumors. *Bioconjug Chem 17*, 1190-9.

(56) Germershaus, O., Neu, M., Behe, M., and Kissel, T. (2007) HER2 Targeted Polyplexes: The Effect of Polyplex Composition and Conjugation Chemistry on in Vitro and in Vivo Characteristics. *Bioconjug Chem*.

(57) Merdan, T., Callahan, J., Petersen, H., Kunath, K., Bakowsky, U., Kopeckova, P., Kissel, T., and Kopecek, J. (2003) Pegylated polyethylenimine-Fab' antibody fragment conjugates for targeted gene delivery to human ovarian carcinoma cells. *Bioconjug Chem 14*, 989-96.

(58) Moffatt, S., Papasakelariou, C., Wiehle, S., and Cristiano, R. (2006) Successful in vivo tumor targeting of prostate-specific membrane antigen with a highly efficient J591/PEI/DNA molecular conjugate. *Gene Ther 13*, 761–772.

(59) Mislick, K. A., and Baldeschwieler, J. D. (1996) Evidence for the role of proteoglycans in cation-mediated gene transfer. *Proc Natl Acad Sci U S A 93*, 12349-54.

(60) Plank, C., Mechtler, K., Szoka, F. C., Jr., and Wagner, E. (1996) Activation of the complement system by synthetic DNA complexes: a potential barrier for intravenous gene delivery. *Hum Gene Ther 7*, 1437-46.

(61) Kunath, K., von Harpe, A., Petersen, H., Fischer, D., Voigt, K., Kissel, T., and Bickel, U. (2002) The structure of PEG-modified poly(ethylene imines) influences biodistribution and pharmacokinetics of their complexes with NF-kappaB decoy in mice. *Pharm Res 19*, 810-7.

(62) Ogris, M., Brunner, S., Schuller, S., Kircheis, R., and Wagner, E. (1999) PEGylated DNA/transferrin-PEI complexes: reduced interaction with blood components, extended circulation in blood and potential for systemic gene delivery. *Gene Ther. 6*, 595-605.

(63) Nguyen, H.-K., Lemieux, P., Vinogradov, S. V., Gebhart, C. L., Guérin, N., Paradis, G., Bronich, T. K., Alakhov, V. Y., and Kabanov, A. V. (2000) Evaluation of polyether-polyethyleneimine graft copolymers as gene transfer agents. *Gene Ther. 7*, 126-138.

(64) Oupicky, D., Howard, K. A., Konak, C., Dash, P. R., Ulbrich, K., and Seymour, L. W. (2000) Steric stabilization of poly-L-Lysine/DNA complexes by the covalent attachment of semitelechelic poly[N-(2-hydroxypropyl)methacrylamide]. *Bioconjug Chem 11*, 492-501.

(65) Deshpande, M. C., Davies, M. C., Garnett, M. C., Williams, P. M., Armitage, D., Bailey, L., Vamvakaki, M., Armes, S. P., and Stolnik, S. (2004) The effect of poly(ethylene glycol) molecular architecture on cellular interaction and uptake of DNA complexes. *J Control Release 97*, 143-56.

(66) Petersen, H., Fechner, P. M., Martin, A. L., Kunath, K., Stolnik, S., Roberts, C. J., Fischer, D., Davies, M. C., and Kissel, T. (2002) Polyethylenimine-graft-poly(ethylene glycol) copolymers: influence of copolymer block structure on DNA complexation and biological activities as gene delivery system. *Bioconjug Chem 13*, 845-54.

(67) Merdan, T., Kunath, K., Petersen, H., Bakowsky, U., Voigt, K. H., Kopecek, J., and Kissel, T. (2005) PEGylation of poly(ethylene imine) affects stability of complexes with plasmid DNA under in vivo conditions in a dose-dependent manner after intravenous injection into mice. *Bioconjug Chem 16*, 785-92.

(68) Bolton, A. E., and Hunter, W. M. (1973) The labelling of proteins to high specific radioactivities by conjugation to a 125I-containing acylating agent. *Biochem J 133*, 529-39.

(69) Acarturk, F. (1989) Preparation of a prolonged-release tablet formulation of diclofenac sodium. Part 1: Using chitosan. *Pharmazie 44*, 547-9.

(70) Thanou, M., Verhoef, J. C., and Junginger, H. E. (2001) Oral drug absorption enhancement by chitosan and its derivatives. *Adv Drug Deliv Rev 52*, 117-26.

(71) Valenta, C., and Auner, B. G. (2004) The use of polymers for dermal and transdermal delivery. *Eur J Pharm Biopharm 58*, 279-89.

(72) Varshosaz, J. (2007) The promise of chitosan microspheres in drug delivery systems. *Expert Opin Drug Deliv 4*, 263-73.

(73) Bowman, K., and Leong, K. W. (2006) Chitosan nanoparticles for oral drug and gene delivery. *Int J Nanomedicine 1*, 117-28.

(74) Mumper, R. J., Wang, J., Claspell, J. M., and Rolland, A. P. (1995) Novel polymeric condensing carriers for gene delivery. *Proc. Intl. Symp. Controlled Rel. Bioact. Mater. 22*, 178–179.

(75) Borchard, G. (2001) Chitosans for gene delivery. *Adv Drug Deliv Rev 52*, 145-50.

(76) Janes, K. A., Calvo, P., and Alonso, M. J. (2001) Polysaccharide colloidal particles as delivery systems for macromolecules. *Adv Drug Deliv Rev 47*, 83-97.

(77) Sato, T., Ishii, T., and Okahata, Y. (2001) In vitro gene delivery mediated by chitosan. effect of pH, serum, and molecular mass of chitosan on the transfection efficiency. *Biomaterials 22*, 2075-80.

(78) Ishii, T., Okahata, Y., and Sato, T. (2001) Mechanism of cell transfection with plasmid/chitosan complexes. *Biochimica Et Biophysica Acta-Biomembranes 1514*, 51-64.

(79) Romoren, K., Pedersen, S., Smistad, G., Evensen, O., and Thu, B. J. (2003) The influence of formulation variables on in vitro transfection efficiency and physicochemical properties of chitosan-based polyplexes. *Int J Pharm 261*, 115-27.

(80) Kiang, T., Wen, J., Lim, H. W., and Leong, K. W. (2004) The effect of the degree of chitosan deacetylation on the efficiency of gene transfection. *Biomaterials 25*, 5293-301.

(81) Danielsen, S., Varum, K. M., and Stokke, B. T. (2004) Structural analysis of chitosan mediated DNA condensation by AFM: influence of chitosan molecular parameters. *Biomacromolecules 5*, 928-36.

(82) Maurstad, G., Danielsen, S., and Stokke, B. T. (2007) The influence of charge density of chitosan in the compaction of the polyanions DNA and xanthan. *Biomacromolecules 8*, 1124-30.

(83) Erbacher, P., Zou, S., Bettinger, T., Steffan, A. M., and Remy, J. S. (1998) Chitosan-based vector/DNA complexes for gene delivery: biophysical characteristics and transfection ability. *Pharm Res 15*, 1332-9.

(84) Jiang, X., Dai, H., Leong, K. W., Goh, S. H., Mao, H. Q., and Yang, Y. Y. (2006) Chitosan-g-PEG/DNA complexes deliver gene to the rat liver via intrabiliary and intraportal infusions. *J Gene Med 8*, 477-87.

(85) Kim, Y. H., Gihm, S. H., Park, C. R., Lee, K. Y., Kim, T. W., Kwon, I. C., Chung, H., and Jeong, S. Y. (2001) Structural characteristics of size-controlled self-aggregates of deoxycholic acid-modified chitosan and their application as a DNA delivery carrier. *Bioconjug Chem 12*, 932-8.

(86) Lee, K. Y., Kwon, I. C., Kim, Y. H., Jo, W. H., and Jeong, S. Y. (1998) Preparation of chitosan self-aggregates as a gene delivery system. *J Control Release 51*, 213-20.

(87) Liu, W. G., Zhang, X., Sun, S. J., Sun, G. J., Yao, K. D., Liang, D. C., Guo, G., and Zhang, J. Y. (2003) N-alkylated chitosan as a potential nonviral vector for gene transfection. *Bioconjug Chem 14*, 782-9.

(88) Yoo, H. S., Lee, J. E., Chung, H., Kwon, I. C., and Jeong, S. Y. (2005) Self-assembled nanoparticles containing hydrophobically modified glycol chitosan for gene delivery. *J Control Release 103*, 235-43.

(89) Uchegbu, I. F., Sadiq, L., Pardakhty, A., El-Hammadi, M., Gray, A. I., Tetley, L., Wang, W., Zinselmeyer, B. H., and Schatzlein, A. G. (2004) Gene transfer with three amphiphilic glycol chitosans--the degree of polymerisation is the main controller of transfection efficiency. *J Drug Target 12*, 527-39.

(90) Gao, S., Chen, J., Xu, X., Ding, Z., Yang, Y. H., Hua, Z., and Zhang, J. (2003) Galactosylated low molecular weight chitosan as DNA carrier for hepatocyte-targeting. *Int J Pharm 255*, 57-68.

(91) Park, I. K., Park, Y. H., Shin, B. A., Choi, E. S., Kim, Y. R., Akaike, T., and Cho, C. S. (2000) Galactosylated chitosan-graft-dextran as hepatocyte-targeting DNA carrier. *J Control Release 69*, 97-108.

(92) Kim, T. H., Park, I. K., Nah, J. W., Choi, Y. J., and Cho, C. S. (2004) Galactosylated chitosan/DNA nanoparticles prepared using water-soluble chitosan as a gene carrier. *Biomaterials 25*, 3783-92.

(93) Satoh, T., Kakimoto, S., Kano, H., Nakatani, M., Shinkai, S., and Nagasaki, T. (2007) In vitro gene delivery to HepG2 cells using galactosylated 6-amino-6-deoxychitosan as a DNA carrier. *Carbohydr Res 342*, 1427-33.

(94) Hashimoto, M., Morimoto, M., Saimoto, H., Shigemasa, Y., and Sato, T. (2006) Lactosylated Chitosan for DNA Delivery into Hepatocytes: The Effect of Lactosylation on the Physicochemical Properties and Intracellular Trafficking of pDNA/Chitosan Complexes. *Bioconjugate Chem. 17*, 309-316.

(95) Mao, H. Q., Roy, K., Troung-Le, V. L., Janes, K. A., Lin, K. Y., Wang, Y., August, J. T., and Leong, K. W. (2001) Chitosan-DNA nanoparticles as gene carriers: synthesis, characterization and transfection efficiency. *J Control Release 70*, 399-421.

(96) Mansouri, S., Cuie, Y., Winnik, F., Shi, Q., Lavigne, P., Benderdour, M., Beaumont, E., and Fernandes, J. C. (2006) Characterization of folate-chitosan-DNA nanoparticles for gene therapy. *Biomaterials 27*, 2060-5.

(97) Chan, P., Kurisawa, M., Chung, J. E., and Yang, Y. Y. (2007) Synthesis and characterization of chitosan-g-poly(ethylene glycol)-folate as a non-viral carrier for tumor-targeted gene delivery. *Biomaterials 28*, 540-9.

(98) Lee, D., Lockey, R., and Mohapatra, S. (2006) Folate receptor-mediated cancer cell specific gene delivery using folic acid-conjugated oligochitosans. *J Nanosci Nanotechnol 6*, 2860-6.

(99) Ouji, Y., Yoshida-Terakura, A., Hayashi, Y., Maeda, I., Kawase, M., Yamato, E., Miyazaki, J., and Yagi, K. (2002) Polyethyleneimine/chitosan hexamer-mediated gene transfection into intestinal epithelial cell cultured in serum-containing medium. *J Biosci Bioeng 94*, 81-3.

(100) Kim, T. H., Kim, S. I., Akaike, T., and Cho, C. S. (2005) Synergistic effect of poly(ethylenimine) on the transfection efficiency of galactosylated chitosan/DNA complexes. *J Control Release 105*, 354-66.

(101) Jiang, H. L., Kim, Y. K., Arote, R., Nah, J. W., Cho, M. H., Choi, Y. J., Akaike, T., and Cho, C. S. (2007) Chitosan-graft-polyethylenimine as a gene carrier. *J Control Release 117*, 273-80.

(102) Jiang, H. L., Kwon, J. T., Kim, Y. K., Kim, E. M., Arote, R., Jeong, H. J., Nah, J. W., Choi, Y. J., Akaike, T., Cho, M. H., et al. (2007) Galactosylated chitosan-graft-polyethylenimine as a gene carrier for hepatocyte targeting. *Gene Ther 14*, 1389-98.

(103) Yu, H., Chen, X., Lu, T., Sun, J., Tian, H., Hu, J., Wang, Y., Zhang, P., and Jing, X. (2007) Poly(l-lysine)-Graft-Chitosan Copolymers: Synthesis, Characterization, and Gene Transfection Effect. *Biomacromolecules 8*, 1425-1435.

(104) Kotze, A. F., Luessen, H. L., de Leeuw, B. J., de Boer, B. G., Verhoef, J. C., and Junginger, H. E. (1997) N-trimethyl chitosan chloride as a potential absorption enhancer across mucosal surfaces: in vitro evaluation in intestinal epithelial cells (Caco-2). *Pharm Res 14*, 1197-202.

(105) Thanou, M., Florea, B. I., Langemeyer, M. W., Verhoef, J. C., and Junginger, H. E. (2000) N-trimethylated chitosan chloride (TMC) improves the intestinal permeation of the peptide drug buserelin in vitro (Caco-2 cells) and in vivo (rats). *Pharm Res 17*, 27-31.

(106) Thanou, M., Florea, B. I., Geldof, M., Junginger, H. E., and Borchard, G. (2002) Quaternized chitosan oligomers as novel gene delivery vectors in epithelial cell lines. *Biomaterials 23*, 153-9.

(107) Mao, S., Shuai, X., Unger, F., Wittmar, M., Xie, X., and Kissel, T. (2005) Synthesis, characterization and cytotoxicity of poly(ethylene glycol)-graft-trimethyl chitosan block copolymers. *Biomaterials 26*, 6343-56.

2 Trastuzumab-Polyethylenimine-Polyethyleneglycol Conjugates for Targeting HER2 Expressing Tumors

Published in Bioconjugate Chemistry 17 (2006) 1190-1199

2.1 Abstract

In this study we describe the synthesis and characterization of a conjugate consisting of poly(ethylene glycol 2000 Da)$_{10}$-graft-poly(ethylene imine 25 kDa) (PEG-PEI) covalently coupled to Trastuzumab (Herceptin®) via N-succinimidyl-3-(2-pyridyldithio)propionate (SPDP) for specific gene delivery to Her2 expressing cell lines. The efficiency of DNA condensation was studied using an ethidium bromide exclusion assay and demonstrated negligible differences compared to PEG-PEI. Conjugate complex sizes were determined by dynamic light scattering to be in a range of 130-180 nm. Zeta potentials at different N/P ratios were close to neutral. Flow cytometry and confocal microscopy revealed efficient binding and uptake of Trastuzumab-PEI-PEG complexes using Her2 positive SK-BR-3 cells. In contrast, binding and uptake into Her2 negative OVCAR-3 cells was negligible. In good correlation with these findings, reporter gene expression using targeted complexes in SK-BR-3 cells was up to 7-fold higher than that of unmodified PEG-PEI complexes. Using OVCAR-3 cells no significant difference in expression efficiencies could be observed between conjugate and PEG-PEI complexes. Inhibition experiments with free Trastuzumab showed a significant decrease in reporter gene expression using SK-BR-3 cells but no decrease using OVCAR-3 cells, strongly supporting a specific Her2-receptor mediated uptake mechanism. Our results suggest that Trastuzumab-PEI-PEG might be a promising new bioconjugate for targeted gene transfer to Her2 positive tumor cells in vivo.

2.2 Introduction

An ideal vector system for gene delivery under *in vivo* conditions needs to meet certain requirements: it should *efficiently* deliver genes to *specific target tissues* with *minimal toxicity* and *immunogenicity*.

Viral vectors are still the most efficient gene delivery systems, but some serious drawbacks such as immune and/or toxic reactions, oncogeniticity and potential virus recombination limit their application (*1, 2*).

Therefore, non-viral vectors may become a promising alternative. Among a multitude of non-viral vectors, poly(ethylene imine) (PEI) gained specific attraction, since it facilitates endosomal release and mediates efficient transfection without the use of endosomolytic reagents by the so-called proton-sponge effect (*3-5*). A major disadvantage of PEI-DNA polyplexes is their positive surface charge, leading to undesired interactions with non-targeted cells, blood components or vessel endothelia (*6, 7*). These interactions not only decrease polyplex blood half-life by fast opsonization and entrapment in fine capillaries, but they also decrease tumor specificity by accumulation of polyplexes in liver, lung and spleen. Furthermore, biocompatibility and toxicity are major problems strongly related to these polyplex characteristics. Therefore, an important goal in developing polycation-based non-viral vectors is the design of polyplexes with decreased tendencies toward aggregation and unspecific adhesion under in vivo conditions.

To improve the aforementioned characteristics, our group (*7, 8*) and others (*9, 10*) have synthesized different poly(ethylene glycol)-grafted PEIs (PEG-PEI) and studied the biophysical and biological properties of the resulting complexes with DNA. Great emphasis was put on defining structure-function relationships between PEI chain length, the degree of substitution, and the MW of PEG chains for optimal complexation and shielding capacities. This research resulted in PEG-graft-bPEI copolymers, which showed good transfection results combined with low cytotoxicity (*7*). Furthermore, some of the resulting polyplexes showed encouraging results in pharmacokinetic studies in mice (*8*). Nevertheless, polymer composition, DNA dose and experimental design strongly influence the outcome of such pharmacokinetic studies as shown by Merdan and coworkers (*11*) and more detailed studies will be needed.

Especially for tumor gene therapy, vectors are desired that show a high specificity for tumor cells while leaving normal cells unaffected. This would offer the possibility of applying high doses of gene constructs with minimal side effects. Several studies described specific ligand-mediated gene transfer using non-viral vectors, e.g. by transferrin (*12, 13*), folate (*14, 15*) saccharides (*9, 16, 17*) or by antibodies or antibody fragments such as anti-CD3 (*13, 18*), anti-PECAM (*19*), anti-OA3 (*20*), anti-GAD (*21*) or anti-PSMA antibodies (*22*). The coupling of antibodies is an advantageous strategy for targeted delivery due to their versatility, the highly specific binding to target cells and, if an appropriate target was chosen, subsequent uptake by receptor mediated endocytosis.

Trastuzumab, a monoclonal antibody directed against the Her2 epitope, offers the possibility of specific targeting of various cancers, such as breast, lung, ovarian and prostate cancers (*23-26*). In normal tissues Her2 is only expressed in low levels and only in certain epithelial cell types (*27*). Upon ligand binding it is fully internalized, which is mimicked by Trastuzumab (*28*). Anti-Her2 antibodies were already successfully used for targeted drug delivery employing immunoliposomes (*29*) or immunoconjugates with different chemo- or radiotherapeutics (*26, 30-32*), in virus-like particles for gene delivery (*33*), and most recently, as targeting moieties coupled to linear (*34*) and branched PEI (*35*).

In these studies, Trastuzumab was coupled with different linkers to unmodified PEI and revealed varying specificity and efficiency depending on the linker chemistry used the degree of substitution, and the N/P ratio. One major drawback in both studies was the use of unmodified linear or branched PEI with the aforementioned disadvantages.

Our aim in this study was the design of a Her2 targeted non-viral vector potentially applicable for in vivo gene therapy. As described above, unmodified branched as well as linear PEIs are not suitable due to their tendency toward aggregation, unspecificity and toxicity. We therefore used PEG grafted branched PEI and modified this copolymer with Trastuzumab using SPDP as a linker. Complexes were characterized by photon correlation spectroscopy (PCS), laser doppler anemometry (LDA), ethidium bromide exclusion and atomic force microscopy (AFM). We studied Her2 expression levels of SK-BR-3 and OVCAR-3 cells using flow cytometry and correlated the findings to the binding, uptake and reporter gene expression of targeted and non-targeted complexes *in vitro*.

Results were verified by competitive inhibition with free Trastuzumab, underlining the receptor dependent manner of uptake and gene expression.

2.3 Materials and Methods

Chemicals and Plasmid. Branched PEI 25 kDa (Polymin, 99% water free) was a kind gift of BASF AG, Ludwigshafen, Germany. Salmon testes DNA and N-succinimidyl-3-(2-pyridyldithio)propionate (SPDP) were purchased from Sigma-Aldrich, Taufkirchen, Germany. Luciferase plasmid (pCMV-Luc) was purchased from the Plasmid Factory, Bielefeld, Germany. Trastuzumab (Herceptin®) was purchased from Roche, Basel, Switzerland. All other chemicals were obtained from Merck, Darmstadt, Germany if not otherwise indicated.

Cell Culture. SK-BR-3 and OVCAR-3 cells were purchased from ATCC, Teddington, UK and maintained in RPMI 1640 (PAA Laboratories, Cölbe, Germany) supplemented with 10% and 20% fetal calf serum (Cytogen, Sinn, Germany), respectively, in humidified atmosphere with 5% CO_2 at 37°C.

Synthesis of PEG-PEI and Trastuzumab-PEG-PEI Conjugates. Poly(ethylene glycol 2000 Da)$_{10}$-graft-poly(ethylene imine 25 kDa) (abbreviated as PEG-PEI) was synthesized and characterized as described previously (*7*). For the synthesis of conjugates, 5 mg of PEG-PEI (equivalent to 2.8 mg of PEI) was dissolved in 1 mL reaction buffer (150 mM sodium chloride; 20 mM 4-(2-hydroxyethyl)-1-piperazine ethane sulfonic acid (HEPES); pH 7.5). 20 µL of a 10 mM solution of SPDP in 100% ethanol were added while stirring and allowed to react for 60 min at room temperature. Purification of the product was performed by gel filtration on a PD-10 column (Amersham Pharmacia Biotech, Freiburg, Germany) in reaction buffer. SPDP-activated PEG-PEI was reduced using 13 µmol Dithiothreitol (DTT) in 500 µL reaction buffer for 1 h at 37°C.

Twenty mg Trastuzumab in reaction buffer were allowed to react with 24 µL of SPDP solution (10 mM in pure ethanol) under stirring at room temperature and were purified according to the procedure described above. SPDP-activated Trastuzumab was added to PEG-PEI-thiopropionate and allowed to react for 24 h at room temperature. Purification of the conjugate was performed by a modified ion exchange chromatography method described by Kircheis et al. (*18*). Briefly, the solvent of the reaction solution was ex-

changed with 150 mM NaCl, 10 mM HEPES pH 7.4 (buffer A) and the solution was applied on two serial HiTrap SP Sepharose HP columns (1 mL column volume, flow rate 1 mL/min, ÄKTAprime System, Amersham Pharmacia Biotech, Freiburg, Germany). After elution of unbound antibody with buffer A, the solvent was changed to 3 M NaCl, 10 mM HEPES pH 7.4 (buffer B) stepwise and the conjugate was eluted. The solvent was changed to 150 mM NaCl solution pH 7.4 in a further gel filtration step and PEI was quantified by copper complexation (*36*). The amount of antibody was determined by UV-spectrometry with background correction using a solution of PEG-PEI of equal concentration with Warburg's formula,

$$c(mg/mL) = 1.55 \times (A_{280} - A_{320}) - 0.76 \times (A_{260} - A_{320})$$

where c is protein concentration in mg/mL calculated with the absorbance at the wavelengths indicated.

Preparation of Polyplexes. Luciferase plasmid and the appropriate amount of polymer were prepared in equal volumes of 150 mM NaCl, pH 7.4. Complexes were formed by adding pCMV-Luc solution to polymer solution followed by intensive mixing. Complexes were allowed to incubate at room temperature for 10 min before use.

Ethidium Bromide Exclusion Assay. DNA condensation was measured by quenching of ethidium bromide as described earlier (*37*). Briefly, 8 µg of salmon testes DNA dissolved in 79 µL water and 50 µL of 60 mM Tris buffer pH 7.4 were added to each well of a 96 well plate. Water was added to give a final volume of 300 µL per well. Subsequently, appropriate volumes of 0.05 mg/mL polymer solutions were added to produce N/P ratios between 0.2 and 4. After a 10 min incubation, 20 µL of a 0.1 mg/mL ethidium bromide solution were added. Solutions were mixed intensively and fluorescence was measured using a fluorescence plate reader (LS 50 B, Perkin Elmer, Rodgau-Jügesheim, Germany) at 518 nm excitation and 605 nm emission wavelengths. Results are given as the mean of triplicate measurements ± standard deviation and as relative fluorescence values, where 100 is the fluorescence of DNA without polycation and 0 is the remaining fluorescence of non-intercalating ethidium bromide.

Photon Correlation Spectroscopy and Zeta Potential Measurements. Hydrodynamic diameters and zeta potentials were determined in a 150 mM NaCl solution employing a

Zetasizer 3000 HS (Malvern Instruments, Herrenberg, Germany; 10 mW HeNe laser, 633 nm) as described previously (*17*). In the PCS measurements, scattered light was detected at a 90° angle through a 400 micron pinhole at a temperature of 25°C. The viscosity (0.88 mPa s) and refractive index (1.33) of distilled water at 25°C was used for data analysis. The accuracy of size measurements was routinely checked using reference polymer particles (Nanosphere Size Standards, 50, 100 and 200 nm, Duke Scientific Corp., Palo Alto, CA, USA). Data were analyzed using the CONTIN algorithm. Determination of the zeta potential of complexes was carried out using the standard electrophoresis cell of the Zetasizer 3000 HS at position 17.0 at 25 °C. Sampling time was set to automatic. 4 µg of luciferase plasmid in 200 µL 150 mM NaCl, pH 7.4, were complexed with the appropriate amount of polymer in the same volume. The accuracy of the instrument was checked with Zeta Potential Transfer Standard (Malvern Instruments, Herrenberg, Germany). Values given are the mean of 5 measurements of the same sample ± standard deviation.

Atomic Force Microscopy. Size and surface morphology of polyplexes was analyzed by atomic force microscopy. Complexes of pCMV-Luc and PEG-PEI or conjugate were prepared as described above immediately after synthesis at an N/P ratio of 3.5. Silicon chips were used as sample support. The chips were incubated with complex suspension for 10 min before drying in a stream of dry nitrogen gas. Samples were investigated within 2 hours of preparation. Microscopy was performed on a vibration and acoustic damped Nanoscope IV Bioscope (Veeco Instruments, Santa Barbara, USA). Commercial pyramidal Si3N4 tips (NCH-W, Veeco Instruments, Santa Barbara, USA) on an I-type cantilever with a length of 125 µm, a resonance frequency of about 220 kHz, and a nominal force constant of 36 N/m were used. All measurements were performed in tapping mode to avoid damage to the sample surface. The scan speed was proportional to the scan size. The scan frequency was between 0.5 and 1.5 Hz. Heights and phase images were recorded simultaneously.

Flow cytometry. For flow cytometry experiments, cells were seeded in 6 well plates at a density of 400,000 cells per well and grown for 24 hours. For HER2 expression experiments cells were detached with trypsin, washed twice with 500 µL PBS at 4°C and cell density was adjusted to 600,000 cells per mL. Cell suspensions were mixed with Trastuzumab solution to give concentrations of 500 µg/mL and 1000 µg/mL Trastuzu-

mab, respectively, and incubated for 15 min at 4°C. After three washings with cold PBS, cells were incubated with 5 µg/mL FITC-goat anti-human antibody (Sigma-Aldrich, Steinheim, Germany) at 4°C for 15 min. After three washings with cold PBS, cells were suspended in 1 ml FACS Flow (BD Biosciences, San Jose, USA) containing 4% paraformaldehyde and stored on ice until analysis.

For polyplex binding experiments, pCMV-Luc was labeled with YOYO-1 (Molecular Probes, Eugene, USA) as described elsewhere (*38*). Cells were incubated for 15 min at 4°C with polyplexes prepared with 10 µg of YOYO-1 labeled pCMV-Luc and the appropriate amount of either PEG-PEI-Trastuzumab or PEG-PEI to obtain an N/P ratio of 3.5. Cells were subsequently washed three times with ice-cold PBS, suspended in 1 ml FACS Flow containing 4% paraformaldehyde and stored on ice until analysis.

Flow cytometry was performed using a FACScan (BD Biosciences, San Jose, USA) equipped with a 488 nm argon-ion laser. The emission filter setting was 530/30 band-pass (FL1). First, forward and sideward scatter sensitivity was adjusted so that all signals were within detection limits. The amplification of fluorescence signals was set to mean fluorescence values of approximately $0.5x10^1$ for untreated cells and settings were kept constant throughout the measurement. Ten thousand events were measured in each sample. Viable cells were gated according to untreated cell samples and only cells within this gate were subjected to further analysis. Data thus obtained were then normalized to the untreated cells. CellQuest 3.3 software (BD Biosciences, San Jose, USA) was used for data acquisition. Data analysis was performed with FCS Express V3 (De Novo Software, Thornhill, Canada).

Confocal laser scanning microscopy. Cells were incubated with either conjugate or PEG-PEI complexes prepared with 1.66 µg YOYO-1 labeled DNA (see flow cytometry) and the appropriate amount of polymer to obtain N/P 3.5 for 20 min at 4°C and for 2 h at 37°C, respectively. Afterwards, cells were washed 3 times with PBS, fixed with 4% paraformaldehyde in PBS for 20 min and subsequently incubated for 20 min with DAPI solution (0,18 µg/mL in PBS) at room temperature. Cells were washed again 3 times, embedded with FluorSave Reagent (Calbiochem, San Diego, USA) and kept on ice until analysis.

A Zeiss Axiovert 100 M microscope coupled to a Zeiss LSM 510 scanning device (Zeiss, Oberkochen, Germany) was used for confocal microscopy. For excitation of YOYO-1 fluorescence an argon laser with an excitation wavelength of 488 nm was used. Fluorescence emission was detected using a 505 nm long-pass filter. Transmission images were obtained in the same scan. In a second scan DAPI was detected using a Coherent Enterprise II 653 laser (Coherent Inc., Santa Clara, USA) with an excitation wavelength of 351 nm and a 385-470 nm band-pass emission filter.

Transfection experiments. Complexes for transfection experiments were prepared using 4 µg of luciferase plasmid per well in 100 µL 150 mM NaCl pH 7.4 and the appropriate amount of polymer in 100 µL of the same solution. Transfection experiments were carried out using PEI, PEG-PEI and conjugated PEG-PEI at N/P ratios of 2.5, 3.5, 7, and 10. SK-BR-3 and OVCAR-3 cells were seeded in 12 well plates at a density of 80,000 cells per well. After 24 h of growth, medium was removed and complexes were added to 1.5 mL fresh medium. For inhibition experiments, 1, 10, or 100 µg/mL of free Trastuzumab was added to fresh media 20 min before addition of the complexes. Medium was changed again after 4 h and the cells were incubated for an additional 44 h.

Luciferase gene expression was quantified using a commercial kit (Promega, Mannheim, Germany) and photon counting on a luminometer (Sirius, Berthold, Pforzheim, Germany). Results were measured in relative light units per second (RLU/s) and afterwards converted to nanograms of luciferase using a standard curve of recombinant luciferase (Promega, Mannheim, Germany). Protein concentration was determined using a modified BCA assay (Perbio Science, Bonn, Germany) with bovine serum albumin as a standard (*39*). All experiments were performed in triplicate and results are expressed as nanograms of luciferase per milligrams of protein.

Statistical analysis. Statistical significance of differences was evaluated by either two-tailed unpaired Student t-test or one-way ANOVA with Dunnett's post test. Level of significance is indicated with a single asterisk if $p \leq 0.05$, two asterisks if $p \leq 0.01$ and three asterisk if $p \leq 0.001$.

2.4 Results

Synthesis of PEG-PEI and PEG-PEI-Trastuzumab. Synthesis resulted in a copolymer consisting of 10 PEG chains of 2 kDa grafted onto a chain of branched PEI with a molecular weight of 25 kDa. Copolymer composition was determined by ^{1}H NMR and FT-IR spectroscopy (*7*).

Purification of PEG-PEI-Trastuzumab by ion exchange chromatography displayed one peak of free unconjugated antibody at low ionic strength conditions. When low ionic buffer A was stepwise substituted with high-ionic buffer B, a second peak was found containing the conjugate. The elution volumes of free antibody and PEG-PEI-Trastuzumab were comparable to those of a blend of Trastuzumab and PEG-PEI. Under the chosen experimental conditions the SPDP linker strategy led to conjugation of Trastuzumab to PEG-PEI with a PEI to antibody ratio of 1:0.2. Variations of Trastuzumab and PEG-PEI amounts as well as SPDP concentrations and reaction times did not increase the conjugation degree.

Ethidium bromide exclusion assay. To probe whether DNA condensation properties were altered by antibody conjugation we performed an ethidium bromide exclusion assay.

Free ethidium bromide shows only weak fluorescence, but its fluorescence is strongly increased when it intercalates into DNA. Condensation of DNA by PEI and other cationic polymers decreases fluorescence by inhibiting this intercalation.

The ethidium bromide exclusion assay with PEG-PEI-Trastuzumab showed only minor differences in shape and position of the curve compared to unmodified PEG-PEI (Figure 1), suggesting no inhibitory effect of antibody-modification to DNA condensation capacity. We assume that PEI and some PEG chains form a core, which is responsible for efficient complexation of DNA, while most of the hydrophilic PEG chains as well as coupled antibody form a shell structure. This accounts for efficient shielding and presentation of the targeting moiety combined with effective complexation of DNA. These findings are in line with results obtained with Fab'-PEI-PEG conjugates (*20*). N/P ratios higher than 4 were not investigated since DNA condensation was almost complete at this point.

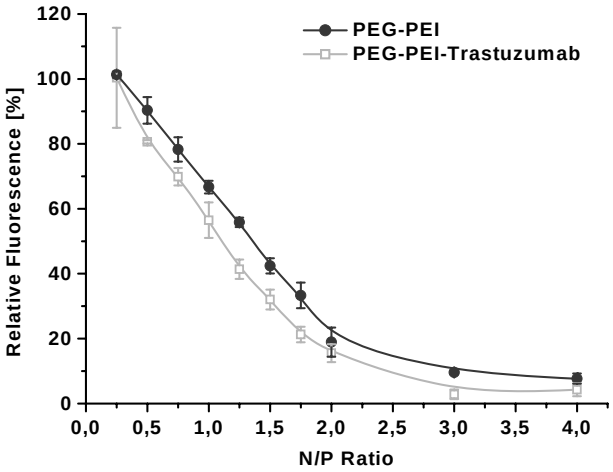

Figure 1. Ethidium bromide exclusion assay comparing unmodified PEG-PEI and PEG-PEI-Trastuzumab. Only minor differences in complexation efficiency were found after conjugation of Trastuzumab.

Hydrodynamic diameter and zeta potential. Hydrodynamic diameters of PEG-PEI-Trastuzumab and PEG-PEI complexes were determined at different N/P ratios using photon correlation spectroscopy (Figure 2). The hydrodynamic diameter decreased with increasing N/P ratio for both targeted and non-targeted complexes. Complex sizes were 237.8 ± 6.1 nm or 181.0 ± 3.8 nm at N/P 2.5 and 165.7 ± 3.2 nm or 128.1 ± 8.2 nm at N/P 10 for PEG-PEI and PEG-PEI-Trastuzumab complexes, respectively. Conjugate complex sizes were significantly smaller than those of PEG-PEI complexes (except at an N/P ratio of 7). Complex sizes of 200 nm and less are favorable for endocytosis (*40*), the proposed route of cell entry for PEI/pDNA complexes (*41, 42*). Therefore, all complexes at N/P 3.5 and higher may be taken up via endocytosis.

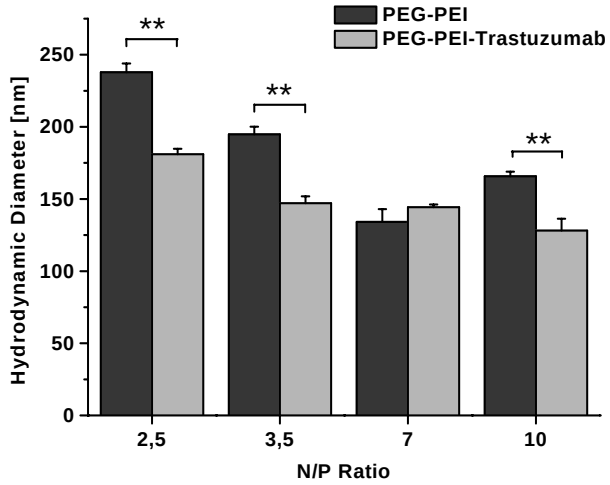

Figure 2. Comparison of hydrodynamic diameters of complexes of PEG-PEI and PEG-PEI-Trastuzumab at different N/P ratios. The PEG-PEI-Trastuzumab complexes are significantly smaller (except N/P 7) than the unmodified PEG-PEI complexes.

Zeta potential measurements revealed nearly neutral complex charges for PEG-PEI-Trastuzumab (maximum of + 5 mV at N/P 3.5) and for PEG-PEI (maximum of + 5 mV at N/P 3.5 and 10) complexes (Figure 3), which are in good correlation with earlier observations with this type of PEG-PEI copolymer (*7, 8, 20*).

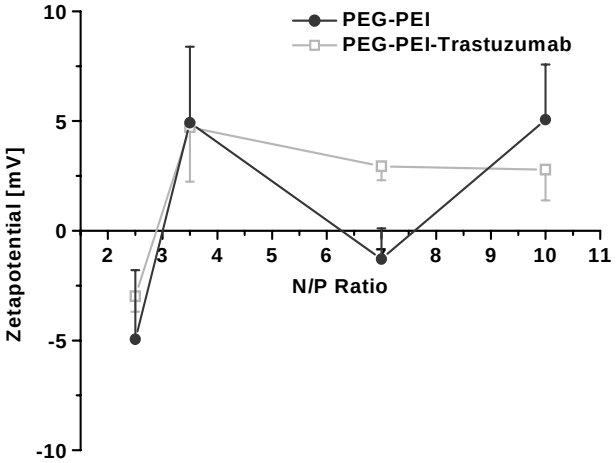

Figure 3. Zeta potential values of PEG-PEI and PEG-PEI-Trastuzumab complexes at different N/P ratios. Slightly negative zeta potential values at N/P 2.5 are due to inefficient complexation of DNA. Overall zeta potential range is -5 to +5 mV, indicating nearly neutral surface charges for all complexes at each N/P ratio tested.

Atomic Force Microscopy. Complexes were imaged using atomic force microscopy with the aim to visualize fine-structural differences in PEG-PEI-Trastuzumab vs. PEG-PEI complexes. The extraordinary high resolution of atomic force microscopy enables the visualization of structures down to the level of antibodies or even DNA strands. In these experiments an N/P ratio of 3.5 was chosen to represent characteristics of complexes used for flow cytometry, confocal microscopy and transfection studies.

PEG-PEI/pDNA complexes depicted in Figure 4 A were of spherical shape with smooth surfaces and nearly homogeneous but fairly soft material characteristics. Mean particles sizes were determined to be 152.2 ± 5.8 nm. The decrease in particle sizes compared to PCS measurements can be explained by sample preparation: Samples were measured in semi-dry state in the case of AFM measurements and dispersed in sodium chloride solution in the case of PCS measurements.

In contrast, complexes of PEG-PEI-Trastuzumab were significantly smaller (Figure 4 B). The mean diameter was determined to be 85.2 ± 4.2 nm. Again complex size was significantly decreased compared to PCS measurements due to different experimental conditions. The complex surface was not as smooth as and even softer than that of PEG-PEI complexes. A small fraction of particles with sizes of about 10-20 nm was seen on and in proximity to the complexes in the case of PEG-PEI-Trastuzumab (see arrows in 4 B). The mean diameter of these particles was determined to be 18.6 nm. In a second experiment, the size of free Trastuzumab antibodies was determined under the same experimental conditions to be between 10 and 20 nm (Figure 4 C). A recently published study by Thomson supports our results on sizes of IgG molecules (*43*). In this study, measurements of IgG sizes under comparable experimental conditions revealed diameters of approximately 9 nm for molecules in “angled” position and approximately 20 nm for the “flat” orientation. We therefore conclude that the small particles found exclusively in PEG-PEI-Trastuzumab samples represent successfully coupled Trastuzumab antibodies. Hence, the presentation of targeting moieties on the complex surface can be directly verified by this method.

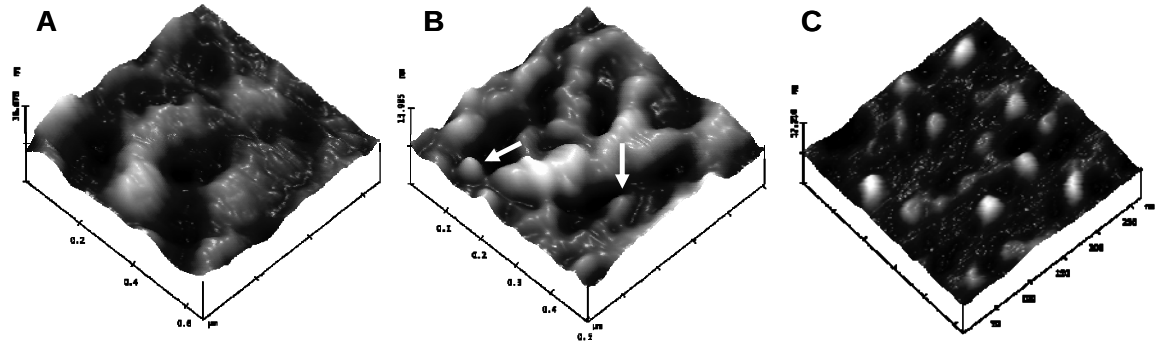

Figure 4. Atomic force micrographs of PEG-PEI/pDNA (A) and PEG-PEI-Trastuzumab/pDNA complexes (B) at N/P 3.5. Free antibody was visualized under the same experimental conditions (C). Arrows in B depict coupled Trastuzumab antibodies.

Flow cytometry. Cell membrane adhesion of complexes at 4°C was tested using flow cytometry. These data were then correlated to the binding of pure Trastuzumab to the corresponding cell line. For complex adhesion experiments, plasmid DNA was labeled using the intercalating dye YOYO-1. Unconjugated and Trastuzumab-conjugated PEG-PEI was then used to prepare complexes with labeled DNA at an N/P ratio of 3.5. After incubation at 4°C, cell-associated fluorescence was quantified.

In the case of Trastuzumab binding studies, Trastuzumab was incubated with the cells and subsequently labeled using a secondary FITC-anti-human antibody. Cell-associated FITC fluorescence was then measured by flow cytometry as well.

OVCAR-3 cells were used as a negative control. Her2 expression was found to be very low using the immunoconjugate of Trastuzumab and FITC-anti-human antibody (Figure 5 A II). When the immunoconjugate was used, the mean fluorescence increased only 4.7-fold compared to unspecific binding of FITC secondary antibody alone. With increasing amounts of Trastuzumab, the mean fluorescence showed no further increase, indicating saturation of receptors at the lowest concentration used (data not shown). These findings are consistent with low receptor expression levels in OVCAR-3 cells determined by Western blotting (*44*).

SK-BR-3 cells are reported to over-express the Her2 antigen (*45*). Fluorescence increased 36-fold using 0.5 mg/mL Trastuzumab subsequently labeled with FITC secondary antibody compared to FITC labeled secondary antibody alone (Figure 5 B II). A

two-fold increase of Trastuzumab concentration resulted in a 1.6-fold increase of relative fluorescence, indicating that in the case of the lower Trastuzumab concentration, a certain number of Her2 receptors were still unsaturated (data not shown).

Unconjugated complexes showed moderate binding to OVCAR-3 cells with a mean fluorescence intensity of 13.28. Using PEG-PEI-Trastuzumab/pDNA complexes, cell adhesion decreased remarkably. The mean fluorescence value was only 8.82 in this case (Figure 5 A I).

Unspecific binding of unconjugated PEG-PEI to Her2 positive SK-BR-3 cells produced a mean fluorescence intensity of 20.25. In contrast, cell associated fluorescence increased 2.4-fold using PEG-PEI-Trastuzumab (mean fluorescence 49.58, Figure 5 B I).

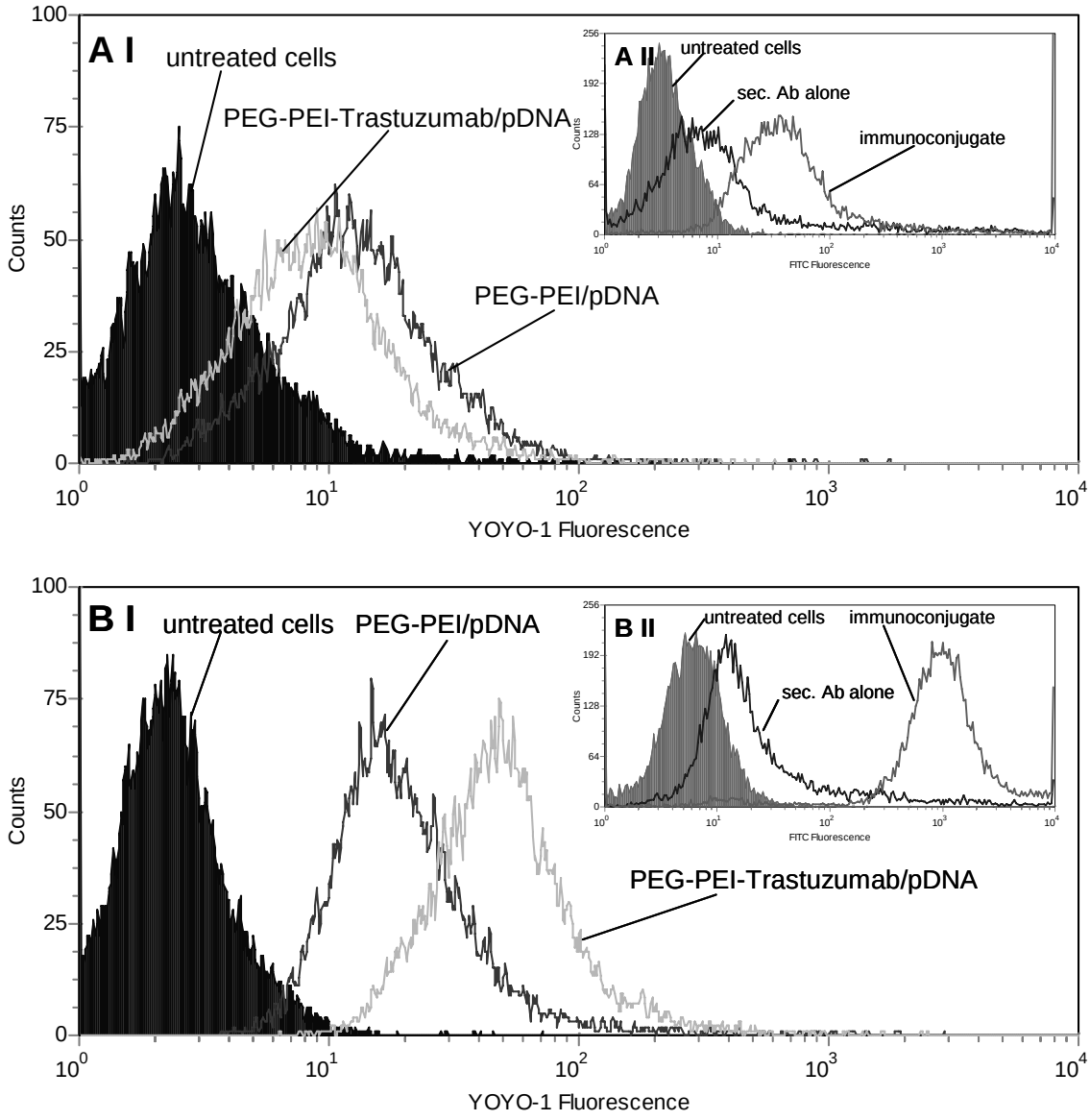

Figure 5. Flow cytometry using OVCAR-3 (A) and SK-BR-3 (B) cells. Cell surface adhesion of targeted and non-targeted PEG-PEI/YOYO-1-pDNA complexes at 4°C were compared in OVCAR-3 and SK-BR-3 cells (A I and B I). These data can be correlated to Her2 expression levels in these cell lines tested by incubation with Trastuzumab at 4°C and subsequent labeling with FITC-anti-human antibody (A II and B II).

Confocal Laser Scanning Microscopy. Uptake of the complexes was studied by confocal microscopy. SK-BR-3 and OVCAR-3 cells were incubated for 20 min or 2 hours at 37°C with complexes composed of either unconjugated or Trastuzumab-conjugated PEG-PEI and YOYO-1 labeled plasmid DNA.

After incubating for 20 min, binding to the cell membrane occurred in both cell lines for unconjugated PEG-PEI while a specific binding was observed only with SK-BR-3 cells if PEG-PEI-Trastuzumab was used (Data not shown).

A similar phenomenon was found when polyplexes were incubated with the cells for 2 hours at 37°C. Comparable cell uptake occurred within this timeframe for both OVCAR-3 and SK-BR-3 cells using PEG-PEI/pDNA complexes (Figure 6 A II and B II). Using PEG-PEI-Trastuzumab/pDNA, only very little intracellular fluorescence was found for OVCAR-3 cells (Figure 6 A I). In contrast, PEG-PEI-Trastuzumab complexes were readily taken up into SK-BR-3 cells (Figure 6 B I).

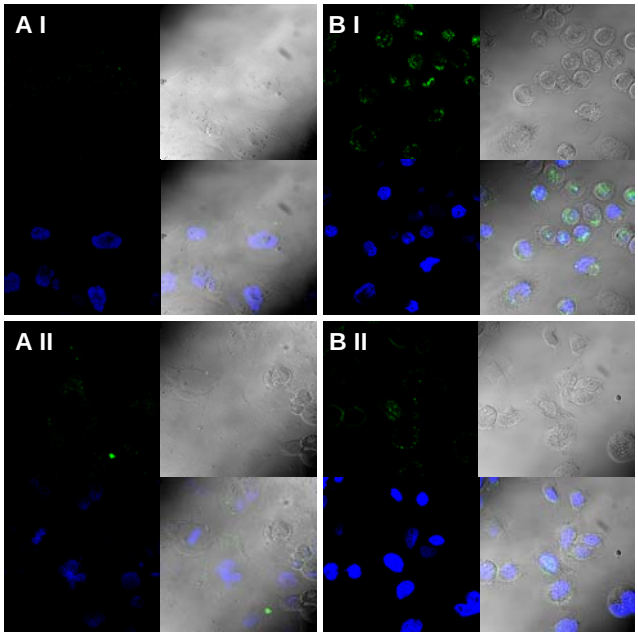

Figure 6. Confocal microscopy images of OVCAR-3 (A) and SK-BR-3 (B) cells. Cells were incubated with PEG-PEI-Trastuzumab/YOYO-1-pDNA (I) or PEG-PEI/YOYO-1-pDNA (II) complexes for 2 hours at 37°C. Upper left: YOYO-1 fluorescence (complexes), upper right: phase contrast transmitted light image, lower left: DAPI fluorescence (cell nuclei), lower right: merge of all channels.

Transfection experiments. The aim of these experiments was to correlate receptor expression levels, binding, and internalization properties with transfection efficiency *in vitro* and to verify the receptor-dependent manner of uptake by competitive inhibition with free Trastuzumab in culture media. As a control, pure plasmid DNA was used for transfection in both cell lines. Luciferase expression levels were not significantly differ-

ent from untreated cells in this case. Unmodified PEI 25 kDa, an efficient transfection reagent under *in vitro* conditions, was used as a positive control in these experiments. As anticipated, complexes of unmodified PEI 25 kDa and pDNA at an N/P ratio of 3.5 showed comparably high transfection efficiencies of 1.1 and 7.0 ng luciferase per mg protein in SK-BR-3 and OVCAR-3 cells, respectively. However, unmodified PEI is not suitable for in vivo gene delivery due to the earlier mentioned disadvantages and serves as a point of reference.

Transfection efficiencies in SK-BR-3 were determined at four different N/P ratios (Figure 7), showing decreasing differences between conjugate and unmodified PEG-PEI with increasing N/P ratio. The overall transfection efficiency increased for both polymers with increasing N/P ratio. For transfection experiments, an N/P ratio of 3.5 was favorable due to the approximately neutral complex charges and appropriate complex sizes for both polymers at this point.

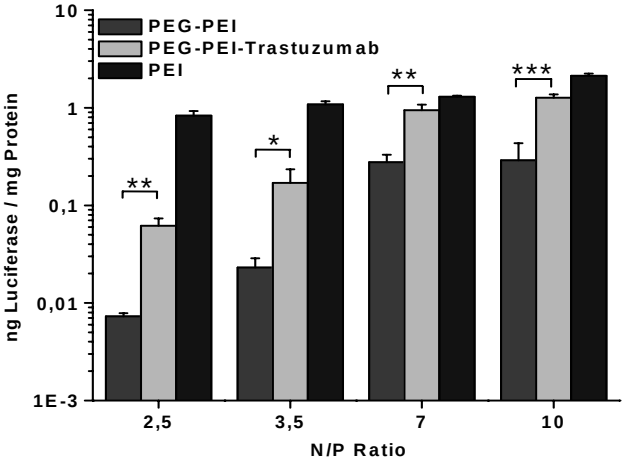

Figure 7. Transfection results using PEG-PEI/pDNA vs. PEG-PEI-Trastuzumab/pDNA complexes at different N/P ratios with SK-BR-3 cells. With increasing N/P ratio transfection efficiency of unconjugated and Trastuzumab-conjugated PEG-PEI complexes increases while differences between transfection efficiency of both complexes decrease. Transfection efficiencies of unmodified PEI 25 kDa are shown for comparison.

Using OVCAR-3 cells, no significant increase in transfection efficiency could be detected with Trastuzumab-conjugate compared to unmodified PEG-PEI and no significant inhibition with free Trastuzumab was possible (Figure 8), which is in excellent agreement with the flow cytometry and confocal microscopy results.

Transfection experiments using SK-BR-3 showed up to seven-fold higher luciferase expression with Trastuzumab-PEG-PEI compared to PEG-PEI at N/P 3.5. Reporter gene expression was in this case significantly inhibited by increasing Trastuzumab concentrations. At 10 and 100 µg/mL Trastuzumab, transfection efficiencies decreased to values that were not significantly different from those of the non-targeted complexes (Figure 8).

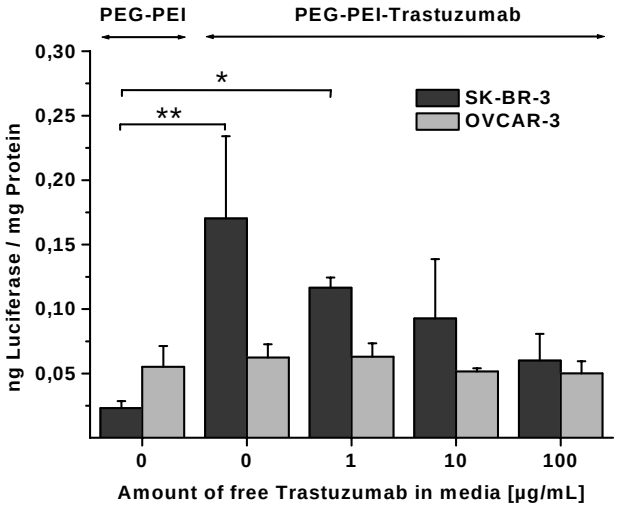

Figure 8. Reporter gene expression using PEG-PEI/pDNA vs. PEG-PEI-Trastuzumab/pDNA complexes at N/P 3.5 in SK-BR-3 and OVCAR-3 cells. In the presence of free Trastuzumab in culture media, transfection efficiency is significantly decreased using SK-BR-3 cells but not in the case of OVCAR-3 cells.

2.5 Discussion

The aim of this study was a detailed physicochemical and biological *in vitro* characterization of an antibody-targeted, surface shielded, PEI-based non-viral vector system for potential *in vivo* application. Previous investigations with pegylated PEIs showed efficient complexation of plasmid DNA combined with suitable complex sizes and a neutral zeta potential (*7*). If these copolymers are modified with targeting moieties such as antibodies, non-specific interactions are minimized and transfection efficiencies in target cells are increased due to specific recognition and subsequent uptake of complexes (*46*). Therefore, PEG-PEIs are favorable for targeted gene delivery *in vivo*.

Recently, Chiu et. al. (*34*) studied conjugates of Trastuzumab with linear PEI (22 kDa). Linear PEI is known to show a high selectivity for the lung if administered systemically (*6, 47*). From this point of view, linear PEI is not the ideal vector system for targeted gene therapy of distant tumors *in vivo*. Chiu et al. used the homo-bifunctional linker Dithio-bis-(succinimidyl propionate) (DSP) to prepare Trastuzumab-conjugated PEI. It was reported that DSP can be used as cross-linking reagent for branched PEI under comparable conditions (*48*). Even by using linear PEI and thereby reducing the amount of reactive amine groups per PEI molecule, intra- and intermolecular cross-linking of PEI cannot be completely ruled out. This may result in an ill-defined complex composition which would not be comparable to linear PEI itself and may lead to significantly altered physicochemical and biological complex properties. Furthermore, the reaction mixture was purified by dialysis, which does not allow separation of conjugate and free antibody. Therefore, in all probability a mixture of L-PEI-Trastuzumab conjugate and free antibody was used by Chiu et al.

Strehblow et al. synthesized conjugates of Trastuzumab and PEI (branched, 25 kDa) using different linker chemistries (*35*). Conjugation of Trastuzumab to PEI via the hetero-bifunctional linker N-succinimidyl-3-(2-pyridyldithio)propionate (SPDP) resulted in non-specific gene expression. The authors suspected that this is due to the blocking of critical amino groups either by the linker or by PEI itself. When Trastuzumab was coupled to PEI by sulfosuccinimidyl 4-(N-maleimidomethyl)cyclohexane-1-carboxylate (SMCC) or 3-(2-(2-(vinylsulfonyl)ethylthio)ethyl)quinazoline-2,4(1H,3H)-dione (IBFB 110001), an effective and specific transfection was reported.

In contrast to the results of Strehblow et al., Kircheis et al. reported successful conjugation of an anti-CD3 antibody to PEI (800 kDa) via SPDP. Using this conjugate, transfection efficiency in CD3 positive Jurkat cells was increased 30-fold, whereas CD3 negative K562 cells showed no increase in transfection efficiency (*18*).

In our study, Trastuzumab was successfully coupled to PEG-PEI via SPDP, enabling specific conjugation without the risk of changing polymer properties by cross-linking. Trastuzumab and PEG-PEI were both activated with SPDP and were then coupled to form PEG-PEI-S-S-Trastuzumab (see Scheme 1).

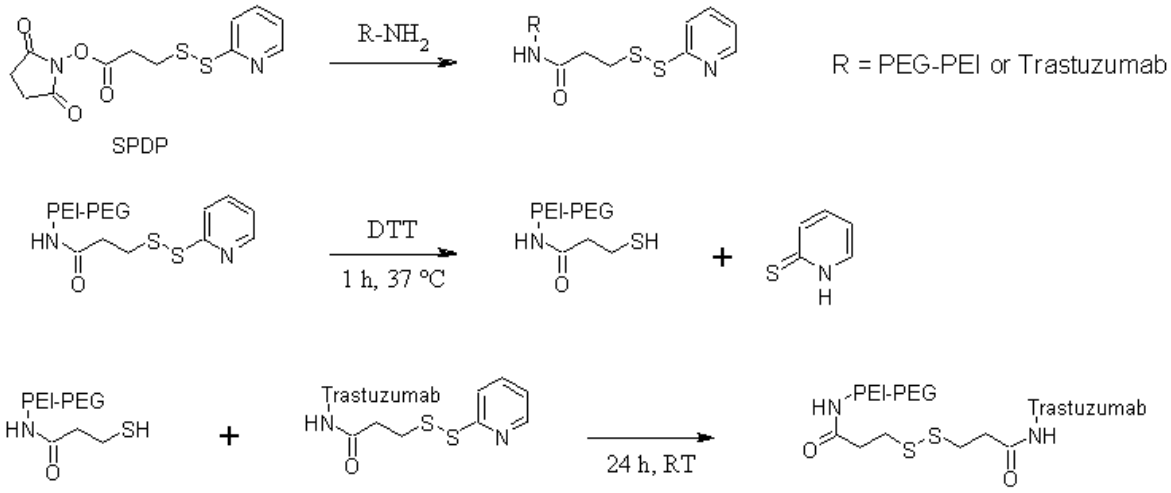

Scheme 1. Synthesis of PEG-PEI-Trastuzumab Conjugate

Apart from a chemically defined polymer composition, our system offers several additional advantages over the Trastuzumab-PEI derivatives mentioned above. Tendency toward aggregation, toxicity, and electrostatic interaction with non-targeted cells are decreased while biocompatibility is increased due to pegylation. On the other hand, endosomal escape and intracellular trafficking of complexes is improved due to potential intracellular cleavability of the disulfide bond between the targeting moiety and the polymer (*48*).

With this conjugation technique, every fifth PEI chain was modified with one Trastuzumab antibody. In contrast, Kircheis et al. report a coupling ratio of about 1:2.8 (PEI:Ab) with PEI 800 kDa (*18*). Coupling efficiencies comparable to PEG-PEI-Trastuzumab conjugates were obtained in a previous study in our laboratory, where conjugation of OV-TL 16 Fab' to PEG-PEI via SPDP resulted in a PEI:Fab' ratio of 1:0.5 (*20*).

Since 31 % of the amino groups of PEI are primary amines (*49*), there is an upper limit for modification with PEG or antibody depending on the molecular weight of PEI, which accounts for reduced degree of antibody modification in our case. Attachment of PEG-chains also increased steric hindrance, so that substitution is also hampered by this effect. Due to the decreased molecular weight of OV-TL 16 Fab' (approximately 50 kDa) compared to Trastuzumab (approximately 150 kDa), reduced steric hindrance may explain the slightly higher conjugation degree in the former case.

Physicochemical properties of the complexes were not significantly influenced by the coupling of Trastuzumab. Complexation efficiencies as well as zeta potential values of the PEG-PEI-Trastuzumab complexes were comparable to PEG-PEI complexes at all N/P ratios tested. Neutral surface charge of complexes is a main prerequisite for *in vivo* applicability. Opsonization, aggregation, and unspecific interactions with blood components, vessel endothelia, and non-targeted cells will be minimized with neutral complexes; therefore, systemic circulation will be prolonged (*8, 12, 50, 51*).

For both PEG-PEI and PEG-PEI-Trastuzumab complexes, the size decreases with increasing N/P ratio due to enhanced complexation of DNA which was shown by the ethidium bromide exclusion experiments. Measurements of hydrodynamic diameters revealed significantly decreased complex sizes of Trastuzumab-conjugate compared to unconjugated complexes (except at N/P ratio 7). This effect may be explained by an increased hydrophilicity of targeted complexes and a decreased interaction between particles due to additional steric shielding by coupled antibody. However, the proposed route of cell entry for these complexes is mainly by clathrin-mediated endocytosis and uptake efficiency may not be significantly affected by particle size as long as complex diameters are within the range of 100-200 nm (*41, 42*).

Detailed analysis of complex shape and surface hardness was performed by atomic force microscopy. AFM measurements of complexes composed of PEI, PEG-PEI or PEG-PEI conjugates and plasmid DNA or oligonucleotides were previously published by several authors (*7, 20, 52, 53*). In all cases, complexes of more or less spherical shape with smooth surfaces were observed. These findings were confirmed for PEG-PEI and PEG-PEI-Trastuzumab complexes in our study. Visualization of coupled antibodies was to the best of our knowledge not previously reported for this type of bioconjugate. Small particles found only in the case of Trastuzumab-PEI-PEG complexes were identified as coupled antibodies by comparing the size and shape of particles to a control sample with pure antibody. A comparable approach was reported by Anabousi et al., who visualized the surface modification of liposomes with transferrin molecules by AFM (*54*). Due to the more rigid and defined shape of liposomes compared to polyplexes, targeting moieties could be visualized more easily in this case. Surface bound water, softness of complexes and possible interactions of antibodies with the polymer impaired a detailed visualization of antibody sub domains as reported in (*43, 55*). How-

ever, AFM measurements verify the presentation of Trastuzumab on the complex surface, which is essential for targeted transfection.

In the next step, specific binding of Trastuzumab-PEI-PEG conjugates was proven by flow cytometry. Receptor expression levels could be directly correlated to the binding of targeted and non-targeted complexes. Even the effect of additional steric shielding by coupled Trastuzumab and therefore decreased binding compared to unmodified complexes was shown in the case of Her2 negative cells. These results are perfectly in line with previously performed flow cytometry experiments with OV-TL 16 Fab'-PEI-PEG conjugates (*20*). Furthermore, confocal laser scanning microscopy showed that the internalization of targeted complexes occurs exclusively in Her2 positive cells. In contrast, uptake of unconjugated complexes was negligible in both Her2 negative and Her2 positive cell lines.

Finally, transfection efficiencies in Her2 positive SK-BR-3 were determined at four different N/P ratios, showing overall increases in transfection efficiencies and decreasing differences between targeted and non-targeted PEG-PEI complexes with increasing N/P ratio. To explain these observations we assume that the conjugate binds to the cell 1) via non-specific interaction of cationic PEI with the cell surface and 2) via specific receptor-mediated interaction. With increasing N/P ratio, the effect of charge mediated binding more and more outweighs the effect of specific binding via antibody-receptor interactions. A comparable effect was observed in different studies in the literature. Conjugation of PEI with anti-PECAM antibody led to efficient transfection of mouse lung endothelial cells, especially at lower N/P ratios (*19*). Targeting of HepG2 cells with galactosylated PEI complexes only showed improved transfection efficiencies for N/P ratios of 3 or lower (*16, 17*). In contrast, no significant difference was found in transfection efficiencies of targeted and non-targeted complexes in Her2 negative cells. Ultimately, inhibition with increasing amounts of free Trastuzumab verified receptor dependent uptake, which matches previous results obtained with different antibodies and antibody fragments (*18, 20, 21, 34, 38*).

Physicochemical and biological properties found in this study give rise to the assumption that this system may be applicable for *in vivo* use. In the next step, the balance between PEG- and Trastuzumab substitution will be optimized to further enhance the tar-

geting effect. Pharmacokinetic, organ distribution, and toxicity studies will then be performed to proceed towards the goal of targeted transfection of tumor tissues *in vivo*.

2.6 Conclusion

We have developed a targeted gene delivery system for highly specific *in vitro* transfection of Her2 positive cell lines which may potentially be applicable for targeted transfection of tumor cells *in vivo*.

Polyplex surface charge was efficiently shielded by modification with PEG and targeting moieties while efficient pDNA complexation was maintained. Hydrodynamic diameters of polyplexes are suitable for possible extravasation and efficient endocytosis. Trastuzumab was shown to be presented on complex surface by AFM and accessibility of antigen-binding domains was verified by flow cytometry and confocal microscopy experiments. Confocal microscopy was also used to demonstrate specific and efficient cellular uptake of targeted complexes. Finally, transfection experiments showed efficient and specific reporter gene expression in Her2 positive cells using targeted complexes. By inhibition with free Trastuzumab, Her2 receptor dependency of reporter gene expression was verified.

2.7 Acknowledgments

We are grateful to Eva Mohr and Nicole Bamberger (Department of Pharmaceutics and Biopharmacy) for their excellent support in cell culture experiments and Dr. Cornelia Brendel (FACS laboratory, Department of Hematology, Oncology and Immunology, University Hospital Marburg) for the generous use of equipment and facilities. We thank Erik Rytting for helpful discussions.

2.8 References

(1) Byrnes, A. P., Rusby, J. E., Wood, M. J., and Charlton, H. M. (1995) Adenovirus gene transfer causes inflammation in the brain. *Neuroscience 66*, 1015-24.

(2) Schreier, H. (1994) The new frontier: gene and oligonucleotide therapy. *Pharm Acta Helv 68*, 145-59.

(3) Behr, J. P. (1997) The proton sponge: A trick to enter cells the viruses did not exploit. *Chimia 51*, 34-36.

(4) Merdan, T., Kunath, K., Fischer, D., Kopecek, J., and Kissel, T. (2002) Intracellular processing of poly(ethylene imine)/ribozyme complexes can be observed in living cells by using confocal laser scanning microscopy and inhibitor experiments. *Pharm Res 19*, 140-6.

(5) Akinc, A., Thomas, M., Klibanov, A. M., and Langer, R. (2005) Exploring polyethylenimine-mediated DNA transfection and the proton sponge hypothesis. *J Gene Med 7*, 657-63.

(6) Chollet, P., Favrot, M. C., Hurbin, A., and Coll, J. L. (2002) Side-effects of a systemic injection of linear polyethylenimine-DNA complexes. *J Gene Med 4*, 84-91.

(7) Petersen, H., Fechner, P. M., Martin, A. L., Kunath, K., Stolnik, S., Roberts, C. J., Fischer, D., Davies, M. C., and Kissel, T. (2002) Polyethylenimine-graft-poly(ethylene glycol) copolymers: influence of copolymer block structure on DNA complexation and biological activities as gene delivery system. *Bioconjug Chem 13*, 845-54.

(8) Kunath, K., von Harpe, A., Petersen, H., Fischer, D., Voigt, K., Kissel, T., and Bickel, U. (2002) The structure of PEG-modified poly(ethylene imines) influences biodistribution and pharmacokinetics of their complexes with NF-kappaB decoy in mice. *Pharm Res 19*, 810-7.

(9) Erbacher, P., Bettinger, T., Belguise-Valladier, P., Zou, S., Coll, J. L., Behr, J. P., and Remy, J. S. (1999) Transfection and physical properties of various saccharide, poly(ethylene glycol), and antibody-derivatized polyethylenimines (PEI). *J Gene Med 1*, 210-22.

(10) Nguyen, H.-K., Lemieux, P., Vinogradov, S. V., Gebhart, C. L., Guérin, N., Paradis, G., Bronich, T. K., Alakhov, V. Y., and Kabanov, A. V. (2000) Evaluation of polyether-polyethyleneimine graft copolymers as gene transfer agents. *Gene Ther. 7*, 126-138.

(11) Merdan, T., Kunath, K., Petersen, H., Bakowsky, U., Voigt, K. H., Kopecek, J., and Kissel, T. (2005) PEGylation of poly(ethylene imine) affects stability of

complexes with plasmid DNA under in vivo conditions in a dose-dependent manner after intravenous injection into mice. *Bioconjug Chem 16*, 785-92.

(12) Kircheis, R., Wightman, L., Schreiber, A., Robitza, B., Rossler, V., Kursa, M., and Wagner, E. (2001) Polyethylenimine/DNA complexes shielded by transferrin target gene expression to tumors after systemic application. *Gene Ther 8*, 28-40.

(13) Buschle, M., Cotten, M., Kirlappos, H., Mechtler, K., Schaffner, G., Zauner, W., Birnstiel, M. L., and Wagner, E. (1995) Receptor-mediated gene transfer into human T lymphocytes via binding of DNA/CD3 antibody particles to the CD3 T cell receptor complex. *Hum Gene Ther 6*, 753-61.

(14) Dauty, E., Remy, J. S., Zuber, G., and Behr, J. P. (2002) Intracellular delivery of nanometric DNA particles via the folate receptor. *Bioconjug Chem 13*, 831-9.

(15) Leamon, C. P., Weigl, D., and Hendren, R. W. (1999) Folate copolymer-mediated transfection of cultured cells. *Bioconjug Chem 10*, 947-57.

(16) Zanta, M. A., Boussif, O., Adib, A., and Behr, J. P. (1997) In vitro gene delivery to hepatocytes with galactosylated polyethylenimine. *Bioconjug Chem 8*, 839-44.

(17) Kunath, K., von Harpe, A., Fischer, D., and Kissel, T. (2003) Galactose-PEI-DNA complexes for targeted gene delivery: degree of substitution affects complex size and transfection efficiency. *J Control Release 88*, 159-72.

(18) Kircheis, R., Kichler, A., Wallner, G., Kursa, M., Ogris, M., Felzmann, T., Buchberger, M., and Wagner, E. (1997) Coupling of cell-binding ligands to polyethylenimine for targeted gene delivery. *Gene Ther 4*, 409-18.

(19) Li, S., Tan, Y., Viroonchatapan, E., Pitt, B. R., and Huang, L. (2000) Targeted gene delivery to pulmonary endothelium by anti-PECAM antibody. *Am J Physiol Lung Cell Mol Physiol 278*, L504-11.

(20) Merdan, T., Callahan, J., Petersen, H., Kunath, K., Bakowsky, U., Kopeckova, P., Kissel, T., and Kopecek, J. (2003) Pegylated polyethylenimine-Fab' antibody fragment conjugates for targeted gene delivery to human ovarian carcinoma cells. *Bioconjug Chem 14*, 989-96.

(21) Jeong, J. H., Lee, M., Kim, W. J., Yockman, J. W., Park, T. G., Kim, Y. H., and Kim, S. W. (2005) Anti-GAD antibody targeted non-viral gene delivery to islet beta cells. *J Control Release 107*, 562-570.

(22) Moffatt, S., Papasakelariou, C., Wiehle, S., and Cristiano, R. (2006) Successful in vivo tumor targeting of prostate-specific membrane antigen with a highly efficient J591/PEI/DNA molecular conjugate. *Gene Ther 13*, 761–772.

(23) Slamon, D. J., Godolphin, W., Jones, L. A., Holt, J. A., Wong, S. G., Keith, D. E., Levin, W. J., Stuart, S. G., Udove, J., and Ullrich, A. (1989) Studies of the HER-2/neu proto-oncogene in human breast and ovarian cancer. *Science 244*, 707-12.

(24) Tripathy, D., and Benz, C. C. (1992) Activated oncogenes and putative tumor suppressor genes involved in human breast cancers. *Cancer Treat Res 63*, 15-60.

(25) Molland, J. G., Barraclough, B. H., Gebski, V., Milliken, J., and Bilous, M. (1996) Prognostic significance of c-erbB-2 oncogene in axillary node-negative breast cancer. *Aust N Z J Surg 66*, 64-70.

(26) Li, Y., Cozzi, P. J., Qu, C. F., Zhang, D. Y., Abbas Rizvi, S. M., Raja, C., and Allen, B. J. (2004) Cytotoxicity of human prostate cancer cell lines in vitro and induction of apoptosis using 213Bi-Herceptin alpha-conjugate. *Cancer Lett 205*, 161-71.

(27) Press, M. F., Cordon-Cardo, C., and Slamon, D. J. (1990) Expression of the HER-2/neu proto-oncogene in normal human adult and fetal tissues. *Oncogene 5*, 953-62.

(28) Harries, M., and Smith, I. (2002) The development and clinical use of trastuzumab (Herceptin). *Endocr Relat Cancer 9*, 75-85.

(29) Park, J. W., Kirpotin, D. B., Hong, K., Shalaby, R., Shao, Y., Nielsen, U. B., Marks, J. D., Papahadjopoulos, D., and Benz, C. C. (2001) Tumor targeting using anti-her2 immunoliposomes. *J Control Release 74*, 95-113.

(30) Gilbert, C. W., McGowan, E. B., Seery, G. B., Black, K. S., and Pegram, M. D. (2003) Targeted prodrug treatment of HER-2-positive breast tumor cells using trastuzumab and paclitaxel linked by A-Z-CINN Linker. *J Exp Ther Oncol 3*, 27-35.

(31) Mandler, R., Wu, C., Sausville, E. A., Roettinger, A. J., Newman, D. J., Ho, D. K., King, C. R., Yang, D., Lippman, M. E., Landolfi, N. F., Dadachova, E., Brechbiel, M. W., and Waldmann, T. A. (2000) Immunoconjugates of geldanamycin and anti-HER2 monoclonal antibodies: antiproliferative activity on human breast carcinoma cell lines. *J Natl Cancer Inst 92*, 1573-81.

(32) Behr, T. M., Behe, M., and Wormann, B. (2001) Trastuzumab and breast cancer. *N Engl J Med 345*, 995-6.

(33) Gleiter, S., and Lilie, H. (2003) Cell-type specific targeting and gene expression using a variant of polyoma VP1 virus-like particles. *Biol Chem 384*, 247-55.

(34) Chiu, S. J., Ueno, N. T., and Lee, R. J. (2004) Tumor-targeted gene delivery via anti-HER2 antibody (trastuzumab, Herceptin(R)) conjugated polyethylenimine. *J Control Release 97*, 357-69.

(35) Strehblow, C., Schuster, M., Moritz, T., Kirch, H. C., Opalka, B., and Petri, J. B. (2005) Monoclonal antibody-polyethyleneimine conjugates targeting Her-2/neu or CD90 allow cell type-specific nonviral gene delivery. *J Control Release 102*, 737-47.

(36) von Harpe, A. (2000) in *Department of Pharmaceutics and Biopharmacy*, Philipps-University, Marburg, Germany.

(37) Petersen, H., Kunath, K., Martin, A. L., Stolnik, S., Roberts, C. J., Davies, M. C., and Kissel, T. (2002) Star-shaped poly(ethylene glycol)-block-polyethylenimine copolymers enhance DNA condensation of low molecular weight polyethylenimines. *Biomacromolecules 3*, 926-36.

(38) Ogris, M., Steinlein, P., Carotta, S., Brunner, S., and Wagner, E. (2001) DNA/polyethylenimine transfection particles: influence of ligands, polymer size, and PEGylation on internalization and gene expression. *AAPS PharmSci 3*, E21.

(39) Hill, H. D., and Straka, J. G. (1988) Protein determination using bicinchonic acid in the presence of sulfhydryl reagents. *Anal Biochem 170*, 203-208.

(40) Mellman, I. (1996) Endocytosis and molecular sorting. *Annu Rev Cell Dev Biol 12*, 575-625.

(41) Grosse, S., Aron, Y., Thevenot, G., Francois, D., Monsigny, M., and Fajac, I. (2005) Potocytosis and cellular exit of complexes as cellular pathways for gene delivery by polycations. *J Gene Med 7*, 1275-86.

(42) Rejman, J., Oberle, V., Zuhorn, I. S., and Hoekstra, D. (2004) Size-dependent internalization of particles via the pathways of clathrin- and caveolae-mediated endocytosis. *Biochem J 377*, 159-69.

(43) Thomson, N. H. (2005) The substructure of immunoglobulin G resolved to 25 kDa using amplitude modulation AFM in air. *Ultramicroscopy 105*, 103-10.

(44) Campiglio, M., Ali, S., Knyazev, P. G., and Ullrich, A. (1999) Characteristics of EGFR family-mediated HRG signals in human ovarian cancer. *J Cell Biochem 73*, 522-32.

(45) Lewis, G. D., Figari, I., Fendly, B., Wong, W. L., Carter, P., Gorman, C., and Shepard, H. M. (1993) Differential responses of human tumor cell lines to anti-p185HER2 monoclonal antibodies. *Cancer Immunol Immunother 37*, 255-63.

(46) Merdan, T., Kopecek, J., and Kissel, T. (2002) Prospects for cationic polymers in gene and oligonucleotide therapy against cancer. *Adv Drug Deliv Rev 54*, 715-58.

(47) Goula, D., Benoist, C., Mantero, S., Merlo, G., Levi, G., and Demeneix, B. A. (1998) Polyethylenimine-based intravenous delivery of transgenes to mouse lung. *Gene Ther 5*, 1291-5.

(48) Gosselin, M. A., Guo, W., and Lee, R. J. (2002) Incorporation of reversibly cross-linked polyplexes into LPDII vectors for gene delivery. *Bioconjug Chem 13*, 1044-53.

(49) von Harpe, A., Petersen, H., Li, Y., and Kissel, T. (2000) Characterization of commercially available and synthesized polyethylenimines for gene delivery. *J Control Release 69*, 309-22.

(50) Ogris, M., Brunner, S., Schuller, S., Kircheis, R., and Wagner, E. (1999) PEGylated DNA/transferrin-PEI complexes: reduced interaction with blood components, extended circulation in blood and potential for systemic gene delivery. *Gene Ther. 6*, 595-605.

(51) Kircheis, R., Blessing, T., Brunner, S., Wightman, L., and Wagner, E. (2001) Tumor targeting with surface-shielded ligand--polycation DNA complexes. *J Control Release 72*, 165-70.

(52) Brus, C., Kleemann, E., Aigner, A., Czubayko, F., and Kissel, T. (2004) Stabilization of oligonucleotide-polyethylenimine complexes by freeze-drying: physicochemical and biological characterization. *J Control Release 95*, 119-31.

(53) Kleemann, E., Dailey, L. A., Abdelhady, H. G., Gessler, T., Schmehl, T., Roberts, C. J., Davies, M. C., Seeger, W., and Kissel, T. (2004) Modified polyethylenimines as non-viral gene delivery systems for aerosol gene therapy: investigations of the complex structure and stability during air-jet and ultrasonic nebulization. *J Control Release 100*, 437-50.

(54) Anabousi, S., Laue, M., Lehr, C. M., Bakowsky, U., and Ehrhardt, C. (2005) Assessing transferrin modification of liposomes by atomic force microscopy and transmission electron microscopy. *Eur J Pharm Biopharm 60*, 295-303.

(55) Thomson, N. H. (2005) Imaging the substructure of antibodies with tapping-mode AFM in air: the importance of a water layer on mica. *J Microsc 217*, 193-9.

3 HER2 Targeted Polyplexes: The Effect of Polyplex Composition and Conjugation Chemistry on in vitro and in vivo Characteristics

Published in Bioconjugate Chemistry 19 (2008) 244-253

3.1 Abstract

Knowledge of the influence of targeting ligands on pharmacokinetics and biodistribution of polymeric non-viral vectors is presently limited. We investigated the properties of three structurally different conjugates of polyethylenglycol-modified polyethylenimine coupled to the HER2 specific antibody Trastuzumab. Unlike polyethylenimine, conjugates formed small (100-230 nm) DNA polyplexes with zeta-potentials of ±2 mV at a broad range of N/P ratios. Stability as assessed by heparin displacement was slightly improved compared to unmodified copolymers. Erythrocyte aggregation and hemolysis were strongly reduced with conjugates. Conjugate polyplexes showed significant differences in specificity and transfection efficiency in vitro. These could be attributed to differences in cell binding and uptake assessed by flow cytometry. Pharmacokinetics of conjugates in mice revealed significant improvements over free plasmid DNA and polyethylenimine. Area under the plasma level-time curve of conjugates was increased up to 48% or 114% compared to polyethylenimine or free plasmid DNA, respectively. Deposition of conjugate polyplexes in lung and spleen was significantly reduced compared to polyethylenimine. Differences could be attributed to antibody conjugation since no significant differences in pharmacokinetics and biodistribution were found between conjugates. These findings demonstrate that conjugated antibodies do not only confer active targeting but significantly improve in vivo properties of polyplexes as well.

3.2 Introduction

Therapeutic nonviral gene delivery holds great potential for the treatment of many acquired and inherited diseases such as viral infections and cancer (*1*). To efficiently achieve in vivo cancer gene therapy, especially to distant tumors or disseminated metastases, systemic administration of such vector systems is indispensable. For this purpose, the vector system should be efficient, non-toxic and specific to its target cells. The vector should as well be easily producible in a tailor-made fashion in large quantities. Cationic polymers, namely poly(ethylene imine) (PEI) are exceptionally suitable for this purpose. PEI is known to exhibit superior transfection properties in vivo owing to its ability to efficiently package, protect and deliver DNA (*2, 3*). Unfortunately, the cationic nature of polymer/DNA complexes (polyplexes) causes aggregation with blood compo-

nents and opsonization in vivo (*4*). Unmodified polyplexes are quickly cleared by first pass organs of the reticuloendothelial system such as liver and spleen or are trapped in lung capillaries (*5-8*). To achieve a "stealth effect" similar to polyethylenglycol (PEG) modified liposomes (*9*). hydrophilic polymers like PEG or poly(*N*-(2-hydroxypropyl)methacrylamide) (pHPMA) were attached before or after complex formation with DNA (*4, 10-12*). This strategy led to reduction of surface charge, increased circulation times (*4, 10*) decreased unspecific transfection (*11, 13*) and improved biocompatibility, solubility and stability for freeze-drying (*14*). Such "stealth" vectors are able to passively target tumor tissues due to the enhanced penetration and retention effect (*7*). To facilitate active tumor targeting in vivo, gene delivery vectors need to be recognized and taken up by the target cells. This can be achieved by coupling of cell binding ligands such as antibodies or peptides (*15-17*).

Several studies using cationic polymers for in vivo gene delivery have been published (*2, 4, 6, 18-20*). The in vivo pharmacokinetics and/or biodistribution of these vectors was less often addressed (*4, 6-8, 10, 12, 21-23*). Only a minority of the studies dealt with the influence of hydrophilic polymers on polyplex disposition and kinetics (*4, 8, 10, 12, 21, 22*). The results of these studies were controversial. While Mullen et al. (*8*), Oupicky et al. (*12*) and Merdan et al. (*21*) found a decreased polyplex stability in circulation after modification with hydrophilic polymers, Ogris et al. (*4*), Kunath et al. (*10*) and Hildebrandt et al. (*22*) reported increased tumor association and/or prolonged kinetics. Due to significant differences in study design, direct comparison of these results proved to be difficult.

Further modification of relatively small cationic polymers or copolymers (typically about 25-75 kDa) with large targeting molecules like transferrin (~80 kDa) or IgG (~150 kDa) caused significant changes of polyplex properties. We hypothesized that targeting ligands do not only mediate active targeting of tumor cells but could also affect in vivo disposition and pharmacokinetics of the vector system. These changes may in effect be as important for efficient transfection of tumors in vivo as efficient binding to the target cells. A literature search on the contribution of targeting antibodies on pharmacokinetics and biodistribution of non-viral vector systems in vivo showed that this question was not systemically addressed so far.

We synthesized three structurally different conjugates consisting of branched PEI, PEG and an antibody, Trastuzumab, directed against HER2. We determined sizes, zeta-potentials and stability parameters of the resulting complexes with DNA at different charge ratios (N/P: polymer nitrogen:DNA phosphate). HER2 positive and –negative cell lines were used to evaluate transfection efficiencies and specificities of conjugates in vitro. Cell binding and uptake was studied by flow cytometry. In vivo pharmacokinetics and biodistribution were determined following tail vein injection of polyplexes in BALB/c mice in a 120 minutes time frame.

3.3 Materials and Methods

Materials: Branched Polyethylenimine (Polymin, 25 kDa) was a gift from BASF (Ludwigshafen, Germany). Luciferase plasmid pCMV-Luc was purchased from Plasmid Factory (Bielefeld, Germany). N-succinimidyl-3-(2-pyridyldithio)propionate (SPDP) was obtained from Sigma-Aldrich (Taufkirchen, Germany). N-hydroxysuccinimidyl ester of orthopyridyl-disulfide polyethylenglycol 2kDa (SPA-PEG(2 kDa)-OPSS) was purchased from Nektar Therapeutics (San Carlos, CA, USA). YOYO-1 iodide was obtained from Invitrogen (Karlsruhe, Germany). Trastuzumab (Herceptin®) was purchased from Roche (Basel, Switzerland). All other chemicals used were of analytical grade.

Cell Culture: SK-BR-3 and OVCAR-3 cells were purchased from ATCC, Teddington, UK and maintained in RPMI 1640 (PAA Laboratories, Cölbe, Germany) supplemented with 10% and 20% fetal calf serum (Cytogen, Sinn, Germany), respectively, in humidified atmosphere with 5% CO_2 at 37°C.

Synthesis of Conjugates: Polyethylenglycol (2 kDa)$_{10}$-graft-polyethylenimine (25 kDa) (abbreviated as PEG(2)-PEI) and Polyethylenglycol (30 kDa)$_{1.1}$-graft-polyethylenimine (25 kDa) (abbreviated as PEG(30)-PEI) copolymers were synthesized and characterized as described previously (*24*). For the synthesis of conjugates based on PEG-PEI copolymers the method described in was refined (*16*). 0.11 µmol of PEG(2 kDa)$_{10}$-PEI or PEG(30 kDa)$_1$-PEI were dissolved in 0.5 mL reaction buffer consisting of 150 mM sodium chloride, 20 mM 4-(2-hydroxyethyl)-1-piperazine ethane sulfonic acid (HEPES), pH 7.5. 0.2 µmol SPDP in 20 µL of 100% ethanol were added while stirring and allowed to react for 60 min at RT. Purification of the product was performed by gel chro-

matography on a PD-10 column (Amersham Pharmacia Biotech, Freiburg, Germany) in reaction buffer. SPDP-activated PEG-PEI was reduced for 1 h at 37°C using an excess of dithiothreitol (DTT) to yield PEG-PEI-SH. Degree of substitution with SH-reactive ortho-pyridyl groups was determined by pyridine-2-thione release upon addition of an excess of DTT (*25*).

In a second synthesis route we used unmodified PEI 25 kDa and covalently coupled Trastuzumab via a hetero-bifunctional PEG linker (SPA-PEG(2 kDa)-OPSS). Reactivity of SPA-PEG-OPSS was determined by pyridine-2-thione release and base catalyzed NHS-ester hydrolysis. 0.12 µmol PEI were dissolved in 1 mL reaction buffer and 1.2 µmol SPA-PEG-OPSS were added in 100 µl 100% ethanol while stirring. The mixture was allowed to react for 1 hour at room temperature and the product was purified by gel chromatography and reduced as described above to yield PEI-PEG-SH. The degree of substitution was determined by pyridine-2-thione release as described above.

0.15 µmol Trastuzumab in reaction buffer were allowed to react with 0.24 µmol of SPDP (10 mM in pure ethanol) under stirring at room temperature and were purified as described above. SPDP-activated Trastuzumab was added to purified, activated PEG-PEI and allowed to react for 24 h at room temperature.

Purification of the conjugates was performed by a modified ion exchange chromatography method first described by Kircheis et al. (*16, 26*). PEI concentration was quantified by copper complexation (*27*). The concentration of Trastuzumab was determined by UV-spectrometry at 280 nm with background correction using a solution of PEG-PEI or PEI of equal concentration.

Formation of Polyplexes: Polyplex formation was performed as described earlier (*16*). Briefly, pDNA was diluted with 150 mM sodium chloride, 10 mM HEPES, pH 7.4 to 0.04 g/L and mixed in equal parts with the appropriate amount of polymer in the same buffer. All experiments were performed at a N/P ratio of 6 and a final pDNA concentration of 0.02 g/L unless stated otherwise.

Size and ζ-potential: Hydrodynamic diameters and zeta-potentials of freshly prepared polyplexes were determined using a Zetasizer Nano ZS (Malvern Instruments, Herrenberg, Germany) equipped with a 4 mW He-Ne laser at a wavelength of 633 nm at 25 °C. Scattered light was detected at a 173° backward scattering angle. The viscosity and re-

fractive index of water at 25 °C was used for data analysis. 500 µl of polyplex solution were prepared and incubated for 10 minutes at RT. Measurements were performed in a folded capillary cell in triplicate. DTS software 4.10 was used for data acquisition and analysis. The accuracy of the instrument was maintained using reference polymer particles (Nanosphere Size Standards of 50, 100 and 200 nm, Duke Scientific Corp., Palo Alto, CA, USA) and with Zeta Potential Transfer Standard (Malvern Instruments, Herrenberg, Germany).

Agarose Gel Electrophoresis: For heparin displacement, 50 µl of polyplex solutions were prepared at N/P 6 and incubated for 10 minutes at RT. Then, polyplexes were challenged with 0.05 to 0.35 U heparin for 30 min at RT. 10% v/v glycerol was added and 10 µl of the solution were carefully applied to a 1% agarose gel in TAE (40 mM Tris/HCl, 1% acetic acid, 1 mM EDTA, pH 7.4) containing 0.6 µg/mL of ethidium bromide. Electrophoresis (Electro-4, Thermo Electron, Waltham, MA, USA) was carried out a constant voltage of 80 V for 1 hour in TAE buffer. Ethidium bromide fluorescence was detected using a gel documentation system (BioDocAnalyze, Biometra, Göttingen, Germany) and images were processed with ImageJ 1.37v (http://rsb.info.nih.gov/ij/) (*28*).

Erythrocyte aggregation and hemolysis: The hemolytic activity and erythrocyte aggregation of polyplexes was investigated as reported earlier (*29*). Briefly, human erythrocytes were isolated from fresh citrated blood from healthy volunteers by centrifugation at 850 x g. Red blood cells were washed in HEPES-buffered saline (HBS) until the supernatant was clear and colorless. Erythrocytes were diluted with HBS to 5 x 10^8 cells/mL. Polyplexes were prepared at N/P 6 in a total volume of 125 µl (DNA concentration 0.1 µg/µL). 1% Triton X-100 in HBS (100% lysis) and pure HBS (0% lysis) were used as control. 40 µL aliquots of polyplex solutions were mixed with 40 µL erythrocyte suspension. Samples were incubated for 30 min at 37 °C under constant shaking. After centrifugation at 850 x g, supernatant was analyzed for hemoglobin release at 415 nm (Ultrospec 3000, GE Healthcare, Munich, Germany). The pellet was resuspended with 500 µl HBS and used for microscopic evaluation of erythrocyte aggregation.

Transfection Experiments: For transfection experiments SK-BR-3 and OVCAR-3 cells were plated at a density of $1x10^4$ cells per well in a 96-well plate. After 24 hours of growth, medium was replaced by 0.2 mL of fresh, complete cell culture medium containing 0, 10, 50 or 250 µg of free Trastuzumab. Cells were incubated for 15 minutes at 37 °C. Polyplexes were prepared in a final volume of 30 µl (containing 0.63 µg pDNA) per well, incubated for 10 minutes at RT and subsequently added to the wells. Medium was exchanged again after 4 hours and cells were incubated for an additional 44 hours.

Luciferase gene expression was quantified using a commercial kit (Promega, Mannheim, Germany) and photon counting on a luminometer (Sirius, Berthold, Pforzheim, Germany). Results were measured in relative light units per second (RLU/s) and converted to nanograms of luciferase using a standard curve of recombinant luciferase (Promega, Mannheim, Germany). Protein concentration was determined using a modified BCA assay (Perbio Science, Bonn, Germany) with bovine serum albumin as a standard (*30*). All experiments were performed in quadruplicate and results were normalized to transfection efficiency of unmodified PEG-PEI copolymers.

Flow Cytometry: For flow cytometry experiments, cells were seeded in 24-well plates at a density of $6x10^4$ cells per well. After 24 hours of growth, cell culture medium was exchanged with 0.5 mL of fresh medium. Polyplexes were prepared in a final volume of 150 µl (containing 2.5 µg YOYO-1 labeled pDNA (*31*)) at N/P 6, incubated for 10 minutes at room temperature and then added to the wells. In the case of polyplex binding experiments, cells were incubated at 4 °C for 15 min before and after addition of polyplexes. Subsequently, cells were washed 2 times with ice cold PBS. For the uptake experiments, cells were incubated with the polyplexes for 3 hours at 37 °C. Cells were then washed 4 times for 3 minutes with 0.5 mg/mL heparin in PBS to remove surface bound polyplexes. Cells were detached with trypsin and suspended in an ice-cold 1:1 mixture of FACS-Flow (BD Biosciences, San Jose, USA) and 4% paraformaldehyde in PBS.

Flow cytometry was performed using a FACScan (BD Biosciences, San Jose, USA) equipped with a 488 nm argon-ion laser. The emission filter setting was 530/30 bandpass. Viable cells were gated according to forward and sideward scatter of untreated cell samples. At least five thousand gated events were collected and subjected to further

analysis. All experiments were performed in triplicate. Results were normalized to binding- or uptake efficiency of the respective unmodified PEG-PEI copolymers, respectively. CellQuest 3.3 software (BD Biosciences, San Jose, USA) was used for data acquisition. Analysis was performed with FCS Express V3 (De Novo Software, Thornhill, Canada).

In vivo experiments: All animal experiments were carried out according to the German law of protection of animal life and approved by an external review committee for laboratory animal care.

Pharmacokinetic and biodistribution studies: 100 ng pCMV-Luc were labeled with 32-P-α-CTP (Hartmann, Germany) using a Nick translation kit N5000 (GE Healthcare, Germany) according to the manufacturer's protocol. The reaction mixture was purified using microspin columns (Wizard SV Gel and PCR Clean-Up System, Promega, Germany) and the labeled plasmid was used immediately after synthesis.

Polyplexes were prepared using 25 µg pCMV-Luc plasmid spiked with ^{32}P labeled plasmid as described earlier (*21*). A volume equal to a dose of 1 µg pCMV-Luc per g mouse of the polyplex solution was injected in anaesthetized male balb/c mice via the tail vein. Blood samples of 25 µL were drawn from the retrobulbar plexus 1, 3, 5, 15, 30, 60 and 120 min post injection. After 120 min, mice were sacrificed by cervical dislocation and organs were excised. Organ samples were dissolved in Soluene 350 (PerkinElmer, Germany) and blood samples were dissolved overnight in a 1:1 mixture of isopropanol/Soluene 350 at 55 °C and subsequently bleached with 200 µL hydrogen peroxide. After addition of 15 mL of scintillation cocktail (Hionic Fluor®, PerkinElmer, Germany) activity of ^{32}P in each sample was determined using a TriCarb 2900 liquid scintillation counter (PerkinElmer, Germany) with a counting time of 10 min, active static controller and half-life correction. Disintegrations per minute (DPM) were calculated with a ^{32}P quench curve using tSIE/AEC as quench indicator. The injected dose was calculated based on activity measurements of the injected solution. All experiments were performed at least in triplicate and the AUC was determined using a non-compartmental mixed logarithmic-linear algorithm. Concentration-time data were fitted to a biexponential disposition function ($C(t) = Ae^{-\alpha t} + Be^{-\beta t}$, iterative reweighing with $1/C_{obs}$) using the software Kinetica 1.1. from Simed (Créteil Cedex, France). Plasmid

concentrations in the samples were calculated as percent of the injected dose per organ or as percent injected dose per mL blood.

3.4 Results

Synthesis of Conjugates: Conjugates were prepared using two different poly-ethylenglycol - polyethylenimine copolymers (*24*). To study the influence of PEGylation, these copolymers represent two extremes concerning the degree of PEGylation and PEG chain length while keeping the weight ratio of PEG to PEI approximately constant. In both cases, the targeting moiety was coupled to PEI via the hetero-bifunctional linker N-succinimidyl-3-(2-pyridyldithio)propionate (SPDP). The degree of substitution with SPDP, determined by pyridine-2-thion release, was 1.5 and 1.7 mole 2-pyridyl disulphide per mole PEI for PEG(2)-PEI and PEG(30)-PEI, respectively. A third conjugate was prepared by modifying PEI with a hetero-bifunctional PEG linker. This synthesis resulted in a degree of substitution of ~10 moles PEG per mole PEI. The degree of substitution with 2-pyridyl disulphide was determined to be 5 moles per mole PEI. Reaction of SPDP with Trastuzumab resulted in a degree of substitution of 1.3 mole 2-pyridyl disulphide per mole antibody. Finally, the degree of substitution of conjugates with Trastuzumab was determined to be 0.74, 1.5 and 0.38 mol/mol Trastuzumab/PEI for PEG(2)-PEI-Trastuzumab, PEG(30)-PEI-Trastuzumab and PEI-PEG(2)-Trastuzumab, respectively (Fig. 1). The overall polymer yield after purification varied between 50 and 70% as determined by copper complexation.

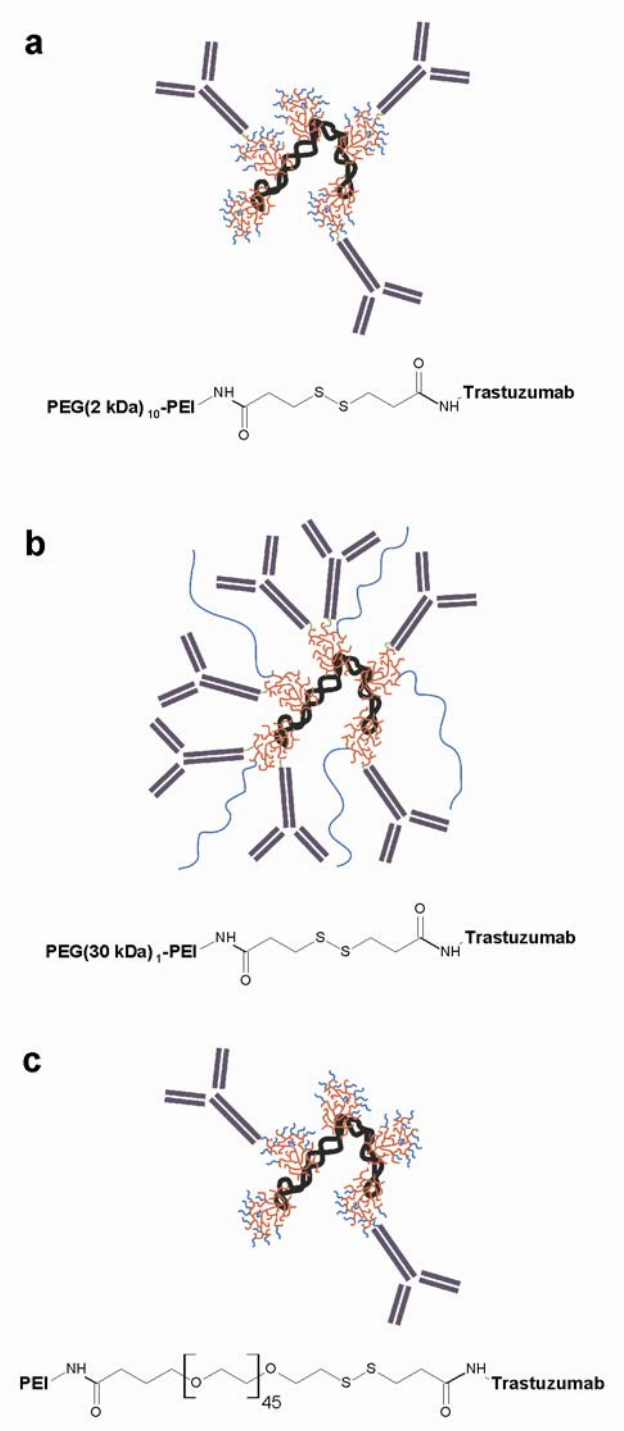

Figure 1. Chemical structure of conjugates and illustration of hypothetical complexes with plasmid DNA (black). Branched PEI 25 kDa (red) was substituted with PEG (light blue) of different molecular weight to different degrees and Trastuzumab (dark blue) was coupled directly to PEI via SPDP (green) in the case of (PEG(2)-PEI-Trastuzumab (a) and PEG(30)-PEI-Trastuzumab (b). PEI-PEG(2)-Trastuzumab (c) was prepared by modification of branched PEI 25 kDa with a hetero-bifunctional PEG linker and Trastuzumab was coupled to the distal end of the PEG chains.

Size and ζ-potential: Hydrodynamic diameters decreased with increasing N/P ratio for all complexes (Fig. 2a). At N/P 6 and 12, all complexes revealed a similar size of 100 to 230 nm, facilitating efficient uptake by absorptive endocytosis (*32*). At N/P 3, PEI formed large complexes of about 1200 nm. Due to efficient shielding, PEG-PEI and conjugate polyplexes were significantly smaller than PEI complexes with sizes of only 100 to 300 nm.

In contrast to PEI polyplexes, which showed high ζ-potentials of about +27 mV at N/P 6 and 12, the surface charge of PEG-PEI polyplexes was significantly reduced (Fig. 2b). Modification of PEG-PEIs with Trastuzumab further decreased ζ-potentials. These polyplexes were near neutral at all N/P ratios tested.

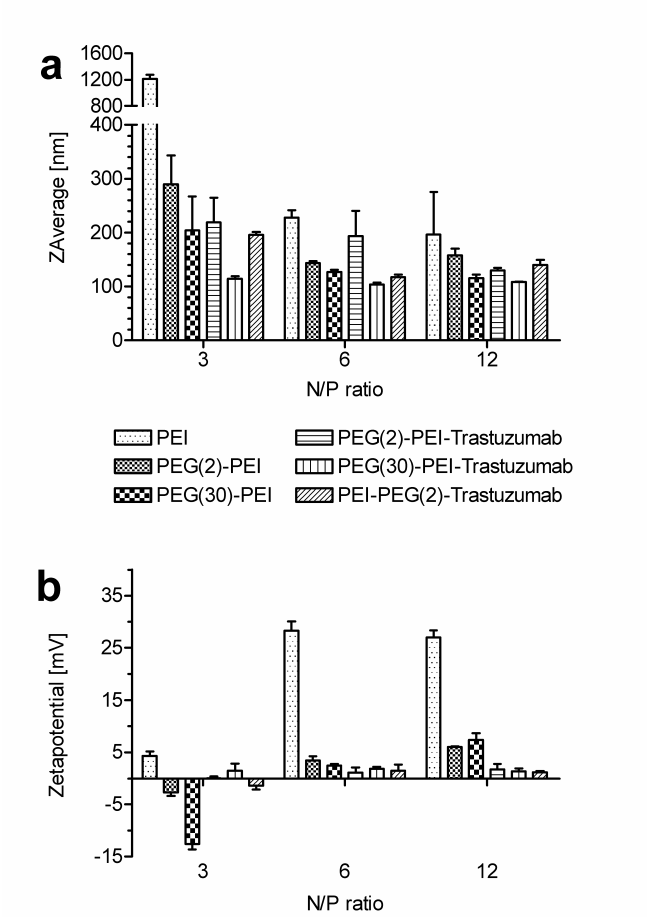

Figure 2. Hydrodynamic diameters (a) and zeta-potentials (b) of polyplexes prepared with pDNA and unmodified polymers or Trastuzumab conjugates at the indicated N/P ratios. Polyplexes were prepared as described in the materials and methods and were measured in a folded capillary cell in quintuplicate (a) or triplicate (b). Values are given as means + SD.

Stability against Heparin Displacement: To evaluate polyplex stability against displacement of pDNA by competing polyanions, the polyplexes were challenged with free heparin (Fig. 3). Heparin amounts as low as 0.1 U displaced DNA from the complex in the case of PEI and PEG-PEI copolymers. Trastuzumab conjugate complexes showed a slightly improved stability against heparin displacement. With these polyplexes, free plasmid DNA was observed at heparin concentrations of 0.20 U and above.

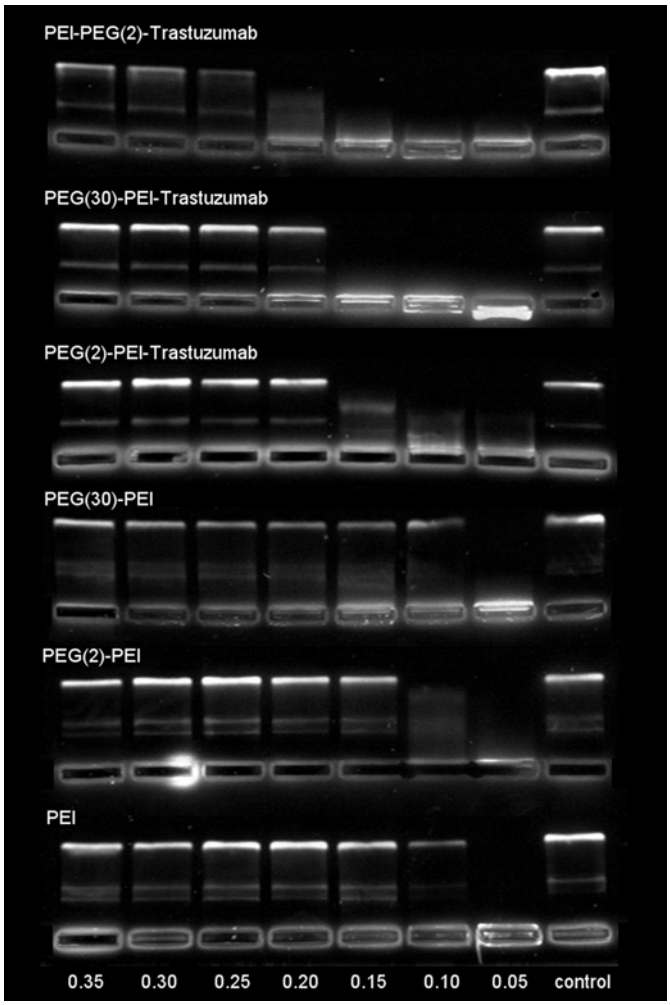

Figure 3. Heparin displacement assay using PEI-, copolymer- and conjugate polyplexes. Polyplexes were formed at N/P 6 and incubated for 30 minutes with increasing heparin concentrations. Free plasmid DNA is shown to the right.

Erythrocyte Hemolysis and Aggregation: Interactions with blood components, namely erythrocytes, are likely to occur after injection of polyplexes into the bloodstream (*4, 33*). The hemolytic activity of polyplexes and the tendency to form aggre-

gates with erythrocytes was studied in an in vitro assay using freshly purified human red blood cells.

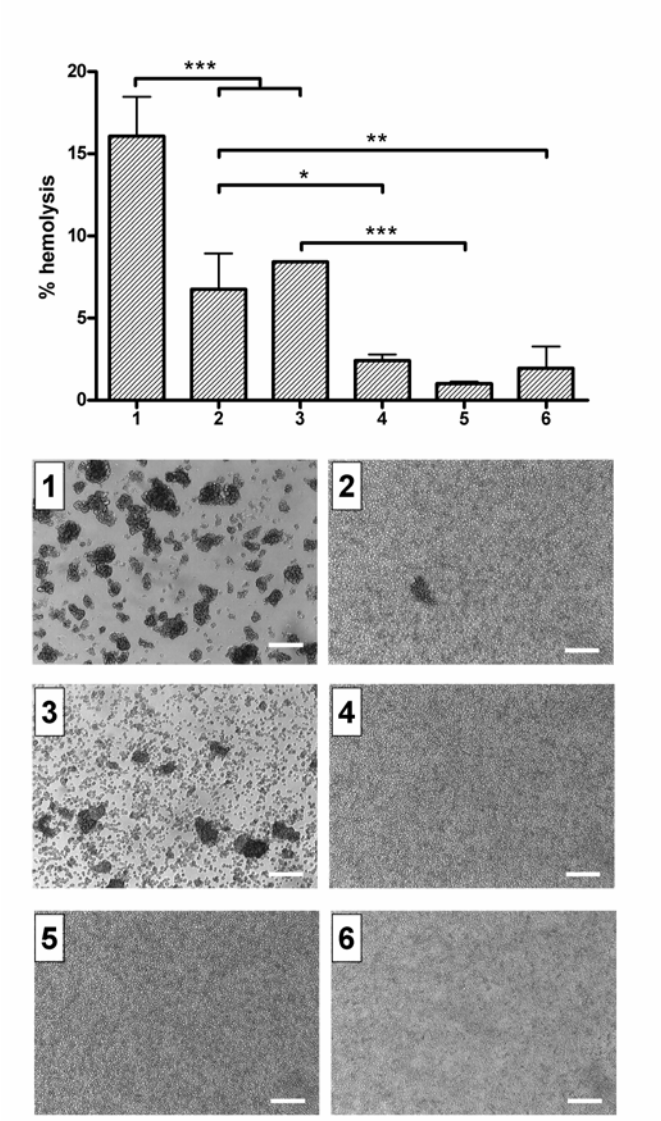

Figure 4. Lysis and aggregation of human erythrocytes induced by polyplexes prepared at N/P 6 with PEI (1), PEG(2)-PEI (2), PEG(30)-PEI (3), PEG(2)-PEI-Trastuzumab (4), PEG(30)-PEI-Trastuzumab (5) and PEI-PEG(2)-Trastuzumab (6). Values are given as means + SD of triplicates. Significance was tested using one-way ANOVA with Bonferroni's multiple comparison test ($p<0.05$; ** $p<0.01$; *** $p<0.001$). Scale bars represent 100 µm.*

For polyplexes prepared with unmodified PEI at N/P 6 hemolysis of 16% of the erythrocytes was found, which is in good correlation with earlier reports (Fig. 4) (*34*). PEGylation of PEI significantly reduced hemolysis both in the case of short (PEG(2)-PEI) and long (PEG(30)-PEI) PEG chains. Modification of PEG-PEI copolymers with Trastuzu-

mab further significantly decreased erythrocyte lysis compared to the unmodified PEG-PEI copolymers. Only 1.0 to 2.4% hemolysis was observed with Trastuzumab conjugates.

Erythrocyte suspensions were then microscopically examined for aggregate formation (Fig. 4). Addition of PEI polyplexes resulted in rapid and extensive erythrocyte aggregation. Interaction with erythrocytes was decreased using PEG-PEI polyplexes but still moderate to severe aggregate formation was found. Using Trastuzumab modified copolymers, no erythrocyte aggregation was seen.

Transfection Experiments: For transfections in vitro, two different cell lines with different HER2 expression levels were used. OVCAR-3 cells were shown to express only low amounts of HER2 and therefore served as a negative control (*16*). In contrast, SK-BR-3 cells are known to over-express HER2 (*16, 35*). Specificity of transfection was evaluated by competitive inhibition with free Trastuzumab during incubation with polyplexes.

In SK-BR-3 cells, PEG(2)-PEI-Trastuzumab showed a significant ($p<0.01$), 6.6-fold increase in reporter gene expression compared to PEG(2)-PEI. Significant inhibition ($p<0.05$) was seen with at least 1.69 µmol/L of free Trastuzumab (Fig. 5a). By contrast, transfection efficiency of PEG(30)-PEI-Trastuzumab was not significantly increased compared to PEG(30)-PEI and no significant inhibition was seen with free Trastuzumab in cell culture media (Fig. 5c). PEI-PEG(2)-Trastuzumab had a reporter gene expression 34-fold higher compared to PEG(2)-PEI. Significant inhibition ($p<0.001$) was achieved with Trastuzumab concentrations as low as 0.34 µmol/L (Fig. 5e). None of the conjugates showed a specific reporter gene expression in HER2 negative OVCAR-3 cells (Figs. 5b, d, f).

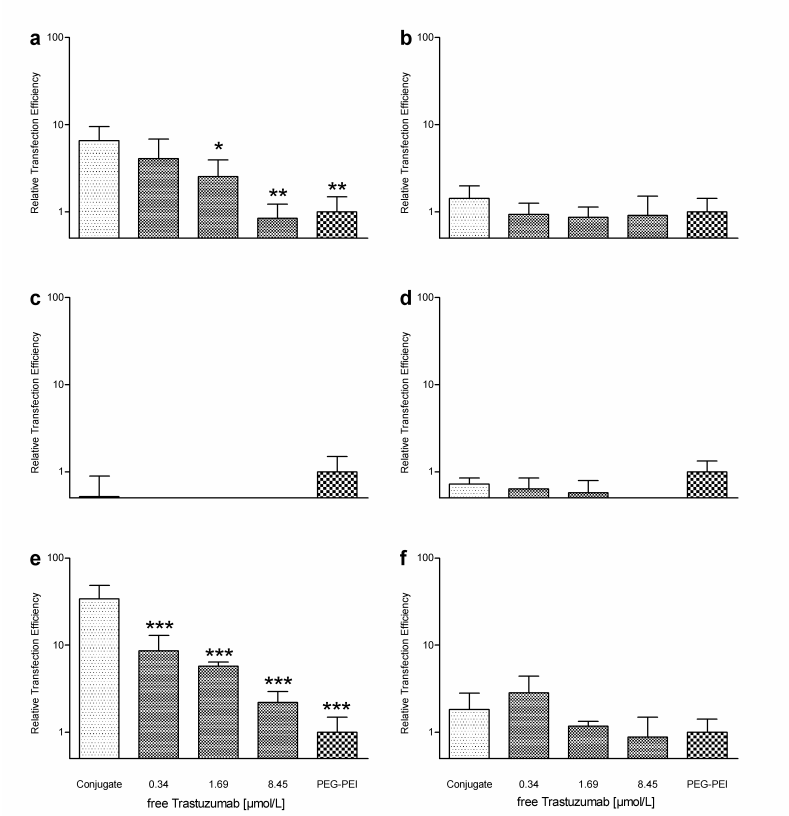

Figure 5. Transfection efficiencies and specificity of conjugates compared to the respective unmodified copolymer in HER2 positive SKBR-3 cells (b, c and e) and HER2 negative OVCAR-3 cells (b, d and f). Polyplexes were formed with pDNA and PEG(2)-PEI-Trastuzumab (a and b), PEG(30)-PEI-Trastuzumab (c and d) and PEI-PEG(2)-Trastuzumab (e and f) at N/P 6. To test the specificity of transfection, cells were incubated with indicated concentrations of free Trastuzumab for 15 minutes before addition of the polyplexes. Values are given as means + SD of quadruplicates. Significance was tested using one-way ANOVA with Dunnett's multiple comparison test with transfection efficiency of conjugate set as control ($p<0.05$; ** $p<0.01$; *** $p<0.001$).*

Flow Cytometry: Binding efficiencies of Trastuzumab conjugates relative to unmodified PEG-PEI copolymers at 4 °C are depicted in Fig. 6a. Increased binding to SK-BR-3 cells was observed for all conjugates. Compared to the respective untargeted copolymer, PEI-PEG(2)-Trastuzumab showed the most efficient binding, followed by PEG(2)-PEI-Trastuzumab and PEG(30)-PEI-Trastuzumab. A smaller increase of binding of conjugates was also found for OVCAR-3 cells. HER2 expression of OVCAR-3 cell was found to be very low but still detectable by flow cytometry (*16*) which may explain the slightly increased binding efficiencies.

To evaluate the uptake of particles, OVCAR-3 and SK-BR-3 cells were incubated with polyplexes for 3 hours at 37 °C. Cell surface-bound polyplexes were then removed and intracellular fluorescence was determined by flow cytometry as well. Figure 6b shows uptake efficiencies of conjugates relative to unmodified PEG-PEI copolymers. A very efficient and specific uptake can be observed for PEI-PEG(2)-Trastuzumab with a 4.3-fold increased uptake compared to the Trastuzumab-free copolymer. PEG(2)-PEI-Trastuzumab also showed a modest increase in uptake efficiency (2.8-fold). PEG(30)-PEI-Trastuzumab showed only a 1.9-fold increase in uptake.

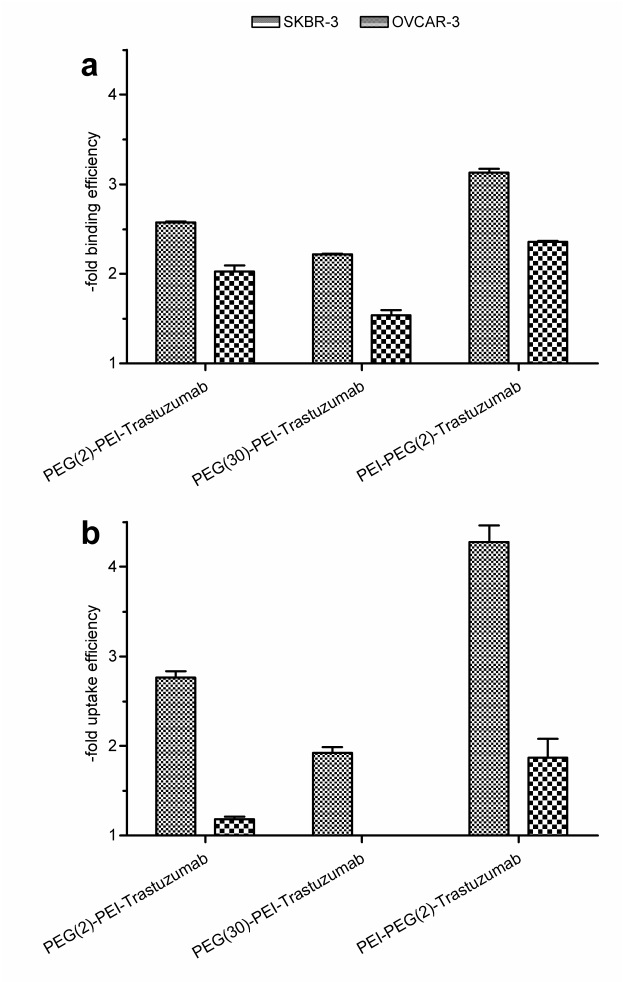

Figure 6. Binding- (a) and uptake efficiencies (b) of polyplexes prepared at N/P 6. Conjugate uptake or binding is shown relative to the corresponding unmodified PEG-PEI copolymer. Polyplexes were incubated with the cells for 15 minutes at 4 °C (a) or 3 hours at 37 °C (b). In the case of uptake experiment (b), cells were washed 4 times with heparin in PBS to dissociate and remove surface bound polyplexes. Cells were then analyzed for mean fluorescence intensity by flow cytometry. Values are given as means + SD of triplicates.

Pharmacokinetics and Biodistribution in mice: For in vivo experiments, polyplexes were injected into the tail vein of male BALB/c mice at a dose of 1 µg/g of radio-labelled DNA per mouse. To ensure the integrity of labeled plasmid, DNA was used immediately after performing the labeling reaction and subsequent purification procedures.

Free pDNA was removed quickly and efficiently from the blood stream. After 60 minutes, only about 1 % of the injected dose per mL (ID/mL) were found in the blood (Fig. 7a), which is in good agreement with earlier reports (*36*). If pDNA was complexed with unmodified PEI, a biphasic disposition with a very rapid decay in the alpha phase was observed. With PEI the onset of the beta phase was earlier and the B value was significantly increased compared to pDNA alone (Table 1). The area under the curve (AUC) was thereby increased from 532.16 to 770.10 % ID min^{-1} mL^{-1}, which again is in excellent agreement with earlier findings (*21*).

	C max [c] [% ID]	A [c] [% ID mL^{-1}]	T $_{1/2\ alpha}$ [c] [min]	B [c] [% ID mL^{-1}]	T $_{1/2\ beta}$ [c] [min]	AUC [d] [% ID mL^{-1} min^{-1}]
PEI	16.11 ± 1.38	17.94 ± 2.87	1.60 ± 0.04 (***/-)	4.45 ± 0.26 (*/-)	108.92 ± 5.10	770.10 ± 169.57 (ns/-)
PEG(2)-PEI-Trastuzumab	17.06 ± 1.13	12.80 ± 2.90	1.57 ± 0.58 (***/ns)	9.54 ± 1.45 (**/*)	85.65 ± 12.34	1139.40 ± 58.55 (***/**)
PEG(30)-PEI-Trastuzumab	14.58 ± 1.94	9.58 ± 5.34	1.95 ± 0.75 (***/ns)	7.71 ± 2.99 (*/ns)	89.23 ± 11.42	1088.12 ± 114.12 (***/*)
PEI-PEG(2)-Trastuzumab	17.65 ± 1.50	14.86 ± 0.68	1.97 ± 0.10 (***/ns)	7.23 ± 1.25 (*/ns)	85.95 ± 26.11	905.79 ± 18.21 (**/ns)
pDNA (pCMV-Luc)	17.35 ± 2.40	14.36 ± 3.05	8.54 ± 0.66 (-/***)	2.18 ± 0.78 (-/*)	205.34 ± 113.24	532.16 ± 20.08 (-/ns)

Table 1: Pharmacokinetic properties of Trastuzumab conjugate- and PEI polyplexes and free plasmid DNA [a, b]

a All values given as means + SD

*b Significance was tested using 1way ANOVA with Bonferroni's multiple comparison test with DNA or PEI (vs. DNA / vs. PEI) set as control (ns: not significant; * p<0.05; ** p<0.01; *** p<0.001)*

c Concentration-time data was fitted to a biexponential disposition function

d AUC was determined using a noncompartmental mixed logarithmic-linear algorithm

All Trastuzumab conjugates were found to improve pharmacokinetics of pDNA with minor differences between conjugates. Complexes composed of PEG(2)-PEI-Trastuzumab showed a significant increase in the B value and AUC compared to PEI polyplexes. Pharmacokinetics of the block-copolymer like PEG(30)-PEI based conjugate were slightly improved compared to PEI. The B value was increased to 7.71 %ID mL^{-1} and AUC was significantly increased over PEI. PEI-PEG(2)-Trastuzumab showed similar kinetics but differences compared to PEI were less pronounced. An increase in B value and AUC compared to PEI was seen but differences were not statistically significant in this case.

Biodistribution of labeled plasmid DNA was assessed 120 minutes post injection (Fig. 7b). Uptake of uncomplexed DNA was negligible in most organs. PEI polyplexes accumulated mainly in the liver, lung, kidneys and spleen. When conjugates were used to prepare polyplexes, main uptake occurred in the liver as well. However, uptake into lung and spleen was significantly decreased for all Trastuzumab conjugates compared to PEI.

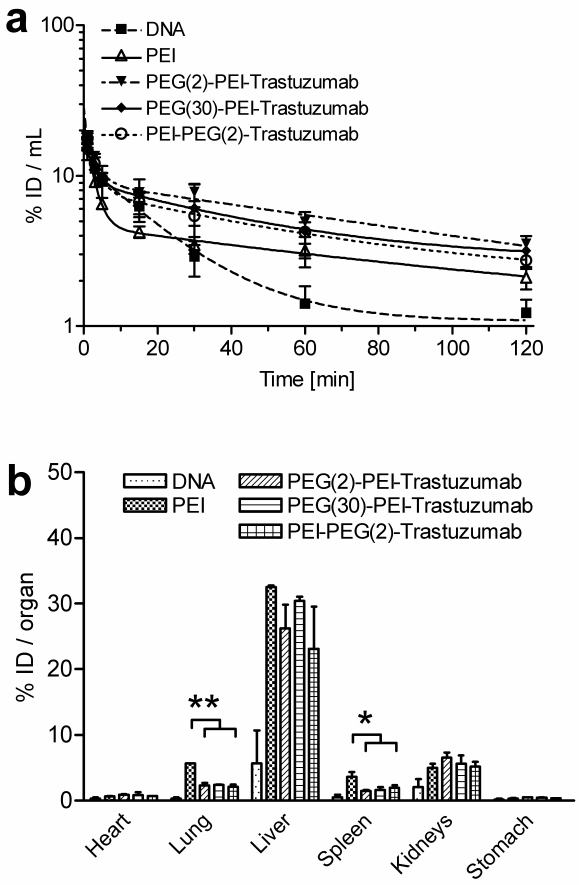

Figure 7. Pharmacokinetic profiles (a) and biodistribution (b) of PEI (open triangle, solid line), PEG(2)-PEI-Trastuzumab (filled triangle, dashed-dotted line), PEG(30)-PEI-Trastuzumab (filled square, solid line) and PEI-PEG(2)-Trastuzumab (open circle, dotted line) polyplexes compared to free plasmid DNA (filled square, dashed line) in male BALB/c mice. Polyplexes were prepared at N/P 6 with 1 µg/g pDNA per mouse and injected via the tail vein in a volume of about 200 µl. Blood samples were taken at indicated time points from the retrobulbar plexus. Organs were withdrawn after 120 min and the amount of radiolabelled plasmid was determined by liquid scintillation counting. Significance was tested using one-way ANOVA and Dunnett's multiple comparison test with PEI polyplexes set as control ($p<0.05$, ** $p<0.01$).*

3.5 Discussion

Several studies on the pharmacokinetics and biodistribution of PEI- (*37, 38*) as well as PEG-PEI/DNA (*4, 10, 21*) polyplexes have been undertaken. Until now, the influence of targeting ligands such as antibodies, antibody fragments or peptides on the pharmacoki-

netics and biodistribution of the resulting vector system was not systemically evaluated. Achievement of high and long lasting blood levels is considered to be a prerequisite for efficient use of non-viral vectors under in vivo conditions. The final goal for the gene delivery system presented in this study was targeting of tumor tissues which will be the subject of a separate investigation. Before addressing this goal the effects of targeting ligands and PEGylation on in vivo pharmacokinetics and distribution needed to be clarified. To elucidate the effects of PEG and antibody, three conjugates were synthesized. These were composed of branched PEI 25 kDa as condensing agent, PEG to reduce non-specific interactions and Trastuzumab as a targeting ligand. Variations included the linker chemistry, PEG chain length and substitution degree (Fig. 1).

The efficacy of non-viral gene delivery systems administered via the intravenous route depends on several crucial parameters: Polyplex size, surface charge, stability in the bloodstream and interaction with blood components are of major importance. One impediment for successful transfection of tumor tissue in vivo is early entrapment of the polyplexes after intravenous injection. Ogris et al., Merdan et al. and Hildebrandt et al. stressed the importance of polyplex size and aggregation behavior in terms of organ distribution (*4, 21, 22*). These investigations showed that deposition in the lung, which is the first capillary bed reached after i.v. injection, as well as lethality after treatment depends on polyplex size and aggregation behavior. It was shown by Petersen et al. that PEI does not produce stable polyplexes especially at low N/P ratios and an increase in complex size over time was observed. In contrast, PEG-PEI copolymers with PEG chains longer than 550 kDa formed stable complexes under these conditions and no aggregation over time occurred (*24*). In our study, unmodified PEI polyplexes formed large particles in micrometer-range at N/P 3 in vitro. In contrast, all PEG-PEI copolymers and Trastuzumab conjugates produced small complexes with DNA with sizes not exceeding 300 nm in a wide range of N/P ratios. After i.v. injection, PEI is known to form aggregates with blood components such as erythrocytes or albumin (*39*). Erythrocyte aggregation and hemolysis studied using human red blood cells showed severe aggregation of erythrocytes with PEI polyplexes. In contrast, PEGylated PEIs showed reduced erythrocyte aggregation and hemolysis, which is in accordance with findings of Petersen et al. (*24*). Most importantly, Trastuzumab modified PEG-PEI copolymers

even surpassed PEG-PEI in these experiments and showed virtually no aggregation or hemolysis of erythrocytes.

The surface charge of polyplexes is an important parameter closely related to the above mentioned characteristics. Zeta-potentials of polyplexes prepared with Trastuzumab conjugates were lower than those of polyplexes prepared with unmodified PEI or with the respective PEG-PEI copolymers. Actually, conjugate polyplexes remained close to neutral in a wide range of N/P ratios due to the additional steric shielding by coupled antibody. Similar shielding effects were observed with transferrin-PEI polyplexes subsequently modified with PEG (*4*) and with PEG-PEI covalently modified with anti-OA3 Fab' (*25*). Ward et al. and Ogris et al. showed that shielded complexes decreased non-specific interactions with blood components and non-targeted cells (*4, 40*). Plank et al. found that positively charged DNA complexes can activate the alternative complement system (*41*). The authors also showed that modification of polylysine/DNA complexes with PEG can considerably reduce complement activation. We speculated that further reduction of surface charge in the case of Trastuzumab modified PEG-PEI polyplexes could result in reduced complement activation.

Polyplexes injected into the circulation encounter relatively harsh conditions such as shear stress during injection and circulation, lytic enzymes and a multitude of salts and proteins which may negatively influence complex integrity and DNA stability (*42, 43*). To investigate complex stability, we tested the susceptibility of polyplexes to heparin displacement. The polyanion heparin releases DNA from polyplexes and is a good measure for complex stability against competing anions. All Trastuzumab conjugates were slightly less susceptible to heparin displacement compared to PEI and their respective unmodified copolymers. We hypothesize that the dense shell formed by PEG and Trastuzumab may prevent heparin from entering the complex as easily as in the case of unmodified PEI polyplexes.

Therefore, all Trastuzumab conjugate complexes appear sufficiently stable to remain intact during circulation and are at the same time less susceptible to aggregation and non-specific interaction than unmodified PEI.

Apart from size and stability, tumor specificity of polyplexes is crucial. The target tissue should ideally be transfected with high efficiency while leaving non-targeted tissues

unaffected. Strehblow et al. showed that conjugation chemistry may have a significant effect on transfection efficiency and specificity in vitro (*44*). In this study, three different linkers were used to prepare HER2 or CD90 targeted conjugates. Using these linkers, major differences in the degrees of conjugation and in target cell specificity of the resulting conjugates were found. Interestingly, none of the conjugates prepared with SPDP as a linker showed target cell specificity. In contrast, SPDP was successfully used as a linker by Merdan et al. and Kircheis et al. under comparable conditions (*25, 26*). Kunath et al. showed that if RGD peptide was used as a targeting moiety, only direct coupling of the peptide to PEI via SPDP mediated efficient and specific transfection while a RGD-PEG-PEI conjugate was inefficient (*45*). In contrast, Moffatt et al. successfully utilized a PEG linker for coupling anti-PSMA antibody to PEI/DNA polyplexes (*17*).

In this study we used three structurally different conjugates which were comparable in physicochemical properties but different in transfection-, binding- and uptake efficiencies. Two conjugates were based on pre-synthesized PEG-PEI copolymers. Trastuzumab was in these cases coupled to the PEI core via SPDP. The PEG(2)-PEI copolymer was well established for conjugation purposes in our laboratory (*16, 25*). To study the influence of PEGylation, PEG(30)-PEI with fewer but longer PEG chains was used as a second copolymer. The PEG content of both copolymers was comparable (45% vs. 56%). PEG-PEI with a lower substitution degree was used to promote substitution with antibody and possibly increase specificity. It was found that the substitution degree could be increased 2-fold by using PEG(30)-PEI compared to PEG(2)-PEI. This in turn decreased reporter gene expression compared to PEG(2)-PEI-Trastuzumab and transfection was non-specific. This result can be explained by a comparably lower binding to target cells and most importantly by lower uptake efficiency as shown by flow cytometry. It was hypothesized, that longer PEG chains may hinder target recognition by partial masking of antigen binding domains. The decrease in uptake efficiency may be contributed to crosslinking of several receptors on the cell surface or inter-cellular crosslinking due to the comparably high antibody substitution degree of this conjugate. For the third conjugate, a PEG linker was used. This enhanced presentation of the targeting moiety and increased the specificity and efficiency of the resulting Trastuzumab conjugate. We

herein showed by flow cytometry analysis that this conjugate was the most efficient in binding and uptake.

As a result, the efficiency of PEG-PEI-antibody conjugates strongly depends on co-polymer composition and conjugation chemistry. In our study, the presentation of antibody at the distal end of a PEG spacer was most efficient. Our second approach of using pre-synthesized PEG-PEI copolymers showed that long PEG chains may hinder the proper presentation of antibody. In contrast, good results were obtained with a PEG-PEI copolymer consisting of shorter PEG blocks with a higher PEG grafting ratio.

In vivo behavior of conjugate polyplexes was compared with unmodified PEI polyplexes as well as with uncomplexed plasmid. Blood levels followed a bi-exponential disposition curve with a rapid distribution phase and a subsequent prolonged elimination phase. PEI polyplexes showed a pronounced distribution phase with a comparably low remaining DNA concentration in blood after distribution. In contrast, Trastuzumab conjugates were more rapidly distributed and higher concentrations remained in circulation after distribution. Elimination half lives of PEI and Trastuzumab conjugate complexes were comparable. Consequently, AUC of Trastuzumab conjugate polyplexes were 18 to 48% higher than AUC of PEI polyplexes and 70 to 114% higher than that of free DNA.

In a previous study, Merdan et al. determined the pharmacokinetic profiles of PEI and PEG(2)-PEI complexes under similar conditions. At a DNA dose of 25 µg/mouse, no significant differences in pharmacokinetics were found between PEI and PEG(2)-PEI polyplexes. Furthermore, the pharmacokinetic profiles showed that DNA is associated with both PEI and PEG(2)-PEI at least until 60 minutes post injection under these conditions (*21*). At a lower DNA dose of 1.5 µg/mouse, significantly increased blood levels were found for pDNA complexed with PEG(2)-PEI compared to PEI. However, at this low dose, complex dissociation indicated by differing pharmacokinetic profiles of radioactively labeled polymer and DNA was observed.

PEI polyplexes are known to rapidly distribute to and remain in highly perfused organs such as liver, lung and spleen.(*20*) These phenomena seem to be in part due to aggregation of polyplexes, interaction with blood components such as erythrocytes and recognition by the reticulo-endothelial system (*4, 24, 39, 43*). By using stealth polyplexes, in

vivo toxicity, aggregation and complement activation can be reduced (*4, 10*). However, studies on PEG-PEI copolymers have shown that PEGylation alone does not significantly improve pharmacokinetics compared to unmodified PEI (*21, 46*). De Wolf et al. recently hypothesized that polyplexes prepared using PEG-grafted PEI (pre-PEGylation approach) are still prone to opsonization and therefore are relatively rapidly eliminated (*46*). Interestingly, post-PEGylated polyplexes, where DNA is first condensed with the unmodified polycation and polyplexes are subsequently PEGylated, seem to be more efficient in improving pharmacokinetics (*7, 40*). However, from our point of view, this approach has serious drawbacks regarding polyplex preparation and characterization, especially in a clinical setting.

In our study, Trastuzumab modified PEG(2)-PEI at the same dose used by Merdan et al. significantly improved pharmacokinetics compared to PEI polyplexes (*21*). Comparable pharmacokinetics were observed for all Trastuzumab conjugates despite their different structure. Trastuzumab modification decreased the surface charge and increased polyplex stability in the case of all three conjugates. Most importantly, aggregation with erythrocytes was strongly decreased with all conjugates. Thereby, entrapment of polyplexes in small capillaries and recognition by the reticulo-endothelial system is reduced and AUC increases. We hypothesized that in the case of the PEG-PEI copolymer used in the study of Merdan et al., PEGylation alone could not sufficiently inhibit erythrocyte aggregation. This might be one of the major reasons that no significant difference between PEI and PEG-PEI was found in this study. This suggests that the additional steric shielding introduced by antibody modification has a stronger effect on pharmacokinetics than the structure of PEG-PEI copolymers or linker chemistry.

The biodistribution of polyplexes was assessed 120 minutes after injection. Using free, uncomplexed plasmid, only minor amounts of radioactivity were found in the liver and in the kidneys, which both are involved in plasmid excretion (*47*). Polyplexes prepared with PEI were taken up mainly by the liver and to a minor extent by lung, spleen and kidneys. The accumulation of polyplexes tended to be increased in highly perfused organs such as liver and kidneys (*47*). Furthermore, liver and spleen possess discontinuous or fenestrated endothelia which may facilitate accumulation of polyplexes (*48*). Finally, positively charged polyplexes can activate the alternative complement system, which will result in enhanced uptake in the liver and spleen (*41, 49*). Lung deposition is

most likely due to aggregation of polyplexes itself or with erythrocytes or both (*4, 21*). With all Trastuzumab conjugates, lung and spleen deposition was significantly reduced compared to PEI. We assume that the nearly neutral zeta-potential and the decreased erythrocyte aggregation mainly accounted for these changes in organ distribution as well.

In summary, the composition of polyplexes affected both, in vitro specificity and in vivo pharmacokinetics. Concerning in vitro transfection efficiency and target cell specificity, PEGylation and linker chemistry were of major importance. Long PEG chains, as used in PEG(30)-PEI-Trastuzumab, hindered proper antigen recognition. The uptake of these polyplexes was decreased potentially due to the high degree of substitution. In contrast, conjugates composed of PEG-PEI with shorter PEG chains or synthesized using a PEG linker successfully transfected the target cells with high specificity. Concerning the situation in vivo, it was found that antibody modification, irrespective of the linker chemistry or the PEG-PEI copolymer used, governed pharmacokinetics and biodistribution. Antibody modification in all cases resulted in higher AUC and lower disposition in lung and spleen compared to PEI polyplexes, which is potentially due to decreased zeta-potentials, improved polyplex stability and decreased interaction with blood components.

3.6 Acknowledgments

We are grateful to Cornelia Brendel (FACS laboratory, Department of Hematology, Oncology and Immunology, University Hospital Marburg) for the generous use of equipment. We are indebted to Eva Mohr (Department of Pharmaceutics and Biopharmacy, Philipps Universität Marburg) for her technical support concerning cell culture. We are grateful to Terry Steele and Olivia Merkel (Department of Pharmaceutics and Biopharmacy, Philipps Universität Marburg) for critical review of the manuscript.

3.7 References

(1) Merdan, T., Kopecek, J., and Kissel, T. (2002) Prospects for cationic polymers in gene and oligonucleotide therapy against cancer. *Adv Drug Deliv Rev 54*, 715-58.

(2) Goula, D., Benoist, C., Mantero, S., Merlo, G., Levi, G., and Demeneix, B. A. (1998) Polyethylenimine-based intravenous delivery of transgenes to mouse lung. *Gene Ther 5*, 1291-5.

(3) Boussif, O., Lezoualc'h, F., Zanta, M. A., Mergny, M. D., Scherman, D., Demeneix, B., and Behr, J. P. (1995) A versatile vector for gene and oligonucleotide transfer into cells in culture and in vivo: polyethylenimine. *Proc Natl Acad Sci U S A 92*, 7297-301.

(4) Ogris, M., Brunner, S., Schuller, S., Kircheis, R., and Wagner, E. (1999) PEGylated DNA/transferrin-PEI complexes: reduced interaction with blood components, extended circulation in blood and potential for systemic gene delivery. *Gene Ther. 6*, 595-605.

(5) Fenske, D. B., MacLachlan, I., and Cullis, P. R. (2001) Long-circulating vectors for the systemic delivery of genes. *Curr Opin Mol Ther 3*, 153-8.

(6) Ward, C. M., Read, M. L., and Seymour, L. W. (2001) Systemic circulation of poly(L-lysine)/DNA vectors is influenced by polycation molecular weight and type of DNA: differential circulation in mice and rats and the implications for human gene therapy. *Blood 97*, 2221-9.

(7) Verbaan, F. J., Oussoren, C., Snel, C. J., Crommelin, D. J., Hennink, W. E., and Storm, G. (2004) Steric stabilization of poly(2-(dimethylamino)ethyl methacrylate)-based polyplexes mediates prolonged circulation and tumor targeting in mice. *J Gene Med 6*, 64-75.

(8) Mullen, P. M., Lollo, C. P., Phan, Q. C., Amini, A., Banaszczyk, M. G., Fabrycki, J. M., Wu, D., Carlo, A. T., Pezzoli, P., Coffin, C. C., and Carlo, D. J. (2000) Strength of conjugate binding to plasmid DNA affects degradation rate and expression level in vivo. *Biochim Biophys Acta 1523*, 103-10.

(9) Woodle, M. C. (1998) Controlling liposome blood clearance by surface-grafted polymers. *Adv Drug Deliv Rev 32*, 139-152.

(10) Kunath, K., von Harpe, A., Petersen, H., Fischer, D., Voigt, K., Kissel, T., and Bickel, U. (2002) The structure of PEG-modified poly(ethylene imines) influences biodistribution and pharmacokinetics of their complexes with NF-kappaB decoy in mice. *Pharm Res 19*, 810-7.

(11) Nguyen, H.-K., Lemieux, P., Vinogradov, S. V., Gebhart, C. L., Guérin, N., Paradis, G., Bronich, T. K., Alakhov, V. Y., and Kabanov, A. V. (2000)

Evaluation of polyether-polyethyleneimine graft copolymers as gene transfer agents. *Gene Ther. 7*, 126-138.

(12) Oupicky, D., Howard, K. A., Konak, C., Dash, P. R., Ulbrich, K., and Seymour, L. W. (2000) Steric stabilization of poly-L-Lysine/DNA complexes by the covalent attachment of semitelechelic poly[N-(2-hydroxypropyl)methacrylamide]. *Bioconjug Chem 11*, 492-501.

(13) Deshpande, M. C., Davies, M. C., Garnett, M. C., Williams, P. M., Armitage, D., Bailey, L., Vamvakaki, M., Armes, S. P., and Stolnik, S. (2004) The effect of poly(ethylene glycol) molecular architecture on cellular interaction and uptake of DNA complexes. *J Control Release 97*, 143-56.

(14) Wagner, E. (2004) Strategies to improve DNA polyplexes for in vivo gene transfer: will "artificial viruses" be the answer? *Pharm Res 21*, 8-14.

(15) Furgeson, D. Y., Yockman, J. W., Janat, M. M., and Kim, S. W. (2004) Tumor efficacy and biodistribution of linear polyethylenimine-cholesterol/DNA complexes. *Mol Ther 9*, 837-45.

(16) Germershaus, O., Merdan, T., Bakowsky, U., Behe, M., and Kissel, T. (2006) Trastuzumab-polyethylenimine-polyethylene glycol conjugates for targeting Her2-expressing tumors. *Bioconjug Chem 17*, 1190-9.

(17) Moffatt, S., Papasakelariou, C., Wiehle, S., and Cristiano, R. (2006) Successful in vivo tumor targeting of prostate-specific membrane antigen with a highly efficient J591/PEI/DNA molecular conjugate. *Gene Ther 13*, 761–772.

(18) Boeckle, S., von Gersdorff, K., van der Peipen, S., Culmsee, C., Wagner, E., and Ogris, M. (2004) Purification of polyethylenimine polyplexes highlights the role of free polycations in gene transfer. *Journal of Gene Medicine 6*, 1102-1111.

(19) Magin-Lachmann, C., Kotzamanis, G., D'Aiuto, L., Cooke, H., Huxley, C., and Wagner, E. (2004) In vitro and in vivo delivery of intact BAC DNA -- comparison of different methods. *J Gene Med 6*, 195-209.

(20) Wightman, L., Kircheis, R., Rossler, V., Carotta, S., Ruzicka, R., Kursa, M., and Wagner, E. (2001) Different behavior of branched and linear polyethylenimine for gene delivery in vitro and in vivo. *J Gene Med 3*, 362-72.

(21) Merdan, T., Kunath, K., Petersen, H., Bakowsky, U., Voigt, K. H., Kopecek, J., and Kissel, T. (2005) PEGylation of poly(ethylene imine) affects stability of complexes with plasmid DNA under in vivo conditions in a dose-dependent manner after intravenous injection into mice. *Bioconjug Chem 16*, 785-92.

(22) Hildebrandt, I. J., Iyer, M., Wagner, E., and Gambhir, S. S. (2003) Optical imaging of transferrin targeted PEI/DNA complexes in living subjects. *Gene Ther 10*, 758-64.

(23) Neu, M., Germershaus, O., Mao, S., Voigt, K. H., Behe, M., and Kissel, T. (2007) Crosslinked nanocarriers based upon poly(ethylene imine) for systemic plasmid delivery: In vitro characterization and in vivo studies in mice. *J Control Release 118*, 370-80.

(24) Petersen, H., Fechner, P. M., Martin, A. L., Kunath, K., Stolnik, S., Roberts, C. J., Fischer, D., Davies, M. C., and Kissel, T. (2002) Polyethylenimine-graft-poly(ethylene glycol) copolymers: influence of copolymer block structure on DNA complexation and biological activities as gene delivery system. *Bioconjug Chem 13*, 845-54.

(25) Merdan, T., Callahan, J., Petersen, H., Kunath, K., Bakowsky, U., Kopeckova, P., Kissel, T., and Kopecek, J. (2003) Pegylated polyethylenimine-Fab' antibody fragment conjugates for targeted gene delivery to human ovarian carcinoma cells. *Bioconjug Chem 14*, 989-96.

(26) Kircheis, R., Kichler, A., Wallner, G., Kursa, M., Ogris, M., Felzmann, T., Buchberger, M., and Wagner, E. (1997) Coupling of cell-binding ligands to polyethylenimine for targeted gene delivery. *Gene Ther 4*, 409-18.

(27) von Harpe, A. (2000) in *Department of Pharmaceutics and Biopharmacy*, Philipps-University, Marburg, Germany.

(28) Rasband, W. S. (1997-2006), U. S. National Institutes of Health, Bethesda, Maryland, USA.

(29) Kloeckner, J., Wagner, E., and Ogris, M. (2006) Degradable gene carriers based on oligomerized polyamines. *Eur J Pharm Sci 29*, 414-25.

(30) Hill, H. D., and Straka, J. G. (1988) Protein determination using bicinchonic acid in the presence of sulfhydryl reagents. *Anal Biochem 170*, 203-208.

(31) Ogris, M., Steinlein, P., Carotta, S., Brunner, S., and Wagner, E. (2001) DNA/polyethylenimine transfection particles: influence of ligands, polymer size, and PEGylation on internalization and gene expression. *AAPS PharmSci 3*, E21.

(32) Mellman, I. (1996) Endocytosis and molecular sorting. *Annu Rev Cell Dev Biol 12*, 575-625.

(33) Dash, P. R., Read, M. L., Barrett, L. B., Wolfert, M. A., and Seymour, L. W. (1999) Factors affecting blood clearance and in vivo distribution of polyelectrolyte complexes for gene delivery. *Gene Ther 6*, 643-50.

(34) Neu, T., Sitterberg, J., Bakowsky, U., and Kissel, T. (2006) Stabilized Nanocarriers for Plasmids Based Upon Cross-linked Poly(ethylene imine). *Biomacromolecules 7*, 3428-38.

(35) Lewis, G. D., Figari, I., Fendly, B., Wong, W. L., Carter, P., Gorman, C., and Shepard, H. M. (1993) Differential responses of human tumor cell lines to anti-p185HER2 monoclonal antibodies. *Cancer Immunol Immunother 37*, 255-63.

(36) Kawabata, K., Takakura, Y., and Hashida, M. (1995) The fate of plasmid DNA after intravenous injection in mice: involvement of scavenger receptors in its hepatic uptake. *Pharm Res 12*, 825-30.

(37) Koshkina, N. V., Agoulnik, I. Y., Melton, S. L., Densmore, C. L., and Knight, V. (2003) Biodistribution and pharmacokinetics of aerosol and intravenously administered DNA-polyethyleneimine complexes: optimization of pulmonary delivery and retention. *Mol Ther 8*, 249-54.

(38) Kunath, K., von Harpe, A., Fischer, D., Petersen, H., Bickel, U., Voigt, K., and Kissel, T. (2003) Low-molecular-weight polyethylenimine as a non-viral vector for DNA delivery: comparison of physicochemical properties, transfection efficiency and in vivo distribution with high-molecular-weight polyethylenimine. *J Control Release 89*, 113-25.

(39) Kircheis, R., Wightman, L., Schreiber, A., Robitza, B., Rossler, V., Kursa, M., and Wagner, E. (2001) Polyethylenimine/DNA complexes shielded by transferrin target gene expression to tumors after systemic application. *Gene Ther 8*, 28-40.

(40) Ward, C. M., Pechar, M., Oupicky, D., Ulbrich, K., and Seymour, L. W. (2002) Modification of pLL/DNA complexes with a multivalent hydrophilic polymer permits folate-mediated targeting in vitro and prolonged plasma circulation in vivo. *J Gene Med 4*, 536-47.

(41) Plank, C., Mechtler, K., Szoka, F. C., Jr., and Wagner, E. (1996) Activation of the complement system by synthetic DNA complexes: a potential barrier for intravenous gene delivery. *Hum Gene Ther 7*, 1437-46.

(42) Fischer, D. (2005) In vivo fate of polymeric gene carriers, in *Biomaterials for Delivery and Targeting of Proteins and Nucleic Acids* (Mahato, R. I., Ed.) pp 295-321, CRC Press.

(43) Sharma, V. K., Thomas, M., and Klibanov, A. M. (2005) Mechanistic studies on aggregation of polyethylenimine-DNA complexes and its prevention. *Biotechnol Bioeng 90*, 614-20.

(44) Strehblow, C., Schuster, M., Moritz, T., Kirch, H. C., Opalka, B., and Petri, J. B. (2005) Monoclonal antibody-polyethyleneimine conjugates targeting Her-2/neu or CD90 allow cell type-specific nonviral gene delivery. *J Control Release 102*, 737-47.

(45) Kunath, K., Merdan, T., Hegener, O., Haberlein, H., and Kissel, T. (2003) Integrin targeting using RGD-PEI conjugates for in vitro gene transfer. *J Gene Med 5*, 588-99.

(46) de Wolf, H. K., Snel, C. J., Verbaan, F. J., Schiffelers, R. M., Hennink, W. E., and Storm, G. (2007) Effect of cationic carriers on the pharmacokinetics and tumor localization of nucleic acids after intravenous administration. *Int J Pharm 331*, 167-75.

(47) Nishikawa, M., Takakura, Y., and Hashida, M. (2005) Theoretical considerations involving the pharmacokinetics of plasmid DNA. *Advanced Drug Delivery Reviews 57*, 675-688.

(48) de Wolf, H. K., Luten, J., Snel, C. J., Oussoren, C., Hennink, W. E., and Storm, G. (2005) In vivo tumor transfection mediated by polyplexes based on biodegradable poly(DMAEA)-phosphazene. *J Control Release 109*, 275-87.

(49) Fischer, D., Osburg, B., Petersen, H., Kissel, T., and Bickel, U. (2004) Effect of poly(ethylene imine) molecular weight and pegylation on organ distribution and pharmacokinetics of polyplexes with oligodeoxynucleotides in mice. *Drug Metab Dispos 32*, 983-92.

4 Establishment and Characterization of a HER2 Tumor Model in SCID Mice and In Vivo Gene Delivery using PEI- and PEI-PEG-Trastuzumab Polyplexes

4.1 Abstract

The aim of this study was A) to establish an in vivo tumor model showing HER2 overexpression and B) to test Trastuzumab targeted PEG-PEI/pDNA vectors for their ability to target tumors in vivo. To establish a tumor model, different HER2 overxpressing cell lines were tested for their ability to generate tumors after subcutaneous injection. Tumors were characterized with respect to their macroscopic and microscopic appearance, their vascularization and HER2 expression. For comparison, Neuro2A tumors, which are an established tumor model for in vivo transfection studies, were used. Compared to Neuro2A, SK-OV-3 tumor tissue appeared to be denser and tumors were surrounded by large blood vessels. In contrast to Neuro2A, fewer capillaries and small blood vessels were found within the tumor tissue in SK-OV-3 by microscopy. These results were verified using anti-CD31 immunofluorescence. HER2 expression levels were studied by immunofluorescence as well and overexpression was only found in SK-OV-3 cells. Trastuzumab-PEG-PEI/pDNA polyplexes were injected into the tail vein and transfection efficiency in main organs and the tumor was compared to non-targeted PEI. Targeted polyplexes failed to selectively transfect the tumors in these experiments. In a second approach, polyplexes were administered by intratumoral injection. In this case, targeted polyplexes showed only a slightly increased efficiency compared to PEI.

4.2 Introduction

One goal of in vivo gene delivery is efficient and specific transfection of distant tissues, such as tumors or disseminated metastasis. Viral vectors, although producing high levels of transduction, have many disadvantages in this direction: Viral vectors are difficult to prepare, lack the ability to be targeted to distinct tissues or cell species, and have drawbacks regarding cytotoxicity and immunogenicity (*1, 2*). Therefore, non-viral vector are regarded as a promising alternative (*3, 4*). Polyethylenimine, one of the most cited polycations for non-viral gene delivery, was not only successfully utilized as transfection reagent in vitro but also proofed to be efficient after intravenous injection in vivo (*5-7*). However, it was repeatedly documented that intravenous injection of unmodified PEI polyplexes results in accumulation of the vector mainly in the lung and liver (*8-10*). A possible solution for this problem is to modify PEI with hydrophilic polymers such as polyethylenglycol (PEG) or poly(*N*-(2-hydroxypropyl)methacrylamide) (pHPMA) (*11, 12*). It was shown for liposomes that PEGylation strongly increased blood circulation times due to decreased unspecific interactions (*13*). However, grafting of PEI with PEG did not in every case result in increased blood levels of polyplexes (*8, 14*). It was hypothesized by de Wolf et al. that polyplexes prepared with PEG-PEI copolymers are still prone to efficient opsonization and therefore prolongation of blood residence time is relatively small compared to results found with PEG-liposomes (*10*). In addition to sufficiently long circulation times in blood, polyplexes need to specifically bind to the desired target tissue. Antibody conjugation was shown to be exceptionally suitable to target PEI polyplexes to a certain tissue (*5*). Furthermore, it was recently shown by us that antibody modification not only potentially increases specificity of vectors but also resulted in increased area under the curve of intravenously injected polyplexes (see chapter 3). Therefore, we sought to study targeting of a subcutaneously growing, HER2 overexpressing tumor with conjugates characterized in chapter 3.

Tumor models that overexpress HER2 are only rarely described in the literature (*15-19*). None of these models was used for transfection studies using PEI polyplexes after intravenous administration. Furthermore, in most of these studies BT-474 cells were injected in SCID mice, which previously received sustained release estradiol pellets. However, this procedure is not in accordance with the application for animal studies in our lab.

Therefore, we sought to screen different HER2 expressing cell lines for their ability to form subcutaneous tumors in SCID mice. The resulting tumors were then macroscopically, histologically and immunonologically characterized. Then, PEI and PEI-PEG-Trastuzumab polyplexes were used to study transfection efficiency after intravenous and intratumoral injection.

4.3 Materials and Methods

Cell Culture. SK-OV-3, BT-474 and SK-BR-3 cells were obtained from ATCC (Manassas, VA, USA) and cultured in Dulbecco's modified Eagle's medium with 4 mM L-glutamine, 4.5 g/L glucose and 10% fetal calf serum (FCS). Cells were collected for injection by washing with PBS without Ca^{2+} and Mg^{2+} and adding trypsin-EDTA to the plate for 5 min at 37 C.

Mouse Tumor Model. All animal procedures were approved and controlled by the local ethics committee and carried out according to the guidelines of the German law of protection of animal life. Female SCID mice were kept in a barrier room under permanent sterile conditions and had continual access to food and water, which were taken ad libitum. Throughout the experiment mice were housed in laminar flow racks under specific pathogen-free conditions, and were monitored daily for general health status. All animals were shaved on the right flank and injected subcutaneously with five million cells in 150 µl (70 µl cell suspension in PBS mixed with 70 µl Matrigel Matrix HC, BD Biosciences). SK-OV-3 tumors grew predictably in all mice and reached a size of 9-11 mm diameter in 10-14 days after injection. The size of the tumor was measured with a digital caliper in three dimensions.

Histology. For histology of tumor tissue, tumors were placed in 4% formalin in phosphate-buffered saline (PBS) for 24 hours prior to being dehydrated in graded solutions of alcohol and xylene and embedded in paraffin. After embedding, 5 µm sections were cut with a RM2265 microtome (Leica, Wetzlar, Germany), and mounted on Superfrost Microscope slides (Menzel, Brausnchweig, Germany). Slides were incubated at 60°C over night. For hematoxylin and eosin (H&E) staining, tissue sections on slides were deparaffinized in xylene for 10 minutes, hydrated in a series of ethanol solutions (100%, 90%, 70%) for 3 minutes each, rinsed in PBS for 2 minutes, stained with hematoxylin

for 20 seconds, and then rinsed in distilled water until excess stain was removed. Tissue sections were then counterstained in an eosin solution for ten minutes, and rinsed in distilled water until excess stain was removed. Tissue sections were dsehydrated in a series of ethanol solutions (70%, 90%, 100%) for 3 minutes each, and then incubated in xylene for 1 minute prior to being coverslipped using Histofluid (Marienfeld, Lauda-Königshofen, Germany).

Immunofluorescence staining. After dissection, tumors were immediately placed in Tissue-Tek mounting medium followed by freezing at -80 C. Sections were cut 5 µm thick on a cryotome (CM3050 S, Leica, Wetzlar, Germany). For immunofluorescence staining microsections were fixed with formaldehyde 4% for 10 min and blocked with PBS/2% FCS for 10 min. For specific staining of endothelial cells, slides were incubated for 2 h with the primary antibody: anti-mouse CD31 [rat], Pharmingen, diluted 1:200. After washing, slides were incubated for 1 h with the secondary antibody: anti-rat Alexa 467, diluted 1:200. Similarly, murine macrophages were stained using a FITC conjugated rat anti mouse F4/80 antibody (Serotec) diluted 1:20. The same procedure was used for HER2 specific staining of tumor sections. Trastuzumab was used as a primary antibody and detected using a FITC-anti-human antibody (Sigma, Taufkirchen, Germany). Finally, sections were stained with DAPI (1 µg/mL) for 20 minutes. Sections were mounted with FluorSave mounting medium, and evaluated under a Zeiss Axiovert 200 fluorescence microscope equipped with an Axiocam CCD camera or a Zeiss Axiovert 100 M fluorescence microscope equipped with a LSM 510 confocal laser scanning device in the case of HER2 staining.

Polyplex preparation and application in tumor-bearing mice. DNA and polymers were diluted in a 1:1 mixture of HBS and HBG, mixed in equal parts and incubated for 10 min at RT before application. In all experiments an N/P ratio of 6 was used. For intravenous injections transfection complexes containing 50 µg DNA in 250 µl were used. In the case of intratumoral application, 100 µl of polyplex solution containing 25 µg DNA were slowly injected into the tumor using an insulin syringe (BD Ultra-Fine, BD Biosciences).

Photon Correlation Spectroscopy: Hydrodynamic diameters of freshly prepared polyplexes were determined using a Zetasizer Nano ZS (Malvern Instruments, Herrenberg,

Germany) equipped with a 4 mW He-Ne laser at a wavelength of 633 nm at 25 °C. Scattered light was detected at a 173° backward scattering angle. The viscosity and refractive index of water at 25 °C was used for data analysis.

Luciferase reporter gene expression in vivo. Animals were sacrificed and organs were resected and homogenized in lysis buffer (Promega, Mannheim, Germany) using an IKA-Homogenizer, snap frozen in liquid nitrogen and stored at -80 °C. The tissue lysates were centrifuged at 4000 g for 10 min at 4 °C to pellet debris. Luciferase activity of an aliquot of the sample was measured for 30 s on a LB9507 luminometer (Berthold, Bad Wildbad, Germany) using a commercial kit (Luciferase Assay System, Promega). Protein concentration was determined using a modified commercial kit (BCA Assay, Pierce) and transfection efficiency was expressed as pg of luciferase per mg of protein (*20*).

4.4 Results and Discussion

4.4.1 Establishment and characterization of a HER2 overexpressing tumor model.

To study HER2 targeted polyplexes in vivo, a tumor model showing HER2 overexpression was developed in SCID mice and tumors were characterized. To augment growth of tumors, Matrigel^{TM} HC was used as a 1:1 mixture with $5x10^6$ tumor cells. The HER2 overexpressing cell lines SK-BR-3, SK-OV-3 and BT-474 were tested for their ability to form tumors in SCID mice after subcutaneous injection. Only SK-OV-3 cells formed tumors of sufficient size and growth rate under these conditions. After injection of $5x10^6$ cells, mice developed tumors with diameters of about 9-11 mm within 10 to 14 days. SK-OV-3 tumors were compared to a well established tumor model, Neuro2A, concerning macroscopic appearance, histology, vascularization and HER2 expression (*6, 21*).

Tumors were macroscopically evaluated concerning tumor structure and vascularization (Figure 1). Both tumors showed no necrotic areas and no cavitation. However, tumor tissue of SK-OV-3 tumors appeared to be more rigid and dense compared to Neuro2A tumors. SK-OV-3 tumors were surrounded by large blood vessels but tumor tissue itself was only sparsely vascularized. In contrast, Neuro2A tumors showed lesser large blood vessels surrounding the tumor but a higher vascularization of tumor tissue.

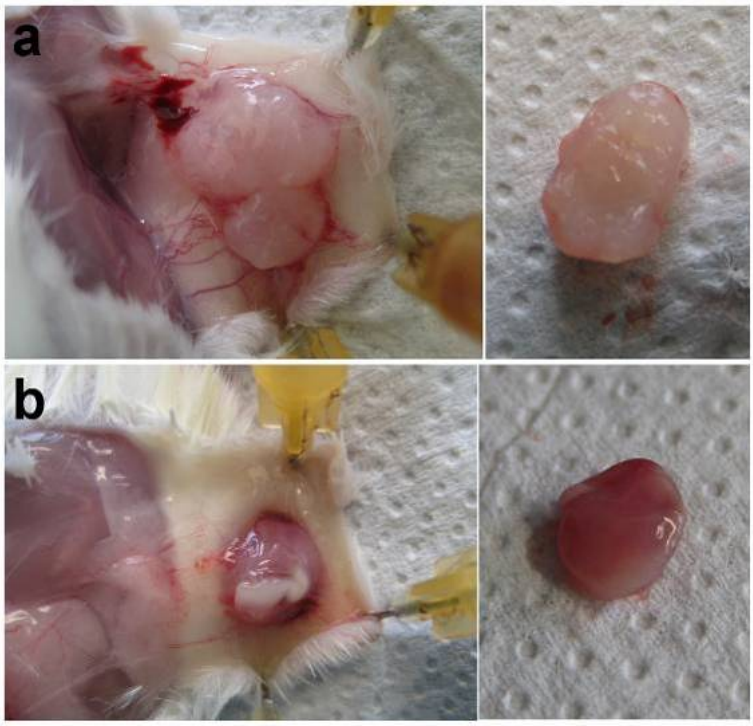

Figure 1. Dissections of SK-OV-3 (a) and Neuro2A (b) tumors showing the macroscopic appearance and internal structure (tumors cut in half).

Tumor fine structure was evaluated on 5 µm sections of paraffin embedded and hematoxylin and eosin (H&E) stained tissues (Figure 2). Again, SK-OV-3 tumors showed a dense inner structure with large amounts of connective tissue while Neuro2A tumors were only loosely organized. Both, SK-OV-3 and Neuro2A tumors showed no necrotic areas. Microvascularization of tumor tissue was also evaluated in H&E stained sections. We found large amounts of capillaries and small blood vessels in Neuro2A tumors. Vascularization of SK-OV-3 tumors was less distinct with only few small blood vessels and capillaries which were mainly associated with connective tissue.

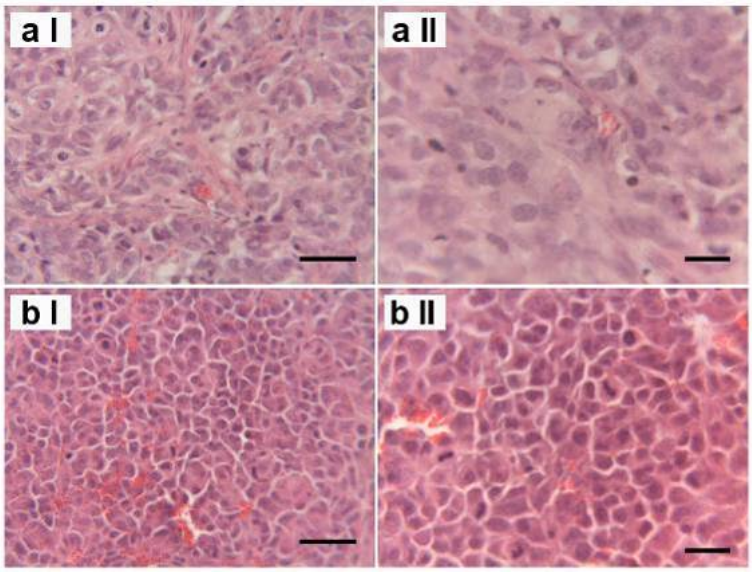

Figure 2. Histology of hematoxylin and eosin stained 5 µm sections of SK-OV-3 (a) and Neuro2A (b) tumors at 25x (I, scale bar represents 50 µm) and 40x (II, scale represents 20 µm) magnification

Tumor vascularization and macrophage infiltration was previously found to be of high importance for the efficiency of gene delivery via the intravenous route. A low vascularization and/or significant macrophage infiltration strongly reduced the efficacy of PEI/DNA polyplexes as well as of transferrin- and EGF-targeted PEI vectors (*21*).

Vascularization of tumors was studied in detail using immunofluorescence staining with CD31 as a primary antibody to detect endothelial cells (Figure 3). Observations made with H&E stained tissue sections were verified using this technique. SK-OV-3 tumors showed medium vascularization consisting mainly of mature blood vessels. In contrast, Neuro2A tumors were nerved with capillaries and immature and discontinuous type blood vessels (compare Figure 2 b and Figure 3). No significant macrophage infiltration was found in both tumors (data not shown).

HER2 expression was studied in cryosections of tumor tissue by immunofluorescence using Trastuzumab as a primary antibody. Again, HER2 negative Neuro2A tumors served as a control (Figure 4). In SKOV-3 tumors the entire tumor mass, excluding connective tissue and blood vessels, was stained positive for HER2. In contrast, Neuro2A tumors showed no HER2 expression.

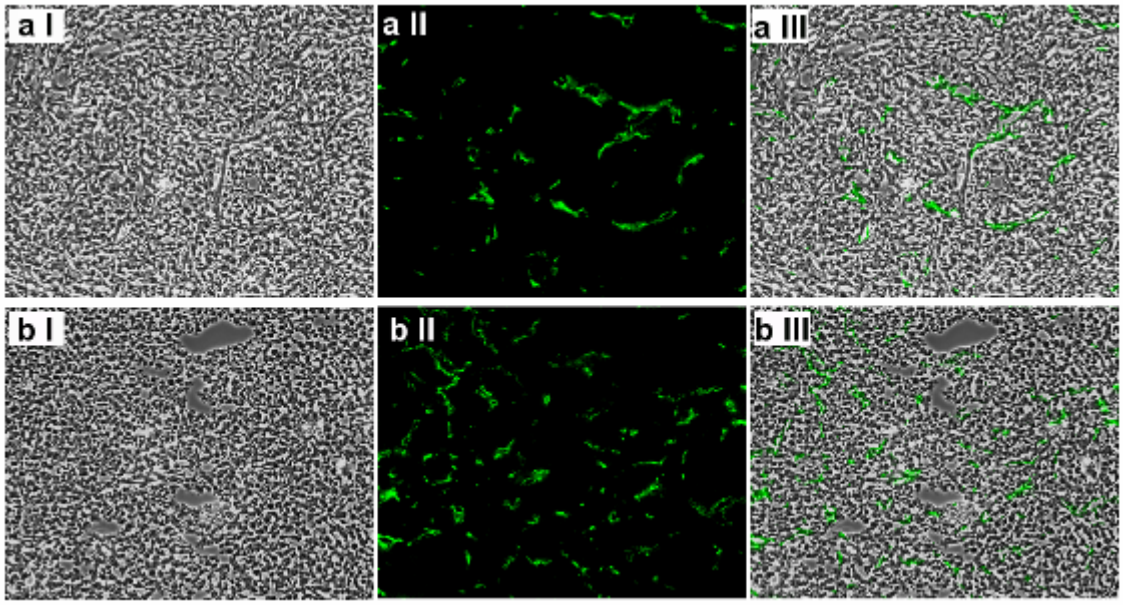

Figure 3. Immunohistochemistry of 5 µm cryosections of SK-OV-3 (a) and Neuro2A (b) tumors. Phase contrast transmitted light image (I), anti-CD31 antibody and secondary Alexa 647-antibody (II) and merge (III).

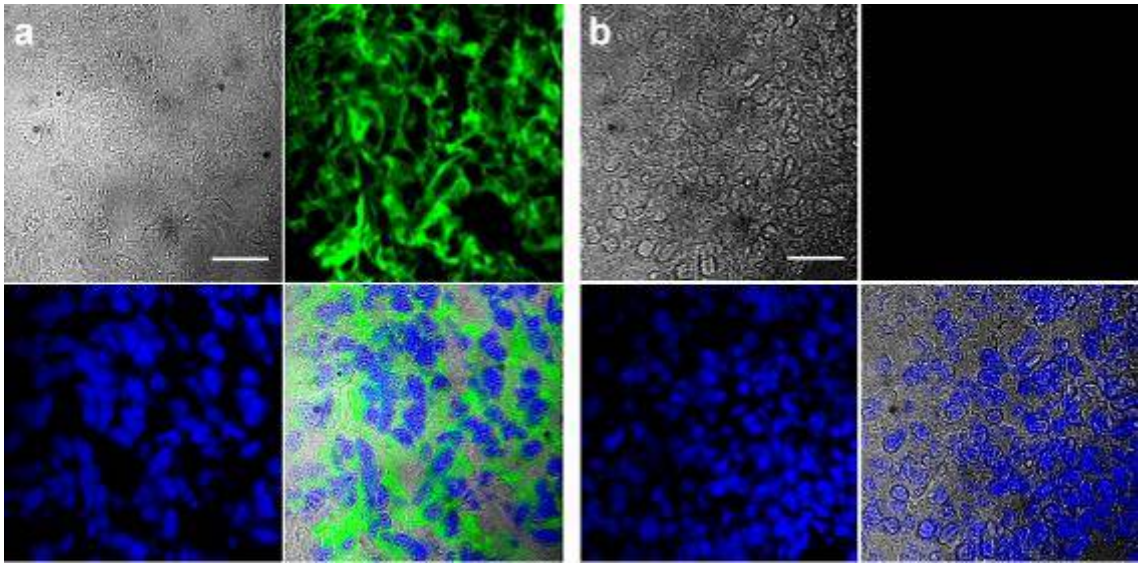

Figure 4. Immunohistochemistry of 5 µm cryosections of SKOV-3 (a) and Neuro2A (b) tumors. HER2 was detected using Trastuzumab as primary and anti-human-FITC as secondary antibody (Bar represents 30 µm). Transmitted light image (upper left), HER2 staining (upper right), staining of nuclei (lower left) and merge (lower right) are shown.

4.4.2 In vivo studies using unmodified PEI and PEI-PEG-Trastuzumab polyplexes

The primary aim of developing a HER2 targeted gene delivery system was to study the efficiency of targeted non-viral vectors after systemic application. Pharmacokinetics and biodistribution of these vectors were studied in mice and showed promising results compared to both unmodified PEI polyplexes and free DNA (see Chapter 3). Therefore, the targeting effect of PEI modified with Trastuzumab via a heterobifunctional PEG linker of 2 kDa was studied using the HER2 overexpressing tumor model characterized above.

Polyplex sizes were determined in 0.5 x HBS by photon correlation spectroscopy. All polyplexes under these conditions formed polyplexes in the range of 180 to 240 nm (Figure 5). Therefore, these polyplexes were regarded suitable for endosomal uptake on one hand and intravenous administration on the other hand.

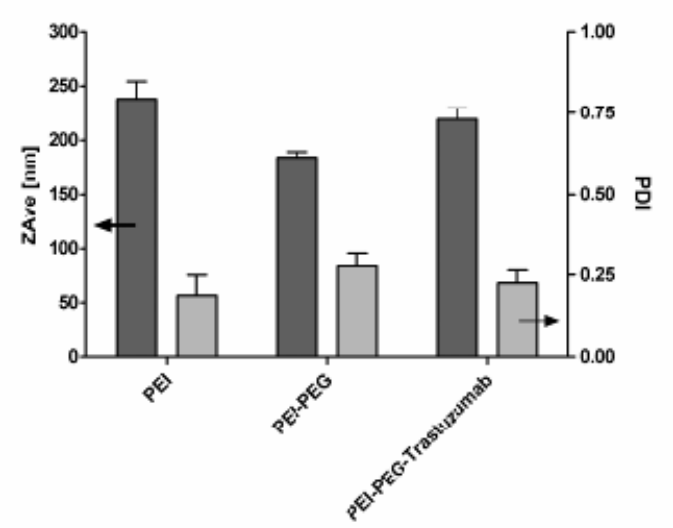

Figure 5: Hydrodynamic diameters and polydispersity indices of PEI, PEI-PEG and PEI-PEG-Trastuzumab polyplexes with pDNA at N/P 6 determined in 0.5 x HBS buffer.

In the first attempt, polyplexes containing 50 µg luciferase-encoding plasmid were administered intravenously via the tail vein. Signs of acute toxicity or lethality after treatment as described by Merdan et al. and Ogris et al. were not observed in our study (*8, 22*). Polyplex injections were well tolerated in all cases. Luciferase expression in main organs and tumor are shown in Figure 6. However, significant luciferase expression was only found in the lung after administration of unmodified PEI polyplexes. As expected, PEG-shielded conjugate polyplexes showed no unspecific transfection of the lung or

other main organs (*8*). But neither PEI nor PEI-PEG-Trastuzumab polyplexes generated significant luciferase expression in the tumor. It was shown by Smrekar et al. that vascularization and macrophage infiltration of tumor tissue are important determinants for the efficiency of non-viral gene delivery systems in vivo. In this study, only well vascularized tumors showing low macrophage infiltration could be transfected efficiently (*21*). To explain our findings we hypothesize that tumor tissue of SK-OV-3 tumors is too sparsely vascularized and especially lacks immature blood vessels and capillaries. Therefore, the tumor vasculature lacks increased permeability as found in Neuro2A tumors. This hypothesis is supported by characterization of tumor tissue described above and by findings of Kong et al. (*23*). The authors investigated extravasation of 100 nm liposomes from tumor microvasculature in vivo in an athymic nude mouse dorsal skin flap window chamber model. In this study no extravasation of liposomes into the tumor interstitium was observed under normothermic conditions.

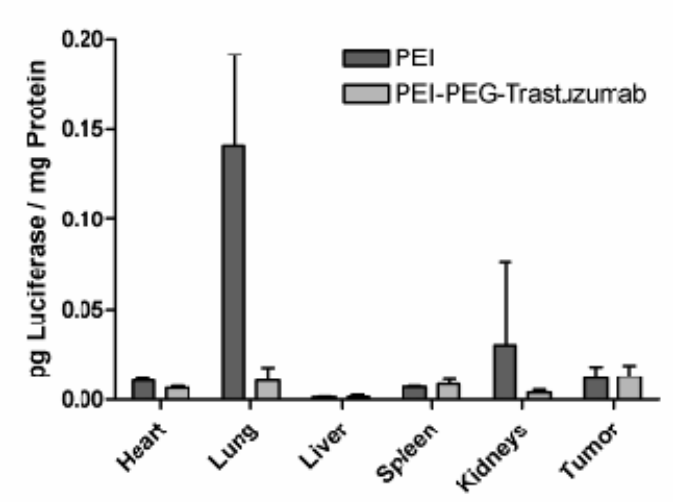

Figure 6: Luciferase expression in the main organs and tumor 48 hours after intravenous application of PEI and PEI-PEG-Trastuzumab polyplexes at N/P 6 and a dose of 50 µg pDNA per mouse.

In a second approach, targeting of HER2 expressing SK-OV-3 tumors was tested by intratumoral administration of polyplexes. For this purpose, 25 µg pDNA were complexed with either PEI or PEI-PEG-Trastuzumab at N/P 6 in a total volume of 100 µl. After 10 minutes incubation, polyplex solution was slowly injected into the tumors using an insulin syringe. The results are shown in Figure 7. A high variability of transfection efficiency was found which is potentially due to low reproducibility of intratumoral

injections. However, using PEI-PEG-Trastuzumab conjugates transfection of the tumor tissue was slightly improved compared to PEI polyplexes, but differences were not statistically significant. A possible solution for this dilemma might be to increase the number of animals per group.

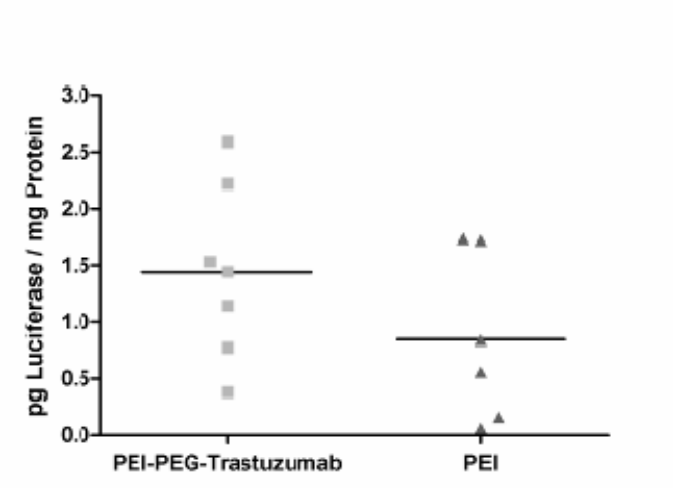

Figure 7. Luciferase reporter gene expression in the tumor 24 hours after intratumoral application of PEI and PEI-PEG-Trastuzumab polyplexes at a dose of 25 µg pDNA per mouse.

To solve all these problems, the current system needs several improvements. Obviously, the chosen tumor model is not perfectly suitable for HER2 targeting of nonviral vectors via the intravenous route. The use of either a BT-474 tumor model (in combination with implantation of an estradiol pellet) or MCF-7 cells stably transfected with HER2 might help to solve these problems (*17, 24*). However, an important question one might raise at this point is which tumor model is able to mimic the situation in patients. In reality one might face situations ranging from easily accessible tumors (represented by Neuro2A tumor model) to tumors showing lower or no accessibility (as in the case of SK-OV-3 tumor model). This issue should be addressed when approaching a specific target tissue and designing an appropriate in vivo model. Secondly, transfection particles need further improvement. Circulation times of targeted vectors were significantly increased compared to non-targeted PEI polyplexes in one of our previous studies (see chapter 3). Nevertheless, polyplex half-life in blood remains to be extremely short compared to PEGylated liposomes (*13*). De Wolf et al. hypothesized that the so called post-PEGylation approach might, at least in part, be a solution for this problem (*10*). However, from our point of view, this approach also has some drawbacks regarding purifica-

tion and characterization of polyplexes, especially in a clinical setting. Another possible improvement might involve additional stabilization of polyplexes by surface-crosslinking as described by Neu et al. (*25, 26*). But in this case again subsequent purification procedures and the necessity to use organic solvents are challenging formulation problems especially regarding later use in humans.

4.5 Conclusion

In this study a tumor model showing HER2 overexpression was successfully developed. SK-OV-3 tumors grew predictably in a time frame of 2 weeks after injection. Furthermore, we intensively characterized tumors with respect to macroscopic appearance, histology, vascularization and HER2 expression. Results were compared to a well established tumor model Neuro2A. SK-OV-3 tumors in these experiments showed significant differences to Neuro2A concerning tumor structure as well as vascularization. Intravenous injection of targeted polyplexes did not result in efficient transfection neither of the tumor nor any other organ. Therefore, targeting via intratumoral injection was evaluated. Using this technique, achieving robust results proved to be far more difficult than with intravenous injection. PEI-PEG-Trastuzumab polyplexes tended to be more effective than PEI polyplexes in these experiments, but differences were not significant.

In general, this study is regarded as a first step towards in vivo targeting of Trastuzumab decorated PEI vectors. Basic knowledge on techniques and underlying problems of establishment of tumor models and major obstacles in in vivo gene delivery was gathered. This knowledge is hoped to trigger further rational design of tumor models as well as of vector systems and finally might result in efficient targeted gene delivery in vivo.

4.6 Acknowledgments

We are indebted to Nicole Tietze, Manfred Ogris and Ernst Wagner (Dept. Pharmaceutical Biology-Biotechnology, LMU München, Germany) for many valuable contributions in terms of scientific discussions, technical assistance and use of equipment and facilities.

4.7 References

(1) Rochlitz, C. F. (2001) Gene therapy of cancer. *Swiss Med Wkly 131*, 4-9.

(2) Brown, M. D., Schatzlein, A. G., and Uchegbu, I. F. (2001) Gene delivery with synthetic (non viral) carriers. *Int J Pharm 229*, 1-21.

(3) Liu, F., and Huang, L. (2002) Development of non-viral vectors for systemic gene delivery. *J Control Release 78*, 259-66.

(4) Boussif, O., Zanta, M. A., and Behr, J. P. (1996) Optimized galenics improve in vitro gene transfer with cationic molecules up to 1000-fold. *Gene Ther 3*, 1074-80.

(5) Moffatt, S., Papasakelariou, C., Wiehle, S., and Cristiano, R. (2006) Successful in vivo tumor targeting of prostate-specific membrane antigen with a highly efficient J591/PEI/DNA molecular conjugate. *Gene Ther 13*, 761–772.

(6) Kircheis, R., Wightman, L., Schreiber, A., Robitza, B., Rossler, V., Kursa, M., and Wagner, E. (2001) Polyethylenimine/DNA complexes shielded by transferrin target gene expression to tumors after systemic application. *Gene Ther 8*, 28-40.

(7) Kircheis, R., Blessing, T., Brunner, S., Wightman, L., and Wagner, E. (2001) Tumor targeting with surface-shielded ligand--polycation DNA complexes. *J Control Release 72*, 165-70.

(8) Merdan, T., Kunath, K., Petersen, H., Bakowsky, U., Voigt, K. H., Kopecek, J., and Kissel, T. (2005) PEGylation of poly(ethylene imine) affects stability of complexes with plasmid DNA under in vivo conditions in a dose-dependent manner after intravenous injection into mice. *Bioconjug Chem 16*, 785-92.

(9) Jeong, G. J., Byun, H. M., Kim, J. M., Yoon, H., Choi, H. G., Kim, W. K., Kim, S. J., and Oh, Y. K. (2006) Biodistribution and tissue expression kinetics of plasmid DNA complexed with polyethylenimines of different molecular weight and structure. *J Control Release*.

(10) de Wolf, H. K., Snel, C. J., Verbaan, F. J., Schiffelers, R. M., Hennink, W. E., and Storm, G. (2007) Effect of cationic carriers on the pharmacokinetics and tumor localization of nucleic acids after intravenous administration. *Int J Pharm 331*, 167-75.

(11) Petersen, H., Fechner, P. M., Martin, A. L., Kunath, K., Stolnik, S., Roberts, C. J., Fischer, D., Davies, M. C., and Kissel, T. (2002) Polyethylenimine-graft-poly(ethylene glycol) copolymers: influence of copolymer block structure on DNA complexation and biological activities as gene delivery system. *Bioconjug Chem 13*, 845-54.

(12) Oupicky, D., Ogris, M., Howard, K. A., Dash, P. R., Ulbrich, K., and Seymour, L. W. (2002) Importance of lateral and steric stabilization of polyelectrolyte gene delivery vectors for extended systemic circulation. *Mol Ther 5*, 463-72.

(13) Woodle, M. C. (1998) Controlling liposome blood clearance by surface-grafted polymers. *Adv Drug Deliv Rev 32*, 139-152.

(14) de Wolf, H. K., Luten, J., Snel, C. J., Oussoren, C., Hennink, W. E., and Storm, G. (2005) In vivo tumor transfection mediated by polyplexes based on biodegradable poly(DMAEA)-phosphazene. *J Control Release 109*, 275-87.

(15) Gilbert, C. W., McGowan, E. B., Seery, G. B., Black, K. S., and Pegram, M. D. (2003) Targeted prodrug treatment of HER-2-positive breast tumor cells using trastuzumab and paclitaxel linked by A-Z-CINN Linker. *J Exp Ther Oncol 3*, 27-35.

(16) Park, J. W., Hong, K., Carter, P., Asgari, H., Guo, L. Y., Keller, G. A., Wirth, C., Shalaby, R., Kotts, C., Wood, W. I., et al. (1995) Development of anti-p185HER2 immunoliposomes for cancer therapy. *Proc Natl Acad Sci U S A 92*, 1327-31.

(17) Kirpotin, D. B., Drummond, D. C., Shao, Y., Shalaby, M. R., Hong, K., Nielsen, U. B., Marks, J. D., Benz, C. C., and Park, J. W. (2006) Antibody targeting of long-circulating lipidic nanoparticles does not increase tumor localization but does increase internalization in animal models. *Cancer Res 66*, 6732-40.

(18) Nielsen, U. B., Kirpotin, D. B., Pickering, E. M., Hong, K., Park, J. W., Refaat Shalaby, M., Shao, Y., Benz, C. C., and Marks, J. D. (2002) Therapeutic efficacy of anti-ErbB2 immunoliposomes targeted by a phage antibody selected for cellular endocytosis. *Biochim Biophys Acta 1591*, 109-118.

(19) Urban-Klein, B., Werth, S., Abuharbeid, S., Czubayko, F., and Aigner, A. (2005) RNAi-mediated gene-targeting through systemic application of polyethylenimine (PEI)-complexed siRNA in vivo. *Gene Ther 12*, 461-6.

(20) Hill, H. D., and Straka, J. G. (1988) Protein determination using bicinchonic acid in the presence of sulfhydryl reagents. *Anal Biochem 170*, 203-208.

(21) Smrekar, B., Wightman, L., Wolschek, M. F., Lichtenberger, C., Ruzicka, R., Ogris, M., Rodl, W., Kursa, M., Wagner, E., and Kircheis, R. (2003) Tissue-dependent factors affect gene delivery to tumors in vivo. *Gene Ther 10*, 1079-88.

(22) Ogris, M., Brunner, S., Schuller, S., Kircheis, R., and Wagner, E. (1999) PEGylated DNA/transferrin-PEI complexes: reduced interaction with blood components, extended circulation in blood and potential for systemic gene delivery. *Gene Ther. 6*, 595-605.

(23) Kong, G., Braun, R. D., and Dewhirst, M. W. (2001) Characterization of the effect of hyperthermia on nanoparticle extravasation from tumor vasculature. *Cancer Res 61*, 3027-32.

(24) Pegram, M., and Ngo, D. (2006) Application and potential limitations of animal models utilized in the development of trastuzumab (Herceptin): a case study. *Adv Drug Deliv Rev 58*, 723-34.

(25) Neu, M., Germershaus, O., Mao, S., Voigt, K. H., Behe, M., and Kissel, T. (2007) Crosslinked nanocarriers based upon poly(ethylene imine) for systemic plasmid delivery: In vitro characterization and in vivo studies in mice. *J Control Release 118*, 370-80.

(26) Neu, T., Sitterberg, J., Bakowsky, U., and Kissel, T. (2006) Stabilized Nanocarriers for Plasmids Based Upon Cross-linked Poly(ethylene imine). *Biomacromolecules 7*, 3428-38.

5 Gene Delivery using Chitosan, Trimethyl Chitosan or Polyethylenglycol-graft-Trimethyl Chitosan Block Copolymers: Establishment of Structure-Activity Relationships in Vitro

Published in Journal of Controlled Release 125 (2008) 145-154

5.1 Abstract

Chitosan, trimethyl chitosan or polyethylenglycol-graft-trimethyl chitosan/DNA complexes were characterized concerning physicochemical properties such as hydrodynamic diameter, condensation efficiency and DNA release. Furthermore, cytotoxicity of polymers and uptake- and transfection efficiency of polyplexes were evaluated in vitro. Under conditions found in cell culture, formation of aggregates of ~1000 nm and strongly decreased DNA condensation efficiency was observed in the case of chitosan polyplexes. These characteristics resulted in only 7% cellular uptake in NIH/3T3 cells and low transfection efficiencies in 4 different cell lines. By contrast, quaternization of chitosan strongly reduced aggregation tendency and pH dependency of DNA complexation. Accordingly, cellular uptake was increased 8.5-fold compared to chitosan polyplexes resulting in up to 678-fold increased transfection efficiency in NIH/3T3 cells. Apart from reduction of the cytotoxicity, PEGylation led to improved colloidal stability of polyplexes and significantly increased cellular uptake compared to unmodified trimethyl chitosan. These improvements resulted in a significant, up to 10-fold increase of transfection efficiency in NIH/3T3, L929 and MeWo cells compared to trimethyl chitosan. This study not only highlights the importance of investigating polyplex stability under different pH- and ionic strength conditions but also elucidates correlations between physicochemical characteristics and biological efficacy of the studied polyplexes.

5.2 Introduction

Chitosan (poly[β-(1-4)-2-amino-2-deoxy-D-glucopyranose]) is a biodegradable biopolymer emerging as a promising non-viral vector for gene delivery (*1*). Chitosan is derived by partial deacetylation of the naturally occurring polysaccharide chitin from crustacean shells. Due to its low toxicity and biocompatibility, chitosan received increasing attention as a versatile excipient. Besides its application in non-viral gene delivery, it was applied in such diverse fields as intestinal delivery of protein drugs, tissue engineering and vaccine delivery (*2-4*).

Due to its apparent pK_a of 6.5, chitosan is only soluble under acidic solutions (*1*). This property causes several problems in the formulation of chitosan/DNA complexes (polyplexes). Typically, complexes of plasmid DNA (pDNA) and chitosan have to be prepared in acidic buffers with low ionic strength. Under these conditions, formation of small and stable polyplexes was reported (*5*). However, only few authors investigated the behavior of the resulting polyplexes under physiologic conditions, e.g. as found after addition to the cell culture media (*6-8*). The development of particle size, zetapotential and polyplex stability in physiologic media are of special importance for cellular uptake and consequently for transfection efficiency. Furthermore, it was shown that chitosan/pDNA polyplexes are highly stable and that release of pDNA is not easily achieved (*6, 9*). It was suggested that this property might contribute to a sustained release of pDNA, leading to a prolonged reporter gene expression compared to standard vectors like polyethylenimine or Lipofectamine® (*9*). Nevertheless, in vitro transfection efficiency of chitosan polyplexes remains poor compared to the above mentioned standards (*10-12*).

To overcome these drawbacks, quaternized chitosan (trimethyl chitosan, TMC) oligomers were used to prepare polyplexes (*10*). These polymers efficiently condensed DNA and formed small polyplexes even at neutral pH. Furthermore, TMC/pDNA complexes increased transfection efficiency 5 to 131-fold compared to naked DNA, whereas efficiency of chitosan polyplexes was only 2 to 4-fold increased (*10*).

In our department, quaternized derivates based on depolymerized chitosan of different molecular weight were synthesized (*13*). To further improve solubility and biocompatibility, a set of polyethylenglycol (PEG) grafted trimethyl chitosan polymers with varying PEG molecular weight and grafting ratio was prepared (*14*). Mao et al. showed that PEG-trimethyl chitosan efficiently complexes insulin and that complexes are readily taken up by Caco-2 cells (*15*).

We now extend this concept to non-viral gene delivery. We hypothesized that hydrodynamic diameters of the complexes affect the efficiency of polyplex uptake, which is one of the major hurdles in the transfection process. As mentioned above, efficient complexation of pDNA resulting in small polyplex sizes and sufficient complex stability under physiological conditions are major problems in gene delivery using chitosan.

These problems can in part be overcome with quaternized chitosan as shown by Thanou et al. (*10*). However, the cytotoxicity of these polymers was also significantly increased compared to unmodified chitosan (*14*). Besides decreasing the cytotoxicity of trimethyl chitosan, PEG grafting was thought to enhance colloidal stability and to help maintaining polyplex sizes under different conditions, potentially resulting in increased uptake efficiency in vitro (*16*).

In this study, we determined physicochemical properties, such as complexation efficiency, particle size, and stability of polyplexes formed with chitosan, trimethyl chitosan and PEG-trimethyl chitosan. We tried to correlate these properties with uptake efficiency of polyplexes assessed by flow cytometry and transfection efficiency in different cell lines under in vitro conditions. Based on these data we elucidate the main factors influencing transfection efficiency of non-viral vectors based on chitosan in vitro.

5.3 Materials and Methods

Materials: Chitosan (MW ~400 kDa, degree of deacetylation 84.7%) was purchased from Fluka (Steinheim, Germany) and depolymerized as described previously (*13*). Trimethyl chitosan (TMC) and PEG-g-TMC were synthesized as described earlier (*14*). Branched polyethylenimine 25 kDa (PEI) was a gift from BASF (Ludwigshafen, Germany). Luciferase encoding plasmid pCMV-Luc was purchased from Plasmid Factory (Bielefeld, Germany).

Cell Culture: NIH/3T3 (mouse embryo; ATCC: CRL-1658), L-929 (mouse subcutaneous connective tissue; ATCC: CCL-1), MeWo (human malignant skin melanoma; ATCC: HTB-65) and A549 (human non-small-cell lung carcinoma; ATCC: CCL-185) cells were purchased from ATCC (Teddington, UK) and maintained in DMEM (PAA Laboratories, Cölbe, Germany) supplemented with 10% fetal calf serum (Cytogen, Sinn, Germany) in humidified atmosphere with 5% CO_2 at 37°C.

Formation of Polyplexes: Polyplex formation was performed under optimal conditions identified in (*17*). Briefly, pDNA was diluted with 15 mM acetate buffer, pH 5.5 to 0.04 g/L and was added to the appropriate amount of polymer in the same buffer in equal parts to obtain the desired polymer nitrogen to DNA phosphate (N/P) ratio. Polyplexes were mixed on a vortex mixer and incubated for 30 minutes at RT before use.

Agarose Gel Electrophoresis: 50 µl polyplex solution was prepared as described above. Where applicable, heparin was added and incubated with polyplexes for 30 minutes at RT. 10% v/v glycerol was added and 20 µl of the solution were applied to a 1% agarose gel in TAE (40 mM Tris/HCl, 1% acetic acid, 1 mM EDTA, pH 7.4) containing 0.6 µg/mL of ethidium bromide. Electrophoresis (Electro-4, Thermo Electron, Waltham, MA, USA) was carried out a constant voltage of 70 V for 45 minutes in TAE buffer. Ethidium bromide fluorescence was detected using a gel documentation system (Bio-DocAnalyze, Biometra, Göttingen, Germany) and images were processed with ImageJ 1.38s (*18*).

Ethidium Bromide Exclusion Assay: DNA condensation was measured by exclusion of ethidium bromide as described earlier (*19*). Briefly, 4 µg of herring testes DNA were complexed with ascending amounts of polymer in a final volume of 280 µl 15 mM sodium acetate buffer, pH 5.5 or HEPES buffered saline solution, pH 7.4, respectively. After incubation for 30 minutes at RT, 20 µl of a 0.1 mg/mL ethidium bromide solution were added and solutions were mixed intensively. Fluorescence was measured using a fluorescence plate reader (LS 50 B, Perkin-Elmer, Rodgau-Jügesheim, Germany) at 518 nm excitation and 605 nm emission wavelengths. Results are given as relative fluorescence intensity values where 1 represents fluorescence of DNA without polycation and 0 represents remaining fluorescence of non-intercalating ethidium bromide. Results are given as means of triplicate measurements.

Size and ζ-potential: Hydrodynamic diameters of undiluted polyplex solutions were determined in a volume of 50 µl. Subsequently, polyplex solutions were diluted with DMEM without FCS to 700 µl and polyplex size measurements were repeated. Measurements were performed using a Zetasizer Nano ZS (Malvern Instruments, Herrenberg, Germany) equipped with a 4 mW He-Ne laser at a wavelength of 633 nm at 25 °C. Scattered light was detected at a 173° backward scattering angle. The viscosity and refractive index of water at 25 °C was used for data analysis. Polyplex solutions were prepared as described above. Hydrodynamic diameters were determined in disposable cuvettes (UVette, Eppendorf, Wesseling-Berzdorf, Germany) at least in sextuplicates and averaged. Zeta potential measurements were performed in a folded capillary cell (Malvern Instruments, Herrenberg, Germany) at least in triplicate. Dispersion Technology Software 5.00 (Malvern Instruments, Herrenberg, Germany) was used for data ac-

quisition and analysis. The accuracy of the instrument was validated using reference polymer particles (Nanosphere Size Standards of 50, 100 and 200 nm, Duke Scientific Corp., Palo Alto, CA, USA) and with Zeta Potential Transfer Standard (Malvern Instruments, Herrenberg, Germany).

Atomic Force Microscopy: Size and surface morphology of polyplexes was analyzed by atomic force microscopy. Complexes of pCMV-Luc and polymers were prepared at an N/P ratio of 30 as described above. Silicon chips were used as sample support. The chips were incubated with complex suspension for 10 min before drying in a stream of dry nitrogen gas. Samples were investigated within 2 hours of preparation. Microscopy was performed on a NanoWizard (JPK Instruments, Berlin, Germany). Commercial silicon nitride tips attached to an I-type cantilever with a length of 230 µm and a nominal force constant of 40 N/m (NSC16 AlBsMicromasch, Estonia) were used. All measurements were performed in intermittent contact mode to avoid damage to the sample surface. The scan frequency was 0.6 Hz and scan size was 5x5 µm.

Cytotoxicity: Cytotoxicity of polymers was determined in quadruplicate by MTT assay according to the method of Mossmann (*20*). NIH/3T3 cells were seeded into 96-well plates at a density of $0.8x10^4$ cells/well. After 24 hours cell culture medium was aspirated and replaced by 200 µl serial dilutions of polymer stock solution in cell culture medium with FCS. The cells were then incubated for 4 or 24 hours at 37 °C, respectively. Afterwards, medium was replaced by DMEM without serum containing 0.5 mg/mL MTT (3-(4,5-dimethylthiazol-2-yl)-2,5-diphenyl tetrazolium bromide, Sigma, Deisenhofen, Germany). After 4 hours incubation at 37 °C in the dark, medium was aspirated and formazan crystals were dissolved in 200 µl dimethylsulfoxide per well. Measurement was performed using an ELISA reader (Titertek Plus MS 212, ICN, Eschwege, Germany) at a wavelength of 570 nm and 690 nm. Relative viability was calculated using 0% (wells without cells) and 100% (wells with untreated cells) controls.

Flow Cytometry: NIH/3T3 **c**ells were seeded in 24 well plates ($6*10^4$ cells/well) 24 hours prior to the experiment. Polyplexes were prepared at N/P 30 for chitosan, TMC50 and PTMC50 and N/P 6 for PEI using 2.5 µg pCMV-Luc per well. DNA was YOYO-1 labeled as described elsewhere (*21*). Cells were incubated with polyplexes for 4 hours at

37 °C in cell culture medium with FCS. Then, cells were washed with PBS once and incubated for 5 minutes with 0.4% trypan blue solution to quench extracellular fluorescence. Cells were detached using trypsin and suspended in a 1:1 mixture of FACSFlow (BD Biosciences, San Jose, CA) and 4% paraformaldehyd in PBS for cell fixation. Suspensions were measured on a FACScan (BD Biosciences, San Jose, CA) with excitation at 488 nm and emission filter set to 530/30 bandpass. 10.000 viable cells were evaluated in each experiment and results are the mean of 3 independent measurements. Data acquisition and analysis was performed using CellQuest Pro (BD Biosciences, San Jose, CA) and FCS Express V3.00 (DeNovo Software, Thornhill, Canada). Results were statistically analyzed using one-way ANOVA with Bonferroni post-tests.

Confocal Laser Scanning Microscopy: $1.5*10^4$ NIH/3T3 cells were seeded per well in 8 well chamber slides (Nunc, Wiesbaden, Germany) and allowed to grow for 24 hours. Polyplexes were prepared as described above using 0.5 µg DNA/well and incubated with the cells for 4 hours at 37 °C in DMEM with FCS. Subsequently, cells were washed with PBS, fixed using 4% paraformaldehyd in PBS, DAPI stained and washed with trypan blue solution as described elsewhere or above (*22*). Finally cells were embedded using FluorSave Reagent (Calbiochem, San Diego, CA). A Zeiss Axiovert 100 M microscope coupled to a Zeiss LSM 510 scanning device (Zeiss, Oberkochen, Germany) was used for confocal microscopy. For excitation of YOYO-1 fluorescence, an argon laser with an excitation wavelength of 488 nm was used. Fluorescence emission was detected using a 505-530 nm bandpass filter. Transmission images were obtained in the same scan. In a second scan, DAPI was detected using a Coherent Enterprise II 653 laser (Coherent, Inc., Santa Clara, CA) with an excitation wavelength of 364 nm and a 385 nm long-pass emission filter.

Transfection Experiments: For transfection experiments $2.5x10^4$ cells were plated per well in a 24-well plate. After 24 hours of growth, medium was replaced by 0.5 mL of fresh, complete cell culture medium. Polyplexes were prepared in a final volume of 100 µl (containing 2 µg pDNA) per well, incubated for 30 minutes at RT and subsequently added to the wells. Medium was exchanged again after 4 hours and cells were incubated for an additional 68 hours. Luciferase gene expression was quantified using a commercial kit (Promega, Mannheim, Germany) and photon counting on a luminometer (Sirius, Berthold, Pforzheim, Germany). Results were measured in relative light units per sec-

ond (RLU/s) and converted to nanograms of luciferase using a standard curve of recombinant luciferase (Promega, Mannheim, Germany). Protein concentration was determined using a modified BCA assay (Perbio Science, Bonn, Germany) with bovine serum albumin as a standard (*23*). All experiments were performed in triplicate and results are expressed as nanograms of luciferase per milligrams of protein. Results were statistically analyzed using two-way ANOVA with Bonferroni post-tests.

5.4 Results and Discussion

Chitosan and chitosan derivatives

Chitosan of different molecular weight and degree of deacetylation was published as potential non-viral gene delivery vector (*9, 24, 25*). These vectors were described to possess a low cytotoxicity, biodegradability and good transfection efficiency. Thanou et al. described a derivative of chitosan, quaternized chitosan (trimethyl chitosan, TMC), showing an increased solubility at physiologic pH and superior transfection efficiency compared to chitosan (*10*). However, quaternization of chitosan was shown to increase cytotoxicity in L929 cells in our laboratory (*14*). To decrease cytotoxicity on the one hand and further increase solubility on the other hand, polyethylenglycol modified TMCs with different grafting ratios and PEG chain lengths were synthesized. A set of PEGylated TMCs was tested for transfection efficiency in NIH/3T3 cells (data not shown) and trimethyl chitosan 50 kDa with PEG chains of 550 Da (TMC 50 kDa-g-PEG (550 Da)$_{116}$, abbreviated as PTMC50) was selected for a more detailed study. Physicochemical and biological properties of PTMC50 were compared to unmodified TMC and chitosan of 50 kDa (abbreviated as TMC50 and C50, respectively) to gain insight into structure-efficiency relationships of these vectors. To be able to objectively compare the properties of our new vectors with well known standards, branched polyethylenimine 25 kDa (PEI) at an optimized nitrogen/phosphate (N/P) ratio of 6 was included in the study.

Physicochemical characterization of polyplexes

An important prerequisite for efficient gene delivery using cationic polymers is the formation of small sized and stable polyplexes with pDNA under physiological conditions

(*26*). The ability of chitosan and chitosan derivatives to complex pDNA was studied by agarose gel electrophoresis (Fig. 1). Polyplexes were prepared at N/P ratios ranging from 0.47 to 30. In accordance with findings by Erbacher et al. (*24*), unmodified chitosan of 50 kDa was found to retard pDNA migration at a N/P ratio of about 2. TMC50 and PTMC50 both showed slightly increased complexation efficiencies, potentially due to the change from acidic to neutral pH during electrophoresis.

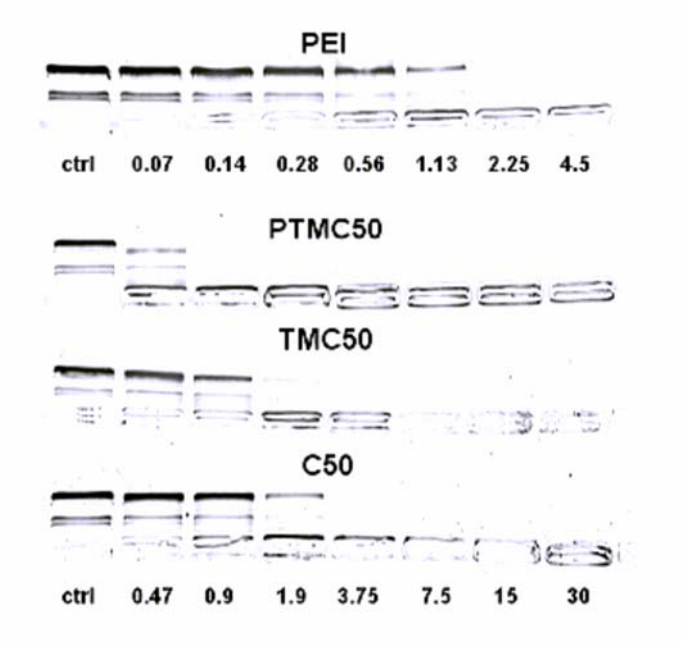

Figure 1. Agarose gel electrophoresis of chitosan, TMC50, PTMC50 and PEI polyplexes. Complexes were prepared at N/P ratios ranging from 0.47 to 30 for chitosans and 0.07 to 4.5 for PEI in 15 mM acetate buffer pH 5.5.

Several studies addressed the influence of ionic strength and pH during chitosan/pDNA polyplex formation (*8, 17, 27*). These parameters were found to significantly influence complex size, zeta potential and stability. To study polyplex formation between and chitosan or modified chitosans at different pH and salt concentrations, ethidium bromide exclusion assays were performed (Fig. 2). When polyplexes were prepared in 15 mM acetate buffer pH 5.5, unmodified chitosan was most efficient in pDNA condensation. The condensation efficiency of TMC50 was comparable with PTMC50 but slightly decreased compared to chitosan. In contrast, if pH was adjusted to 7.4 and ionic strength was higher, condensation efficiency of unmodified chitosan was strongly decreased due to the reduction of the degree of ionization and solubility (*27*). DNA condensation of

TMC50 and PTMC50 was less affected by changes in pH and ionic strength. Our results confirm the hypothesis that quaternized chitosans bind stronger to DNA than the unmodified polymer at neutral pH (*10*). Furthermore, our experiments show that PEGylation did not negatively affect condensation properties of quaternized chitosan neither under acidic, low ionic strength nor under physiological conditions.

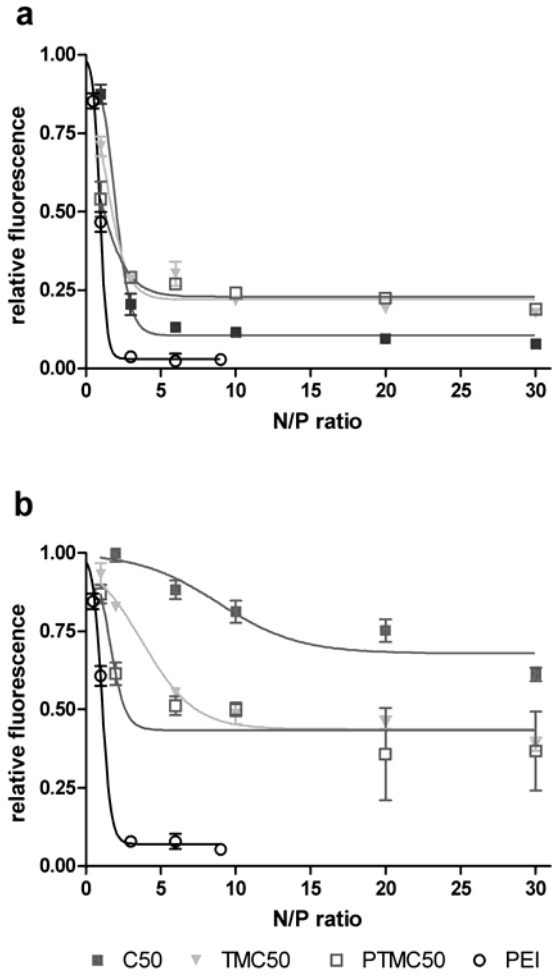

Figure 2. DNA condensation efficiency of polymers studied by ethidium bromide exclusion assay. Experiments were performed under acidic, low ionic conditions (a) and under conditions resembling characteristics of cell culture media (b).

In the next step, hydrodynamic diameters and morphology of polyplexes were evaluated by photon correlation spectroscopy (PCS) and atomic force microscopy (AFM). To resemble conditions after polyplex formation on the one hand and after addition of polyplexes to cell culture media on the other hand, sizes were determined in acetate buffer and after dilution 1:14 with DMEM by PCS (Fig. 3).

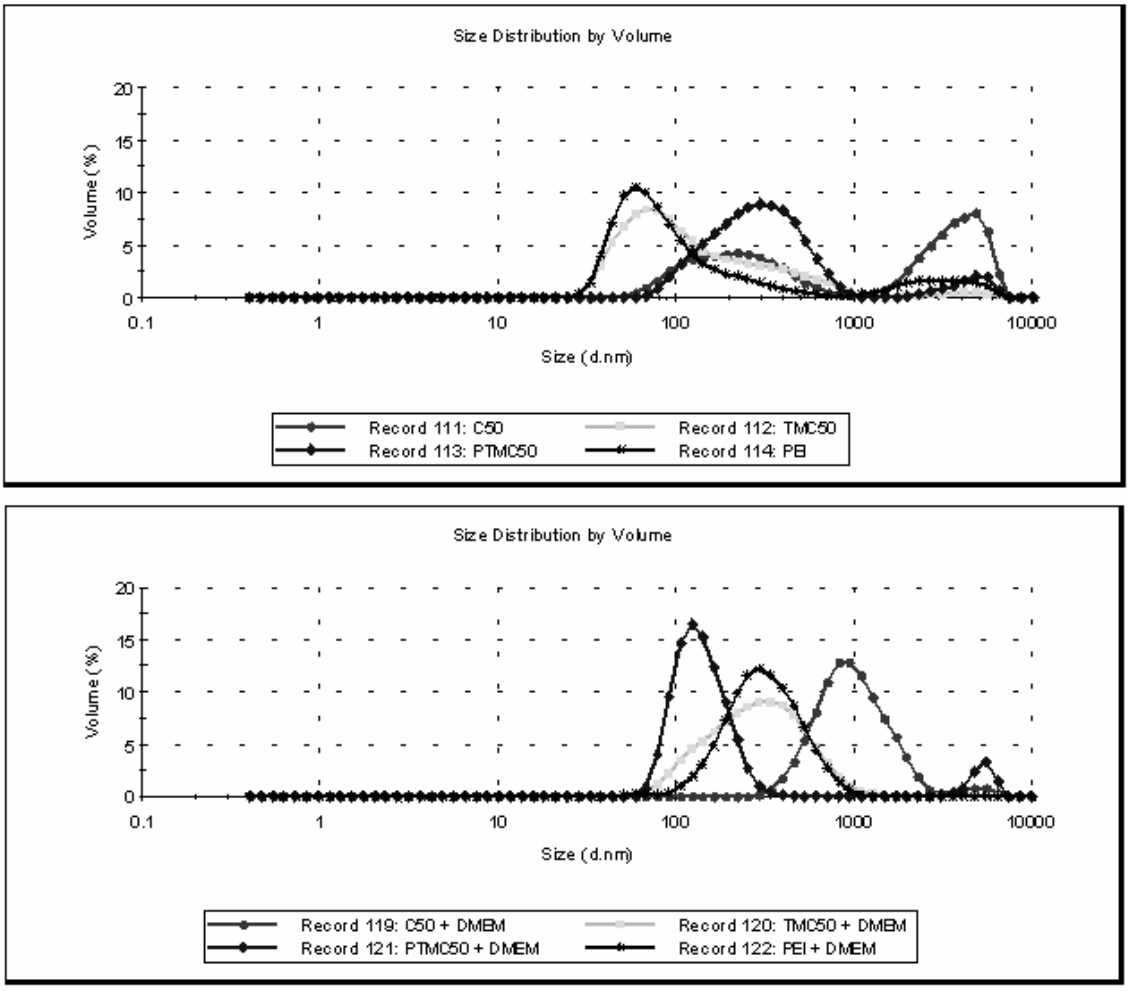

Figure 3. Size distributions by volume of polyplexes at N/P 30 (chitosans) and N/P 6 (PEI) prepared in 15 mM sodium acetate buffer pH 5.5 (top) and after dilution with DMEM (bottom).

When polyplexes were prepared in acetate buffer (15 mM, pH 5.5) at N/P 30, chitosan produced a bimodal distribution with particles of 244 nm (154 nm peak width, 48% volume) and 3768 nm (1301 nm peak width, 52% volume). Bimodal distributions were also found with TMC50, PTMC50 and PEI polyplexes. However, > 80% (volume) comprised particles of 174 nm (181 nm peak width), 311 nm (167 nm peak width) and 105 nm (95 nm peak width), respectively (Fig. 3). Atomic force microscopy confirmed formation of spherical complexes in all cases, which were accompanied to a smaller or bigger extent by particle aggregates (Fig. 4).

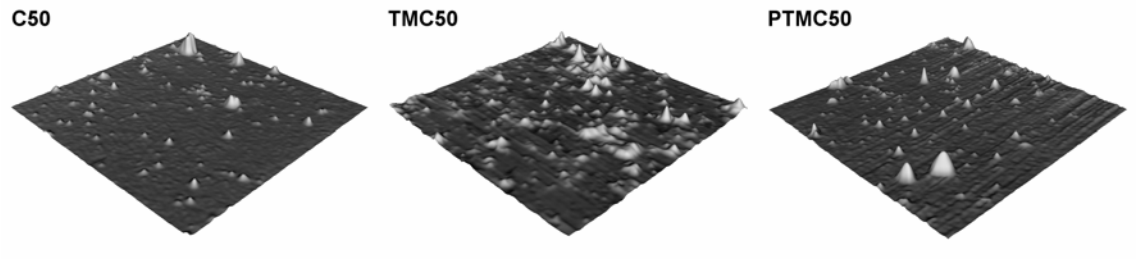

Figure 4. AFM topography images of polyplexes prepared in 15 mM acetate buffer pH 5.5 at N/P 30. Edge length: 5x5 µm.

After dilution with DMEM (ionic strength 166 mM, pH 7.4), a remarkable increase in polyplex sizes of chitosan/pDNA particles to 1049 nm (471 nm peak width) was seen. Results by Erbacher et al. and Strand et al., which described a bimodal size distribution and formation of aggregates for chitosan/pDNA polyplexes under physiologic conditions support these findings (*24, 27*). TMC50 polyplexes showed only a moderate increase of polyplex sizes to 334 (206 nm peak width) after dilution. In contrast, the size of PTMC50 polyplexes decreased after dilution with DMEM to 142 nm (48 nm peak width). We hypothesize that free chitosan in solution and chitosan polymers on the surface of polyplexes are discharged due to the change in pH after addition of DMEM. Charge repulsion between polyplexes is decreased, causing the formation of aggregates. In the case of quaternized chitosan ionization of the polymer is less dependent on the pH of the solution (compare Fig. 2) and discharging of polyplex surface is diminished. With PTMC50 aggregate formation is additionally reduced due to stabilization by PEG chains. Under the conditions chosen here, a moderate increase of hydrodynamic diameter to 344 nm (165 nm peak width) was found for PEI polyplexes after dilution with DMEM.

Chitosan/pDNA polyplexes were shown to be very stable under acidic and low ionic strength conditions by ethidium bromide exclusion experiments and laser light scattering. However, after changing to physiological conditions, chitosan polyplexes tend to form aggregates and show a decreased binding affinity for pDNA. Chitosan polyplexes showed neutral zeta potentials of 0.95 ± 2.56 mV potentially due to the low degree of ionization under these conditions (*27*). Similar findings were published by Mao et al. showing that zeta potential dramatically dropped at a pH of around 7. In this study, electrostatically neutral particles were found at pH 7.0-7.4 (*8*). In contrast, positive zetapo-

tentials were found for TMC50 polyplexes (6.47 ± 0.27 mV). This can be explained by the decreased pH dependency of ionization in the case of quaternized chitosan. As expected, PEGylation of TMC 50 kDa resulted in a reduction of zeta potential of polyplexes (0.01 ± 0.02 mV) due to steric shielding of the surface. PEI polyplexes exhibited the highest zeta potential of 9.11 ± 0.97 mV.

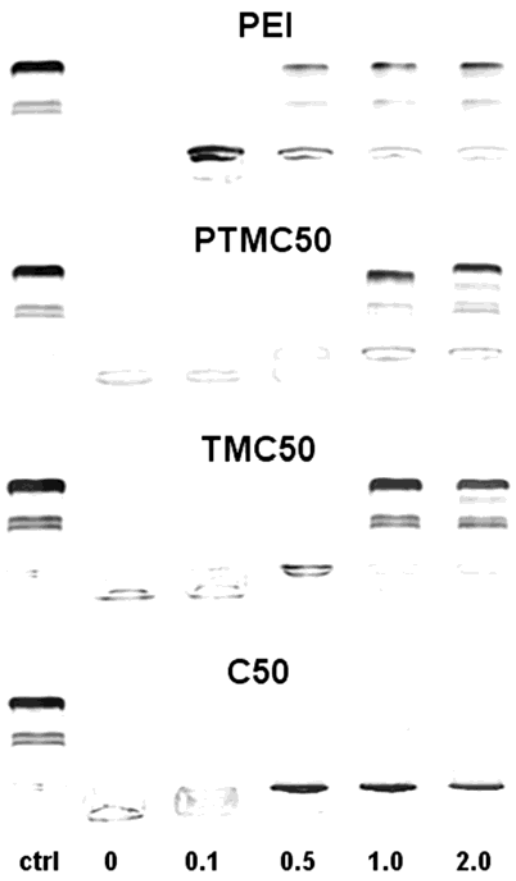

Figure 5. DNA release studied by heparin displacement. Polyplexes prepared at N/P 30 (chitosans) or N/P 6 (PEI) were challenged with increasing amounts of heparin for 30 minutes at RT. Uncomplexed plasmid DNA is shown as control.

The polyanion heparin is capable of displacing pDNA from polyplexes with high efficiency and was used to study pDNA release (Fig. 5). Using chitosan/pDNA complexes even with heparin amounts as high as 2 units, no migration of pDNA was observed, which correlates well with earlier findings of MacLaughlin et al. and Koping-Hoggard et al. (*25, 28*). In contrast, 1 unit of heparin was sufficient to fully release pDNA from polyplexes prepared with both TMC50 and PTMC50. Mao et al. reported that PEGyla-

tion of PEI decreased PEG-PEI/siRNA polyplex stability against heparin displacement in a PEG chain length-dependent way (*29*). The susceptibility to heparin displacement increased with decreasing PEG chain length in this study. Glodde et al. reported that in the case of PEG-PEI/oligonucleotide polyplexes the PEG grafting density also influenced polyplex stability (*30*). With higher degree of substitution, polyplex stability decreased using these PEG-PEI polyplexes. However, this phenomenon was not observed with PTMC50 in our experiments. As shown with ethidium bromide exclusion experiments, PEGylation did not negatively influence polyplex formation with pDNA, which results in comparable stability against heparin displacement. The high stability of chitosan/pDNA complexes was suggested to be a major rate limiting step for intracellular release of pDNA and therefore is a major drawback for efficient transfection (*7, 25*). Koping-Hoggard et al. addressed this problem by using easily dissociated chitosan oligomer polyplexes. With these polyplexes, a faster onset of transfection and a higher reporter gene expression were observed both in vitro and in vivo (*28*). Obviously, a fine balance between polyplex stability and pDNA release is essential for efficient transfection. TMC50 and PTMC50 showed an improved pDNA release compared to chitosan polyplexes and might therefore be advantageous for transfection. Using very high heparin amounts plasmid topology was subtly changed after displacement from polyplexes. An additional band appeared between the supercoiled and linear plasmid isoforms accounting for 5, 6 and 8% of total fluorescence in the case of TMC50, PTMC50 and PEI polyplexes, respectively. We explain this by subtle changes in the tertiary structure of supercoiled DNA upon binding of polycations as described by Lobo et al. (*31*).

Biological characterization of polyplexes

One of the most cited advantages of chitosan is its low toxicity and good biodegradability (*26, 32*). However, good biocompatibility of unmodified chitosan is accompanied by low solubility at physiological pH. Quaternization of chitosan was shown to improve both solubility and DNA binding efficiency (*10*) but on the other hand significantly increased cytotoxicity in our hands (*14*). Toxicity is a major issue with many non-viral vectors and a rough correlation between toxicity and transfection efficiency was often found (*33*). MTT assays were performed to evaluate the metabolic activity of NIH/3T3 cells treated with the different polymers after 4 hours, which resembles transfection

conditions, and after 24 hours. In accordance with findings of Mao et al. using L929 cells, cytotoxicity of PTMC50 was significantly decreased compared to unmodified TMC50 (Fig. 6) (*14*). After 24 hours incubation, IC_{50} value of PTMC50 was 42.1 µg/mL, while TMC50 showed a 4.4-times higher toxicity with an IC_{50} value of 9.6 µg/mL respectively. The same trends were found after 4 hours incubation. PEI is known to show a comparably high cytotoxicity in vitro. After 24 hours incubation, an inhibitory concentration of 6.1 µg/mL was found with this polycation. However, PEI amounts needed for efficient DNA complexation and transfection are about 20-fold lower than with TMC50.

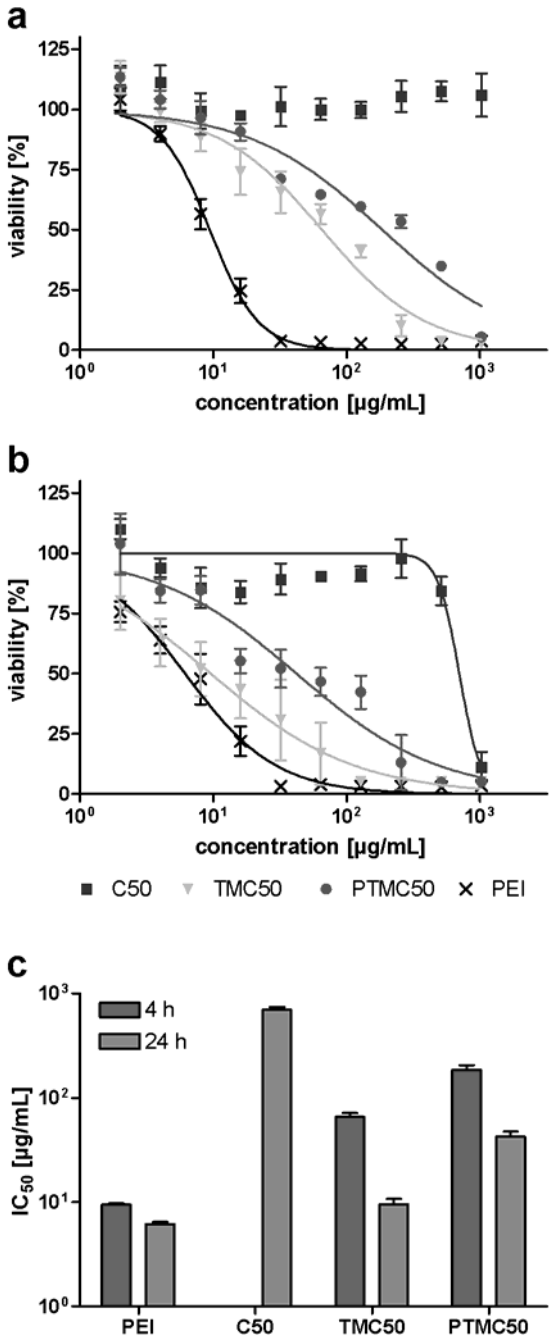

Figure 6. Cytotoxicity of polymers studied by MTT assay. NIH/3T3 cells were incubated with polymers for 4 (a) or 24 hours (b) and IC50 values were calculated (c).

The first step in transfection is cellular binding and uptake of polyplexes. Uptake of large and electrostatically neutral particles as found with chitosan/pDNA polyplexes is disfavored (*1, 34, 35*) and was shown to be very low by fluorescence microscopy (*25, 36*). To evaluate the ability of the different polyplexes to trigger uptake, we used flow

cytometry. DNA was fluorescently labeled using YOYO-1, an intercalating dye with high affinity to dsDNA (*21*). Figure 7 shows representative dot plots of polyplex uptake in NIH/3T3 cells after 4 hours. Using PEI polyplexes cellular uptake was observed in the vast majority of the cells. The percentage of YOYO-1 positive cells in the case of C50 was only 7.3%, but significantly different from untreated cells. Polyplex uptake strongly increased to 62.4% using TMC50 and uptake efficiency of PTMC50 was significantly increased compared to TMC50 despite its lower zeta potential.

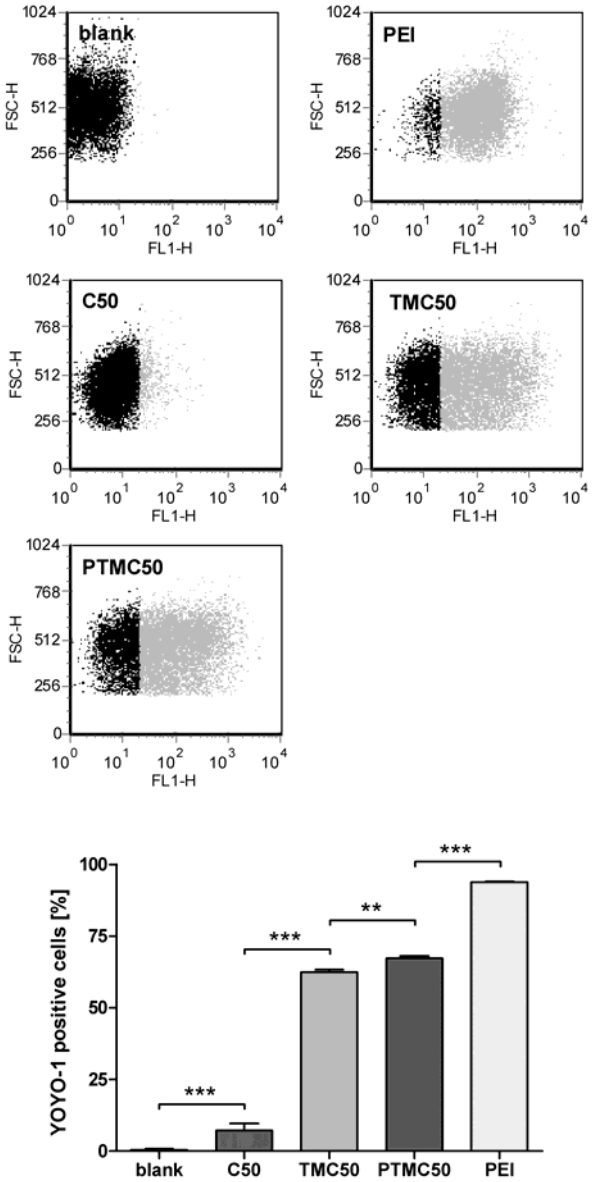

Figure 7. Cellular uptake of polyplexes studied by flow cytometry. NIH/3T3 cells were incubated for 4 hours at 37 °C with polyplexes prepared with fluorescently labeled DNA at N/P 30 in the case of chitosan and N/P 6 in the case of PEI. Top: plots of forward scatter against fluo-

rescence intensity for the different polyplex preparations. Black represents cells with fluorescence intensity of untreated cells, green represents cell with higher fluorescence intensity than blank cells. Bottom: Percentage of cells being positive for fluorescently labeled DNA. Significance was tested using one way ANOVA and Bonferroni post test. Two asterisks: $p < 0.01$, three asterisks: $p < 0.001$.

Polyplex uptake can follow different pathways such as clathrin-mediated endocytosis, macropinocytosis and uptake via raft/caveolae (*37-39*). However, the route of polyplex uptake resulting in efficient transfection is not yet clearly identified and may depend both on the cell line and polyplexes studied (*37, 39, 40*). Grosse et al. showed that polyplex size as well is an important determinant for uptake mechanism (*41*). In the case of PEI polyplexes it is believed that clathrin-mediated endocytosis is a main contributor to efficient transfection in a variety of cell lines (*40, 42-44*). However, other routes are also discussed (*39, 45*). The mechanism of cellular uptake and release of chitosan polyplexes was less often addressed. The few available studies reported that these particles are efficiently internalized by clathrin-mediated endocytosis as well (*46, 47*). Furthermore, the proposed mechanism of intracellular release of chitosan polyplexes is similar to that proposed for PEI polyplexes (*6, 47*).

Polyplex uptake was further studied by confocal laser scanning microscopy, enabling the sub-cellular localization of polyplexes. Again, pDNA was labeled using YOYO-1 and incubated with the cells for 4 hours. As found with flow cytometry, chitosan polyplex uptake was negligible (Fig. 8). Complexes of TMC50 were internalized to a higher extent. However, in many cells large aggregates were found. Distribution of PTMC50 polyplexes was more even and a lower tendency to aggregation was seen. Striking differences were found between uptake of chitosan based vectors and PEI. Using PEI, particles were smaller and accumulation near the nucleus was observed in many cells. In contrast, TMC50 and PTMC50 polyplexes remained near the cell surface as well defined particles. We are currently studying the uptake and release mechanism of chitosan polyplexes in more detail and will published these results soon.

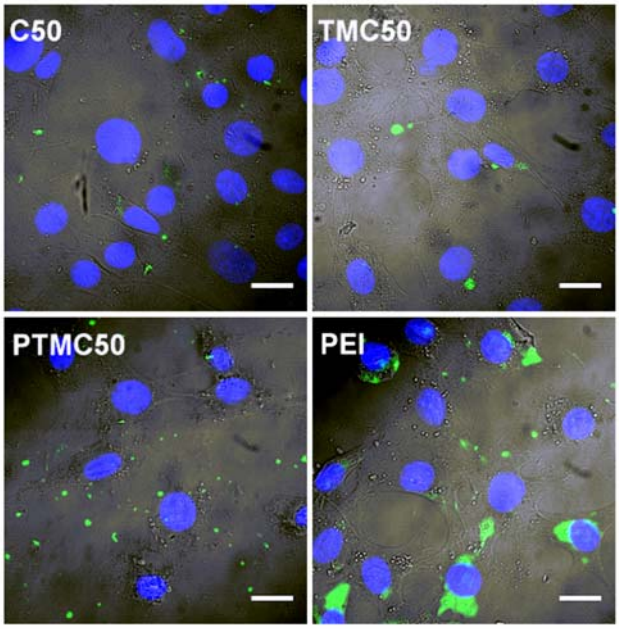

Figure 8. Confocal laser scanning microscopy of NIH/3T3 cells treated with chitosan, TMC50, PTMC50 and PEI polyplexes for 4 hours at 37 °C. Blue: nucleus (DAPI), green: YOYO-1 labeled DNA. Scale bar: 20 µm.

In preliminary experiments we determined the transfection efficiency of different chitosans and chitosan derivatives prepared at N/P ratios between 5 and 30 in NIH/3T3 cells (data not shown). In accordance with earlier reports, we found that transfection efficiency of TMC and PEG-TMCs increased with increasing N/P ratio (*10*). N/P ratios between 10 and 30 were found to result in significant transfection of NIH/3T3 cells and were used for further studies. Transfection efficiency of the selected chitosan, TMC and PEG-TMC polymers was evaluated in two murine (NIH/3T3 and L929) and two human (MeWo and A549) cell lines. Reporter gene expression of trimethyl chitosan polyplexes at N/P 30 was up to 678-fold (C50 vs. TMC50 in NIH/3T3) increased compared to polyplexes prepared with unmodified chitosan. Thanou et al. found similar results using trimethyl chitosan oligomers. In this study, transfection efficiency of quaternized polymers was up to 131-fold increased compared to naked DNA at comparable DNA/polymer ratios (*10*). At a charge ratio of 30, PTMC50 significantly increased transfection efficiency in 3 of 4 cell lines compared to both C50 and TMC50. Reporter gene expression was increased 4- (NIH/3T3) to 10-fold (L929) compared to TMC50. In MeWo cells luciferase expression of PTMC50 was 7-fold increased compared to TMC50, and transfection efficiency was not significantly different from PEI polyplexes

at an N/P ratio of 6. However, luciferase expression in A549 cells was low with all polymers used, including PEI. A549 cells are known to show some resistance to transfection and very high N/P ratio are needed to achieve significant reporter gene expression (*48*) We hypothesize that cell type specific characteristics such as charge density of the cell surface and differential internalization routes account for the differences in transfection efficiencies in our study. Furthermore, we found that cell lines that are easily transfectable with PEI also showed higher gene expression with chitosan derivatives and vice versa. One might therefore hypothesize that the main hurdles for efficient transfection are similar for PEI and chitosan vectors. However, in-depth studies on route of uptake and intracellular processing of chitosan based polyplexes are necessary to fully answer this question.

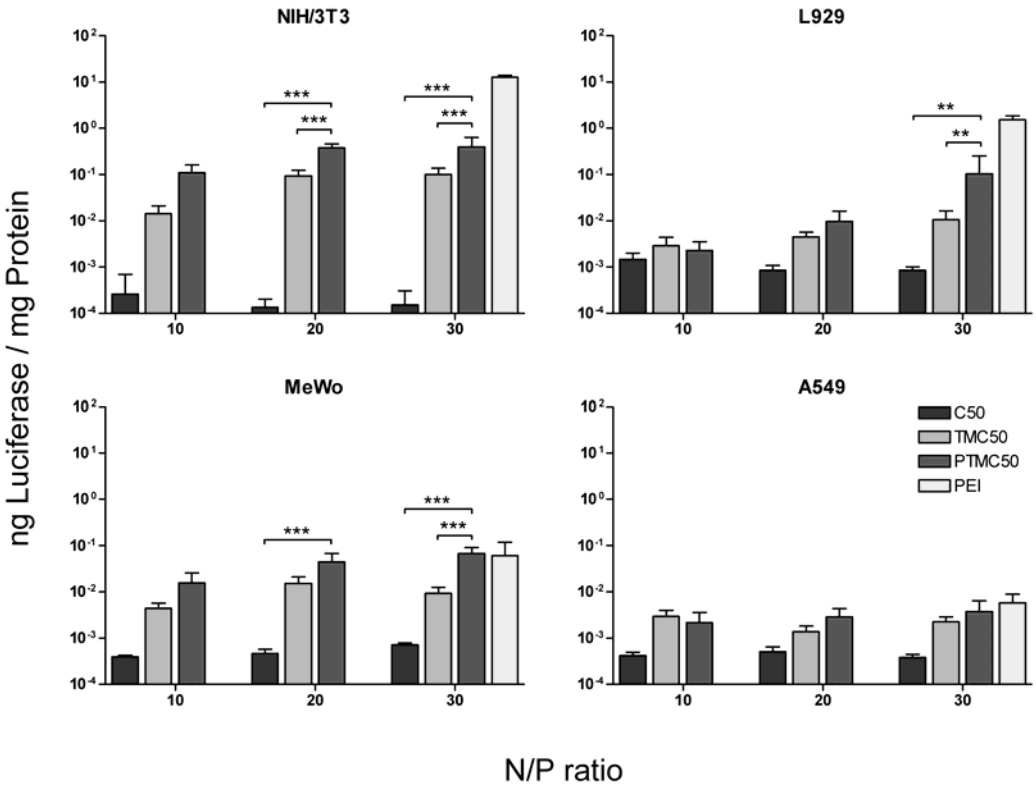

Figure 9. Luciferase expression in different cell lines following treatment with chitosan, TMC50 and PTMC50 polyplexes at different N/P ratios. PEI at N/P 6 is included for comparison of transfection efficiency. Significance was tested using two-way ANOVA with Bonferroni post test. Two asterisks: $p < 0.01$, three asterisks: $p < 0.001$.

5.5 Conclusion

To achieve efficient gene delivery in vitro, several obstacles have to be overcome (*5*). We tried to elucidate the limiting steps in transfection of cultured cells for non-viral vectors based on chitosan. Chitosan formed small polyplexes under acidic conditions. However, after addition to cell culture medium, severe polyplex aggregation was observed. Furthermore, chitosan polyplexes were electrostatically neutral under physiological conditions. These characteristics account for the very low internalization efficiencies observed by FACS and CLSM, which finally results in low transfection efficiency under in vitro conditions. Also, release of pDNA from chitosan polyplexes was shown to be inefficient by heparin displacement, which potentially further decreased their transfection efficiency.

Trimethylation of chitosan was described to significantly increase transfection efficiency. However, the main factors for the increased efficiency were unclear (*10*). Here we demonstrated that polyplex stability under physiological conditions is strongly increased with TMCs compared to chitosan, resulting in decreased polyplex sizes under physiological conditions. Furthermore, complexation of pDNA with TMC50 produced polyplexes with positive surface charges at pH 7.4. Consequently, polyplex uptake was far more efficient with TMC50- compared to chitosan polyplexes. Moreover, subsequent pDNA release is improved compared to chitosan polyplexes, enabling transcription and finally reporter gene expression. However, cytotoxicity of chitosan was significantly increased after trimethylation, which might be a major disadvantage of these vectors.

PEGylation was shown to strongly decrease cytotoxic effects and further increased solubility of TMC. Furthermore, we found that colloidal stability was increased by PEG grafting, resulting in a decrease of polyplex sizes under physiological conditions and increased polyplex uptake compared to unmodified TMC50. Both decreased cytotoxicity and increased uptake efficiency finally accounted for up to 10-fold improved transfection efficiency compared to trimethyl chitosan.

In summary we demonstrated that cellular uptake in conjunction with polyplex stability under physiological conditions are major hurdles for chitosan based gene delivery systems. Furthermore, we elucidated the major factors leading to increased transfection

efficiency of trimethyl chitosan- and PEG-trimethyl chitosan polyplexes. Therefore, this study not only highlights the importance of investigating polyplex stability under physiological condition but also contributes to the rationale design of new chitosan based vectors.

5.6 Acknowledgments

We would like to thank Eva Mohr (Department of Pharmaceutics and Biopharmacy) for excellent technical assistance and Cornelia Brendel (Flow Cytometry Core Facility, Department of Hematology, Oncology and Immunology, University Hospital Marburg) for generous use of equipment. We are grateful to Juliane Nguyen (Department of Pharamceutics and Biopharmacy) for critical review of the manuscript.

5.7 References

(1) Guang Liu, W., and De Yao, K. (2002) Chitosan and its derivatives--a promising non-viral vector for gene transfection. J Control Release 83, 1-11.

(2) Davis, S. S. (2006) The use of soluble polymers and polymer microparticles to provide improved vaccine responses after parenteral and mucosal delivery. Vaccine 24 Suppl 2, S2-7-10.

(3) George, M., and Abraham, T. E. (2006) Polyionic hydrocolloids for the intestinal delivery of protein drugs: alginate and chitosan--a review. J Control Release 114, 1-14.

(4) Di Martino, A., Sittinger, M., and Risbud, M. V. (2005) Chitosan: a versatile biopolymer for orthopaedic tissue-engineering. Biomaterials 26, 5983-90.

(5) Borchard, G. (2001) Chitosans for gene delivery. Adv Drug Deliv Rev 52, 145-50.

(6) Ishii, T., Okahata, Y., and Sato, T. (2001) Mechanism of cell transfection with plasmid/chitosan complexes. Biochimica Et Biophysica Acta-Biomembranes 1514, 51-64.

(7) Sato, T., Ishii, T., and Okahata, Y. (2001) In vitro gene delivery mediated by chitosan. effect of pH, serum, and molecular mass of chitosan on the transfection efficiency. Biomaterials 22, 2075-80.

(8) Mao, H. Q., Roy, K., Troung-Le, V. L., Janes, K. A., Lin, K. Y., Wang, Y., August, J. T., and Leong, K. W. (2001) Chitosan-DNA nanoparticles as gene carriers: synthesis, characterization and transfection efficiency. J Control Release 70, 399-421.

(9) Koping-Hoggard, M., Tubulekas, I., Guan, H., Edwards, K., Nilsson, M., Varum, K. M., and Artursson, P. (2001) Chitosan as a nonviral gene delivery system. Structure-property relationships and characteristics compared with polyethylenimine in vitro and after lung administration in vivo. Gene Ther 8, 1108-21.

(10) Thanou, M., Florea, B. I., Geldof, M., Junginger, H. E., and Borchard, G. (2002) Quaternized chitosan oligomers as novel gene delivery vectors in epithelial cell lines. Biomaterials 23, 153-9.

(11) Lee, D., Zhang, W., Shirley, S. A., Kong, X., Hellermann, G. R., Lockey, R. F., and Mohapatra, S. S. (2007) Thiolated chitosan/DNA nanocomplexes exhibit enhanced and sustained gene delivery. Pharm Res 24, 157-67.

(12) Yu, H., Chen, X., Lu, T., Sun, J., Tian, H., Hu, J., Wang, Y., Zhang, P., and Jing, X. (2007) Poly(l-lysine)-Graft-Chitosan Copolymers: Synthesis, Characterization, and Gene Transfection Effect. Biomacromolecules 8, 1425-1435.

(13) Mao, S., Shuai, X., Unger, F., Simon, M., Bi, D., and Kissel, T. (2004) The depolymerization of chitosan: effects on physicochemical and biological properties. Int J Pharm 281, 45-54.

(14) Mao, S., Shuai, X., Unger, F., Wittmar, M., Xie, X., and Kissel, T. (2005) Synthesis, characterization and cytotoxicity of poly(ethylene glycol)-graft-trimethyl chitosan block copolymers. Biomaterials 26, 6343-56.

(15) Mao, S., Germershaus, O., Fischer, D., Linn, T., Schnepf, R., and Kissel, T. (2005) Uptake and transport of PEG-graft-trimethyl-chitosan copolymer-insulin nanocomplexes by epithelial cells. Pharm Res 22, 2058-68.

(16) Petersen, H., Fechner, P. M., Martin, A. L., Kunath, K., Stolnik, S., Roberts, C. J., Fischer, D., Davies, M. C., and Kissel, T. (2002) Polyethylenimine-graft-poly(ethylene glycol) copolymers: influence of copolymer block structure on DNA complexation and biological activities as gene delivery system. Bioconjug Chem 13, 845-54.

(17) Romoren, K., Pedersen, S., Smistad, G., Evensen, O., and Thu, B. J. (2003) The influence of formulation variables on in vitro transfection efficiency and physicochemical properties of chitosan-based polyplexes. Int J Pharm 261, 115-27.

(18) Rasband, W. S. (1997-2006), U. S. National Institutes of Health, Bethesda, Maryland, USA.

(19) Petersen, H., Kunath, K., Martin, A. L., Stolnik, S., Roberts, C. J., Davies, M. C., and Kissel, T. (2002) Star-shaped poly(ethylene glycol)-block-polyethylenimine copolymers enhance DNA condensation of low molecular weight polyethylenimines. Biomacromolecules 3, 926-36.

(20) Mosmann, T. (1983) Rapid colorimetric assay for cellular growth and survival: application to proliferation and cytotoxicity assays. J Immunol Methods 65, 55-63.

(21) Ogris, M., Steinlein, P., Carotta, S., Brunner, S., and Wagner, E. (2001) DNA/polyethylenimine transfection particles: influence of ligands, polymer size, and PEGylation on internalization and gene expression. AAPS PharmSci 3, E21.

(22) Germershaus, O., Merdan, T., Bakowsky, U., Behe, M., and Kissel, T. (2006) Trastuzumab-polyethylenimine-polyethylene glycol conjugates for targeting Her2-expressing tumors. Bioconjug Chem 17, 1190-9.

(23) Hill, H. D., and Straka, J. G. (1988) Protein determination using bicinchonic acid in the presence of sulfhydryl reagents. Anal Biochem 170, 203-208.

(24) Erbacher, P., Zou, S., Bettinger, T., Steffan, A. M., and Remy, J. S. (1998) Chitosan-based vector/DNA complexes for gene delivery: biophysical characteristics and transfection ability. Pharm Res 15, 1332-9.

(25) MacLaughlin, F. C., Mumper, R. J., Wang, J., Tagliaferri, J. M., Gill, I., Hinchcliffe, M., and Rolland, A. P. (1998) Chitosan and depolymerized chitosan oligomers as condensing carriers for in vivo plasmid delivery. J Control Release 56, 259-72.

(26) Mansouri, S., Lavigne, P., Corsi, K., Benderdour, M., Beaumont, E., and Fernandes, J. C. (2004) Chitosan-DNA nanoparticles as non-viral vectors in gene therapy: strategies to improve transfection efficacy. Eur J Pharm Biopharm 57, 1-8.

(27) Strand, S. P., Danielsen, S., Christensen, B. E., and Varum, K. M. (2005) Influence of Chitosan Structure on the Formation and Stability of DNA-Chitosan Polyelectrolyte Complexes. Biomacromolecules 6, 3357-66.

(28) Koping-Hoggard, M., Varum, K. M., Issa, M., Danielsen, S., Christensen, B. E., Stokke, B. T., and Artursson, P. (2004) Improved chitosan-mediated gene delivery based on easily dissociated chitosan polyplexes of highly defined chitosan oligomers. Gene Ther 11, 1441-52.

(29) Mao, S., Neu, M., Germershaus, O., Merkel, O., Sitterberg, J., Bakowsky, U., and Kissel, T. (2006) Influence of polyethylene glycol chain length on the physicochemical and biological properties of poly(ethylene imine)-graft-poly(ethylene glycol) block copolymer/SiRNA polyplexes. Bioconjug Chem 17, 1209-18.

(30) Glodde, M., Sirsi, S. R., and Lutz, G. J. (2006) Physiochemical properties of low and high molecular weight poly(ethylene glycol)-grafted poly(ethylene imine) copolymers and their complexes with oligonucleotides. Biomacromolecules 7, 347-56.

(31) Lobo, B. A., Rogers, S. A., Choosakoonkriang, S., Smith, J. G., Koe, G., and Middaugh, C. R. (2002) Differential scanning calorimetric studies of the thermal stability of plasmid DNA complexed with cationic lipids and polymers. J Pharm Sci 91, 454-66.

(32) Nordtveit, R. J., Vaarum, K. M., and Smidsroed, O. (1996) Degradation of partially N-acetylated chitosans with hen egg white and human lysozyme. Carbohydrate Polymers 29, 163-167.

(33) Godbey, W. T., Wu, K. K., and Mikos, A. G. (2001) Poly(ethylenimine)-mediated gene delivery affects endothelial cell function and viability. Biomaterials 22, 471-80.

(34) Lorenz, M. R., Holzapfel, V., Musyanovych, A., Nothelfer, K., Walther, P., Frank, H., Landfester, K., Schrezenmeier, H., and Mailander, V. (2006) Uptake

of functionalized, fluorescent-labeled polymeric particles in different cell lines and stem cells. Biomaterials 27, 2820-8.

(35) Chung, T. H., Wu, S. H., Yao, M., Lu, C. W., Lin, Y. S., Hung, Y., Mou, C. Y., Chen, Y. C., and Huang, D. M. (2007) The effect of surface charge on the uptake and biological function of mesoporous silica nanoparticles in 3T3-L1 cells and human mesenchymal stem cells. Biomaterials 28, 2959-66.

(36) Issa, M. M., Koping-Hoggard, M., Tommeraas, K., Varum, K. M., Christensen, B. E., Strand, S. P., and Artursson, P. (2006) Targeted gene delivery with trisaccharide-substituted chitosan oligomers in vitro and after lung administration in vivo. J Control Release 115, 103-12.

(37) Goncalves, C., Mennesson, E., Fuchs, R., Gorvel, J. P., Midoux, P., and Pichon, C. (2004) Macropinocytosis of polyplexes and recycling of plasmid via the clathrin-dependent pathway impair the transfection efficiency of human hepatocarcinoma cells. Mol Ther 10, 373-85.

(38) Manunta, M., Nichols, B. J., Hong Tan, P., Sagoo, P., Harper, J., and George, A. J. (2006) Gene delivery by dendrimers operates via different pathways in different cells, but is enhanced by the presence of caveolin. J Immunol Methods 314, 134-46.

(39) Rejman, J., Bragonzi, A., and Conese, M. (2005) Role of clathrin- and caveolae-mediated endocytosis in gene transfer mediated by lipo- and polyplexes. Mol Ther 12, 468-74.

(40) von Gersdorff, K., Sanders, N. N., Vandenbroucke, R., De Smedt, S. C., Wagner, E., and Ogris, M. (2006) The Internalization Route Resulting in Successful Gene Expression Depends on both Cell Line and Polyethylenimine Polyplex Type. Mol Ther 14, 745-753.

(41) Grosse, S., Aron, Y., Thevenot, G., Francois, D., Monsigny, M., and Fajac, I. (2005) Potocytosis and cellular exit of complexes as cellular pathways for gene delivery by polycations. J Gene Med 7, 1275-86.

(42) Mennesson, E., Erbacher, P., Piller, V., Kieda, C., Midoux, P., and Pichon, C. (2005) Transfection efficiency and uptake process of polyplexes in human lung endothelial cells: a comparative study in non-polarized and polarized cells. J Gene Med 7, 729-38.

(43) Merdan, T., Kunath, K., Fischer, D., Kopecek, J., and Kissel, T. (2002) Intracellular processing of poly(ethylene imine)/ribozyme complexes can be observed in living cells by using confocal laser scanning microscopy and inhibitor experiments. Pharm Res 19, 140-6.

(44) Khalil, I. A., Kogure, K., Akita, H., and Harashima, H. (2006) Uptake pathways and subsequent intracellular trafficking in nonviral gene delivery. Pharmacol Rev 58, 32-45.

(45) van der Aa, M. A., Huth, U. S., Hafele, S. Y., Schubert, R., Oosting, R. S., Mastrobattista, E., Hennink, W. E., Peschka-Suss, R., Koning, G. A., and Crommelin, D. J. (2007) Cellular Uptake of Cationic Polymer-DNA Complexes Via Caveolae Plays a Pivotal Role in Gene Transfection in COS-7 Cells. Pharm Res 24, 1590-8.

(46) Huang, M., Ma, Z., Khor, E., and Lim, L. Y. (2002) Uptake of FITC-chitosan nanoparticles by A549 cells. Pharm Res 19, 1488-94.

(47) Hashimoto, M., Morimoto, M., Saimoto, H., Shigemasa, Y., and Sato, T. (2006) Lactosylated Chitosan for DNA Delivery into Hepatocytes: The Effect of Lactosylation on the Physicochemical Properties and Intracellular Trafficking of pDNA/Chitosan Complexes. Bioconjugate Chem. 17, 309-316.

(48) Dailey, L. A., Kleemann, E., Merdan, T., Petersen, H., Schmehl, T., Gessler, T., Hanze, J., Seeger, W., and Kissel, T. (2004) Modified polyethylenimines as non viral gene delivery systems for aerosol therapy: effects of nebulization on cellular uptake and transfection efficiency. J Control Release 100, 425-36.

6 Kinetics and Mechanism of Uptake of Chitosan, Trimethyl Chitosan and PEG-Trimethyl Chitosan Polyplexes in L929 mouse fibroblasts and A549 human alveolar epithelial cells

In preparation for Journal of Gene Medicine

6.1 Abstract

Background: Cellular uptake pathways and intracellular processing of non-viral vectors are important steps towards efficient reporter gene expression.

Methods: Several specific inhibitors of cellular uptake- or intracellular processing pathways were used to study uptake and transfection efficiency of polyplexes in A549 and L929 cells. In this respect, we also determined uptake kinetics and the colloidal stability of polyplexes.

Results: Chitosan polyplexes showed severe aggregation in physiological media and cellular uptake was low. To a lesser extent aggregation was also observed with polyethylenimine (PEI) polyplexes, but cellular uptake efficiency was less affected. Trimethyl chitosan (TMC) and its PEG derivative (PTMC) showed virtually no aggregation. Cellular uptake was strongly increased compared to PEI polyplexes in L929 cells and was as high as PEI uptake in A549. Uptake kinetics were similar for all polyplexes in L929 cells, while PEI polyplexes were faster internalized than TMC or PTMC polyplexes in A549 cells. In L929 cells the main uptake pathway was clathrin-mediated endocytosis accompanied by uptake via caveolae in the case of TMC and PTMC polyplexes. Clathrin-mediated endocytosis strongly influenced transfection efficiency. In A549 cells, uptake mainly occurred by clathrin-mediated endocytosis accompanied by macropinocytosis but transfection mainly depended on the former.

Conclusions: While certain differences in polyplex uptake and its effect on transfection were found, these could not fully explain the difference in transfection efficiency of PEI versus chitosan vectors. Therefore we conclude that, besides uptake pathways, other steps in the transfection process such as intracellular release or vector unpacking are equally important for efficiency.

6.2 Introduction

Several years ago, non-viral gene delivery has emerged as a promising alternative to viral gene delivery due to its lower immunogenicity, better target ability, lack of pathogenicity and ease of pharmaceutical production (*1*). However, non-viral vectors still suffer from relative low gene transfer efficiency compared to viral vectors. Therefore, a major goal in this field of research is the search for safe vectors with higher efficiency.

In recent years, chitosan, a biodegradable polysaccharide derived from crustacean shells, has been explored for non-viral gene delivery (*2-4*). Chitosan was shown to possess low toxicity, both in animals and humans (*5, 6*). However, chitosan also shows major drawbacks such as low solubility at neutral pH and relative low gene transfer efficiency (*7-9*). Quaternization of chitosan was shown to enhance solubility and transfection efficiency but on the other hand also increased cytotoxicity (*10, 11*). Polyethylenglycol modification of quaternized chitosan significantly reduced cytotoxicity while maintaining or even increasing transfection efficiency (*11, 12*). However, transfection efficiency of these improved chitosan vectors remains to be low as compared to polyethylenimine (PEI) polyplexes, which served as a standard preparation in these experiments.

Non-viral gene delivery is a multistep process as outlined by Bally et al. (*13*). To realize the final therapeutic effect, the exogenous gene must cross several barriers. These barriers include cell surface binding of the non-viral vector, traversing the plasma membrane, escaping lysosomal degradation and overcoming the nuclear envelope. In this study we focused on cellular uptake mechanisms and the effect on uptake and transfection efficiency of chitosan and PEI polyplexes. Cellular uptake of polyplexes can occur via different pathways which are quite similar to the entry pathways of virus particles (*14*). The best-characterized uptake mechanism is the clathrin dependent pathway. Polyplexes taken up by clathrin-mediated endocytosis will be trafficked to early and late endosomes that ultimately fuse with lysosomes (*15*). Non-clathrin dependent pathways can be divided into caveolin-mediated endocytosis, macropinocytosis and phagocytosis. Phagocytosis is limited to specialized cells such as macrophages and monocytes whereas both uptake via caveolae and macropinocytosis can occur in all cells (*16*).

Caveolae were identified by early microscopists as smooth-surfaced flask-shaped pits of 55-65 nm (*17*). Caveolin-1 was later identified as molecular marker closely related with caveolae. In lymphocytes where caveolins are not expressed, the expression of caveolin-1 was sufficient to induce the de novo formation of caveolae (*18*). Unlike clathrin-mediated endocytosis, abundance of caveolea strongly differs in different cells (*17*). Importantly, cellular entry via caveolae is a nonacidic and nondigestive route of internalization, rendering it interesting for non-viral gene delivery (*16*). However, caveolae are small in size, slowly internalized and they represent only a small fluid phase volume. Therefore, it was questioned if caveolae can significantly contribute to constitutive endocytosis (*16*). Macropinocytosis describes the actin-driven formation of large endocytic vesicles. Macropinosomes are uncoated, do not concentrate receptors and strongly differ in size, being as large as 5 µm (*19*). These vesicles can acidify but do not intersect with lysosomes. Furthermore, macropinosomes are thought to be inherently leaky compared to other types of endosomes (*20*). These attributes of macropinocytosis might be advantageous for cellular entry of non-viral vectors (*15, 16*).

The efficiency of PEI mediated gene delivery has long been known to depend on endosomal acidification facilitating endosomal release by the so-called proton sponge effect (*21, 22*). Recently, it was reported that other endocytic pathways may contribute to gene expression as well. Huth et al. showed that PEI-coated superparamagnetic iron oxide gene vectors are taken up via both clathrin- and caveolin-mediated endocytosis in HeLa cells (*23*). Similar results were found by Rejman et al. in A549 and HeLa cells using PEI polyplexes (*24*). Van der Aa et al. found that transfection of COS7 cells with PEI polyplexes was completely lost after blocking caveolae-mediated uptake (*25*). A study of von Gersdorff et al. revealed that the uptake pathway mediating successful gene expression depended on both polyplex type applied and on the cell line used (*26*). In this study, clathrin-mediated endocytosis and uptake via caveolae were identified as main pathways of cellular entry of linear and/or branched PEI polyplexes in HeLa and HUH-7 cells, while clathrin-mediated endocytosis alone contributed to successful gene expression in COS-7 cells. Grosse et al. studied uptake of different polyplexes in airway epithelial cells using electron microscopy discovering that internalization of polyplexes was size-dependent (*27*). Large particles were internalized by macropinocytosis, intermediate (100-200 nm) by clathrin-mediated endocytosis while small particles entered

the cells via caveolae. In sharp contrast, Rejman et al. found that internalization of fluorescent latex beads <200 nm involved clathrin mediated endocytosis while large particles were predominantly taken up via caveolae (*28*). However, due to significant differences in the properties of polyplexes of pDNA and cationic polymers and latex particles the significance of these results for non-viral gene delivery can be questioned. Studies on route of uptake of chitosan or chitosan derivatives and its polyplexes with pDNA are rare. The uptake of fluorescently labeled chitosan nanoparticles prepared by ionotropic gelation was compared with that of chitosan molecules in A549 cells by Huang et al. (*29*). In this study, clathrin-mediated uptake was identified to mainly contribute to particle uptake, while inhibition with filipin had no effect. Hashimoto et al. studied uptake of polyplexes of pDNA with lactosylated chitosan or unmodified chitosan in HepG2 cells (*30*). Transfection was inhibited by Bafilomycin A_1, a proton pump inhibitor. Furthermore, the authors found that transfection efficiency of chitosan polyplexes was increased after microtubule perturbation by nocodazole. These characteristics point to cellular uptake via clathrin mediated endocytosis and release of chitosan polyplexes from early or late endosomes.

To further investigate chitosan polyplex uptake in comparison with uptake of PEI complexes, we used specific uptake inhibitors in two different cell lines and studied their effect on uptake- and transfection efficiency. Furthermore, hydrodynamic diameters, colloidal stability of polyplexes, and uptake kinetics were studied. By specific inhibition of different uptake pathways we show that both PEI and chitosan derivative uptake potentially occurs via both clathrin- and caveolin-dependent endocytosis in L929 cells. Efficient transfection in this cell line mainly involved clathrin-mediated endocytosis. In A549 cells, besides the clathrin-dependent pathway, macropinocytosis contributed to uptake especially in the case of chitosan derivatives. However, transfection again mainly depended on clathrin-mediated endocytosis.

6.3 Materials and Methods

Materials. Chitosan (MW ~400 kDa, degree of deacetylation 84.7%) was purchased from Fluka (Steinheim, Germany) and depolymerized as described in (*11*) to obtain chitosan of 100 kDa. Trimethyl chitosan 100 kDa (TMC) with a degree of substitution of 40% was prepared as described in (*11*). TMC was subsequently modified with 28 moles

polyethylenglycol of 5 kDa per mole TMC (PTMC) as described previously (*11*) Branched polyethylenimine 25 kDa (PEI) was a kind gift from BASF (Ludwigshafen, Germany) and was used as supplied. Luciferase encoding plasmid pCMV-Luc was purchased from Plasmid Factory (Bielefeld, Germany). All other chemicals used in this study were at least of analytical grade.

Cell culture. L929 (mouse subcutaneous connective tissue; ATCC: CCL-1) and A549 (human non-small-cell lung carcinoma; ATCC: CCL-185) cells were purchased from ATCC (Teddington, UK) and maintained in Dulbecco's Modified Eagle's Medium (DMEM, PAA Laboratories, Cölbe, Germany) supplemented with 10% fetal calf serum (FCS, Cytogen, Sinn, Germany) in humidified atmosphere with 5% CO_2 at 37°C.

For flow cytometry experiments, cells were seeded at a density of $3*10^4$ cells per well in 24 well plates and incubated for 24 hours before the experiment. For transfection experiments, 1 day before the experiment cells were seeded at a density of $1.5*10^4$ cells per well of 24 well plates.

DNA labeling and polyplex preparation. pCMVLuc was diluted in 15 mM sodium acetate buffer pH 5.5 to 0.08 g/L and mixed with an equal volume of YOYO-1 solution in the same buffer to produce a final solution of 0.04 g/L pDNA with one YOYO-1 molecule per 200 basepairs similar to (*31*). After incubation for at least one hour at RT in the dark, labeled pDNA was used to prepare polyplexes with chitosan or PEI.

Unlabeled or labeled pDNA (0.04 g/L) was mixed thoroughly with the appropriate amount of polymer solution in an equal volume of 15 mM sodium acetate buffer pH 5.5. After mixing, polymers and DNA were allowed to anneal for 30 min at RT in the dark. Subsequently, polyplexes were directly added to the cell culture media.

Size and aggregation kinetics. In this experiment, unlabeled pDNA was used to prepare polyplexes as described above. Polyplexes were prepared in a final volume of 100 µl (corresponding to 2 µg of pDNA) at N/P 20 in the case of chitosans and N/P 9 in the case of PEI and polyplex sizes were determined with six successive measurements in disposable cuvettes (UVette, Eppendorf, Wesseling-Berzdorf, Germany). Then, polyplex solutions were diluted with DMEM without FCS to 1 ml and 60 successive measurements (each ~0.9 min) were performed. Measurements were performed using a Zetasizer Nano ZS (Malvern Instruments, Herrenberg, Germany) equipped with a 4 mW He-

Ne laser at a wavelength of 633 nm at 25 °C. Scattered light was detected at a 173° backward scattering angle. The viscosity and refractive index of water at 25 °C was used for data analysis. Dispersion Technology Software 5.00 (Malvern Instruments, Herrenberg, Germany) was used for data acquisition and analysis. The accuracy of the instrument was validated using reference polymer particles (Nanosphere Size Standards of 50, 100 and 200 nm, Duke Scientific Corp., Palo Alto, CA, USA).

Kinetics of uptake. L929 and A549 cells were incubated with labeled polyplexes for 0.25, 0.5, 0.75, 1.0, 1.5, 2.0, 3.5 and 5 hours at 37 °C. Then cells were treated with 0.04% trypan blue solution for 5 min to quench extracellulary bound polyplexes and subsequently washed with PBS. Cells were detached with trypsin and suspended in a 1:1 mixture of FACSFlow (BD Biosciences, San Jose, CA) and 4% paraformaldehyd in PBS for cell fixation. Cell suspension was measured on a FACScan (BD Biosciences, San Jose, CA) with excitation at 488 nm and emission filter set to 530/30 bandpass. 10.000 viable cells were evaluated in each experiment and results are represented as mean of 3 independent measurements. Data acquisition and analysis was performed using CellQuest Pro (BD Biosciences, San Jose, CA) and FCS Express V3.00 (DeNovo Software, Thornhill, Canada).

Route of Uptake. Prior transfection, L929 and A549 cells were treated with the following inhibitors in FCS-free DMEM: chlorpromazine 10 µg/mL, filipin III 5 µg/mL, nystatin10 µg/mL, wortmannin 12.8 ng/mL, methyl-β-cyclodextrin 6.6 mg/mL, and sucrose 0.45 M. After 30 min incubation polyplexes were added to the medium and cells were incubated for an additional 3 hours at 37 °C. Cells were then prepared for flow cytometry as described above. Results were calculated relative to untreated and blank cells with geometric mean fluorescence of cells solely treated with polyplexes set to 1 and fluorescence of blank cells set to 0.

Route of Transfection. For inhibition of transfection, cells were treated as described in section route of uptake. In transfection experiments chloroquine 75 µM and nocodazole 5 µg/mL was additionally included. Cells were incubated with polyplexes and inhibitory drugs for 3 h. Then, medium was replaced by fresh DMEM with FCS and cells were incubated an additional 45 hours. Luciferase gene expression was quantified using a commercial kit (Promega, Mannheim, Germany) and photon counting on a luminometer

(Sirius, Berthold, Pforzheim, Germany). All experiments were performed in triplicate and results were expressed relative to cells treated with polyplexes only (set to 1).

6.4 Results and Discussion

6.4.1 Size and aggregation kinetics

Hydrodynamic diameters in preparation buffer as well as development of polyplex size under simulated cell culture conditions were determined by photon correlation spectroscopy. Polyplex sizes in 15 mM sodium acetate buffer pH 5.5 are shown in figure 1a. All polymers formed polyplexes with hydrodynamic diameters below 150 nm (ZAve). Size of polyplexes decreased in the order C > TMC = PTMC > PEI. Volume distributions of polyplexes are shown in figure 2 (left side; 15 mM NaAc, pH 5.5). It was noticed that size distributions of C and TMC polyplexes were larger compared to those of PEI and PTMC polyplexes. Similar results were obtained when size distributions of chitosan 50kDa and its TMC and PTMC derivatives were studied using PCS and atomic force microscopy in an earlier study (*12*). In this study size distributions especially of TMC and chitosan were broad and often bimodal while PEI produced very small polyplexes.

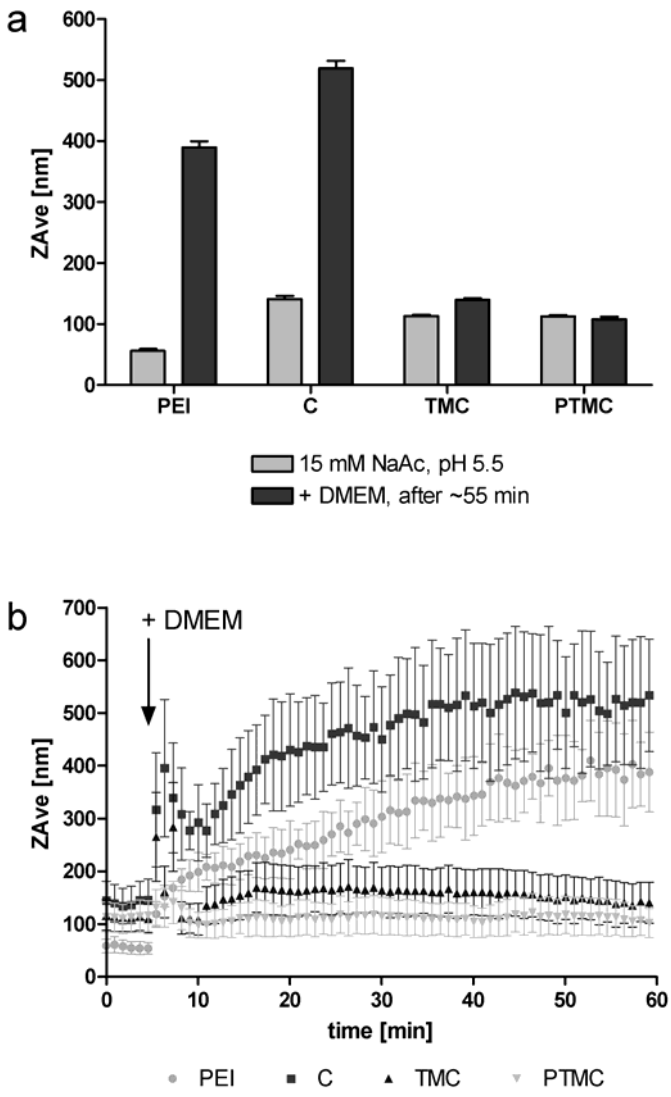

Figure 1: Aggregation kinetics of chitosan (C), trimethyl chitosan (TMC), PEG-trimethyl chitosan (PTMC) and polyethylenimine (PEI) polyplexes. A) Polyplex sizes before (15 mM NaAc, pH 5.5) and 55 minutes after addition of DMEM. Values given as arithmetic mean ± standard deviation of 6 measurements. B) Aggregation kinetics of polyplexes. At the indicated timepoint polyplex solutions were diluted with DMEM and development of polyplex size was followed over approximately 55 minutes. Values given as ZAverage of each measurement ± polydispersity in nm.

Polyplex aggregation kinetics upon addition of DMEM was studied over approximately 55 minutes by PCS (Figure 1 a and b). Chitosan polyplexes formed large aggregates immediately after addition of DMEM. Aggregation leveled off after about 40 minutes and sizes remained relatively constant thereafter. PEI polyplexes showed similar aggre-

gation kinetics. Polyplex sizes strongly increased immediately upon addition of cell culture media and aggregate sizes then slowly increased until the end of the measurement. Comparable results were found when PEI polyplexes at N/P10 were challenged with PBS or increasing salt concentration and polyplex aggregation was followed by turbidity, AFM and PCS measurements (*32, 33*). In contrast, neither TMC nor PTMC showed a tendency to aggregation under these conditions. Polyplex size distributions before and after incubation with cell culture medium are shown in figure 2. PEI and chitosan polyplexes aggregated into large particles while virtually no change in the size distributions of PTMC polyplexes were observed. In the case of TMC, virtually no changes in ZAverage were found but volume distribution was broader and bimodal after incubation with DMEM.

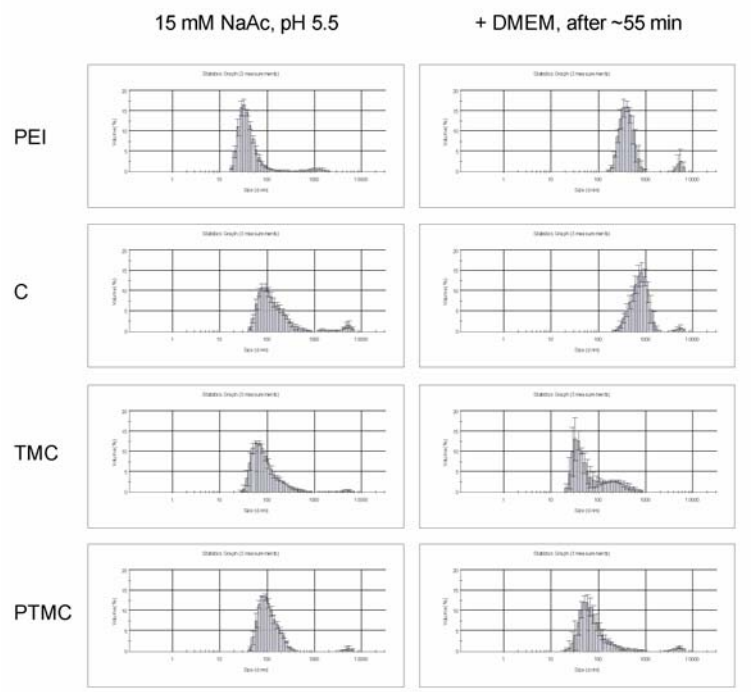

Figure 2: Volume distributions of polyplexes prepared with PEI or chitosan derivates before (left side) and after incubation for approximately 55 min with DMEM (right side). Distributions shown are the mean ± standard deviation of 3 measurements.

Trimethylation of chitosan was already shown to significantly reduce the pH dependency of DNA condensation of chitosan and to strongly increase transfection efficiency (*10, 12*). Furthermore, PEGylation of quaternized chitosan was in the case of chitosan

derivatives of 50 kDa shown to increase colloidal stability of polyplexes which we show herein holds true for 100 kDa chitosan derivatives as well (*12*).

Recent reports indicated that particle size is an important factor for the efficiency and route of cellular entry (*27, 28, 34*). Therefore, the observed differences in colloidal stability of polyplexes may have a significant impact on uptake route and –kinetics.

6.4.2 Efficiency and Kinetics of Polyplex Uptake

Polyplex uptake was studied by flow cytometry. Plasmid DNA was labeled using the intercalating dye YOYO-1. Upon binding to DNA YOYO-1 fluorescence is increased up to 1000-fold, making it a very selective nucleic acid stain. Uptake kinetics of polyplexes prepared using labeled DNA was followed in a 5 hours timeframe. Trypan blue incubation was used to quench fluorescence from cell surface bound polyplexes. Two different cell lines, L929 and A549 cells were used in these studies. It was previously found that A549 cells are relatively resistant to transfection both with PEI as well as with chitosan or quaternized chitosan polyplexes. In contrast, transfection of L929 cells with these vectors is more efficient as previously shown (*12*).

Internalization kinetics was evaluated concerning a) the total amount of internalized pDNA estimated by the shift in geometric mean fluorescence of the cell population after incubation with polyplexes (Figure 3 a and b) and b) the percentage of cells showing fluorescence above the threshold set with untreated cells (Figure 3 c and d).

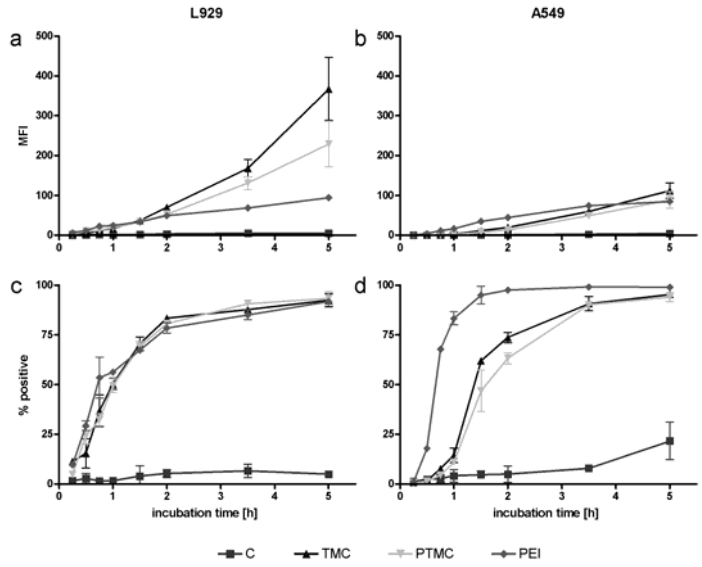

Figure 3: Kinetics of polyplex uptake in L929 (a and c) and A549 cells (b and d). Geometric mean fluorescence of the cell population (a and b) or percentage of YOYO-1 positive cells (c and D) was determined over 5 hours incubation at 37 °C. Values given as mean ± standard deviation of 3 measurements.

Analysis of the total amount of internalized polyplexes revealed that polyplexes prepared using unmodified chitosan were only slowly and ineffectively internalized in both cell lines. In contrast, internalization of PEI-, TMC and PTMC polyplexes was much more efficient. Concerning the total amount of polyplexes taken up, TMC and PTMC in A549 cells were as efficient as and in L929 cells even outperformed PEI polyplexes. As shown above chitosan 100 kDa produced condensed particles with pDNA in the preparation medium but fast and severe aggregation was observed upon mixing with DMEM. The increase in particle size correlates well with the decreased uptake efficiency. Similarly, the uptake efficiency of PEI polyplexes is relatively low in both cell lines. Issa et al. obtained comparable results studying polyplexes with chitosan oligomers and trisaccharide-substituted chitosan oligomers by fluorescence microscopy (*35*). In this study, a positive correlation between cellular uptake, polyplex size and finally transfection efficiency was found. Cellular uptake of polyplexes in the case of chitosan oligomers was strongly reduced due to insufficient colloidal stability of these polyplexes. Mac Laughlin et al. also explained the low transfection efficiency of chitosan polyplexes with low internalization efficiency (*36*). However, no clear correlation between colloidal stability and internalization efficiency was drawn in this study. A similar correlation between size

and uptake efficiency was found in the study of Zuhorn et al. where internalization of radioactively labeled lipoplexes was studied by scintillation counting (*34*).

The second approach of analysis was to determine the percentage of YOYO-1 positive cells over time. Kinetics of polyplex uptake in L929 cells was very similar for PEI, TMC and PTMC polyplexes. Polyplex internalization was seen within 45 to 60 min in 50% and within 100 to 115 min in 75% of the cells. In A549 cells, PEI internalization was somewhat faster with 50% of positive cells in 40 min and 75% in 53 min. In contrast, internalization of TMC and PTMC polyplexes was slightly slower in this cell line. Cellular uptake in 50% of the cell population was seen within 82 to 96 min and the 75% level was reached after 125 to 150 min with these polyplexes. Again, uptake of chitosan complexes was low with only 5% and 21% of YOYO-positive cells after 5 hours of incubation in L929 and A549 cells, respectively.

Based on kinetics and efficiency of uptake one could hypothesize that the route of uptake is identical for all polyplexes in L929 cells while significant differences in uptake route could be expected in the case of A549 cells.

6.4.3 Effect of inhibitors on cellular uptake

To study cellular uptake mechanisms we sought to characterize polyplex internalization in the presence of specific inhibitors of cellular uptake pathways. Plasmid DNA was fluorescently labeled using the intercalating dye YOYO-1. After incubation for 3 hours, cell surface bound fluorescence was quenched by incubation with trypan blue and remaining fluorescence from internalized polyplexes was analyzed by flow cytometry. In all experiments, blank cells and cells which were treated with fluorescently labeled polyplexes only were used as 0% and 100% control, respectively. Due to very low initial uptake, analysis of inhibition of chitosan polyplex uptake was not feasible. We therefore limited further analysis on TMC, PTMC and PEI polyplexes, which showed reasonable uptake efficiency.

The route of uptake of non-viral vectors is a field which is currently under intensive investigation. Studying PEI complexes in COS-7 cells, van der Aa et al. found that polyplexes were taken up both via caveolae and clathrin-mediated endocytosis but only caveolae-mediated uptake resulted in efficient transfection (*25*). Similar results were found by Reijman et al. for A549 and HeLa cells (*24, 37*). Studies performed by Grosse

et al. support these findings. The authors showed that uptake of PEI polyplexes in cystic fibrosis airway epithelial cells depend on actin filaments while microtubules are involved in trafficking of polyplexes towards the nucleus (*38*). In contrast, Mennesson et al. found that PEI polyplexes were mainly taken up by clathrin-mediated endocytosis in human lung endothelial cells (*39*). Goncalves et al. studying histidinylated polylysine polyplexes in HepG2 cells showed that polyplexes were internalized by clathrin mediated endocytosis and macropinocytosis (*40*). Looking at transfection efficiency, inhibitors of clathrin mediated endocytosis completely prevented reporter gene expression in this study while inhibitors of macropinocytosis had no effect. Studies on size-dependence of cellular uptake performed by Rejman et al. found that microspheres of 200 nm and less entered cells through clathrin-coated pits by a microtubule dependent pathway (*28*). Microspheres with a diameter of 500 nm underwent a slow, microtubule independent uptake that was inhibited by amiloride and cytochalasin D. The authors deduced that the particles were taken up via caveolae. As caveolae typically are around 60 nm in size and intracellular transport also depends on microtubules, this finding was somewhat surprising and a clear explanation is currently lacking (*15*). Grosse et al. also studied the size-dependence of internalization in human tracheal epithelial cells and found that large polyplexes were mainly internalized by macropinocytosis, intermediate sized (100-200 nm), ligand-coupled polyplexes were taken up by clathrin-mediated endocytosis and small PEI polyplexes entered the cells via caveolae (*27*).

A main problem of most of these studies is that authors are dealing with a moving target in several ways: Inhibition of a cellular uptake pathway might trigger the activation of another which might then affect both uptake and transfection results (*41*). Inhibitors of certain cellular uptake pathways often also affect others, e.g. microtubule depolymerization by nocodazole might affect clathrin-mediated endocytosis as well as uptake via caveolae or inhibitors of actin such as cytochalasin D may affect caveolae and macropinocytosis (*15*). Furthermore, non-viral vectors are seldom monodispersed and particle size may vary by time and depending on the environment. Lastly, another important factor influencing the route of uptake is cell line evaluated as shown by Manunta et al. and von Gersdorff et al. (*26, 41*).

The results of uptake studies performed with PEI, TMC and PTMC polyplexes in L929 and A549 cells are shown in figure 4. Having previous studies and most common uptake

mechanism in mind we focused on a) clathrin mediated endocytosis, b) uptake via caveolae, and c) macropinocytosis. Chlorpromazine and hypertonic treatment were used for specific inhibition of clathrin mediated endocytosis (*42, 43*). The sterol binding drugs filipin and nystatin are known to form complexes with cholesterol (*44*) and interact with cellular uptake via caveolae (*45*). Macropinocytosis was specifically inhibited by wortmannin (*46-48*). Methyl-β-CD, which extracts free cholesterol from membranes (*49*), affects both clathrin- and caveolae-mediated uptake (*50-52*).

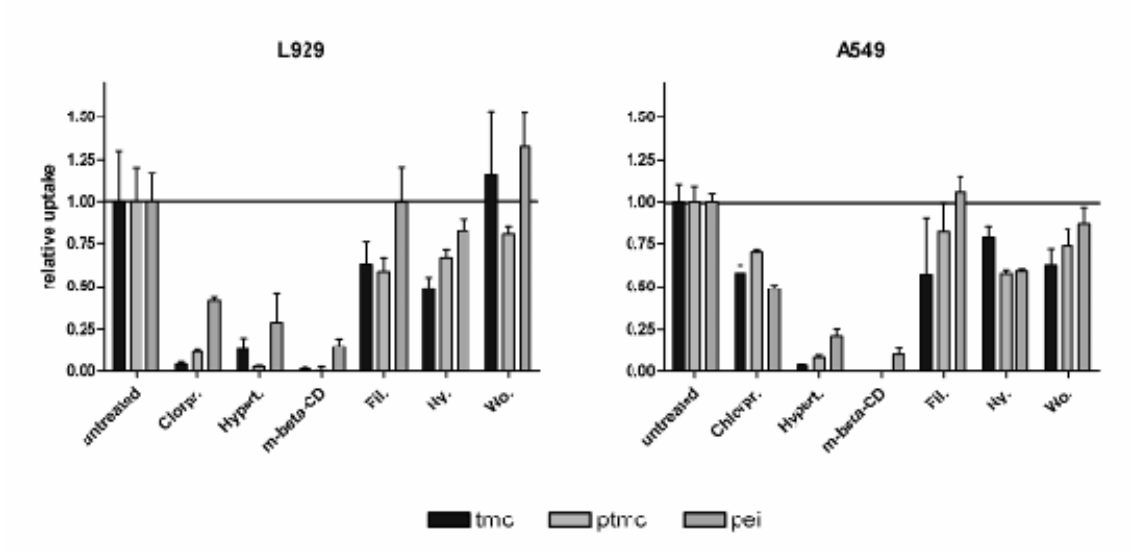

Figure 4: Cellular uptake of polyplexes in L929 and A549 cells after coincubation with inhibitors of different uptake pathways. Inhibitors were incubated with the cells for 30 min in DMEM without FCS before polyplexes were added. After 3 hours incubation with polyplexes and inhibitors, cell were washed with trypan blue and intracellular fluorescence was quantified by flow cytometry. Results given as mean ± standard deviation of 3 measurements.

In L929 cells, uptake of all polyplexes was strongly inhibited by chlorpromazine, hypertonic treatment and methyl-β-CD. Furthermore, uptake of TMC and PTMC polyplexes was inhibited by nystatin and filipin. In A549 cells, similar to L929 cells, a strong effect of hypertonic treatment and methyl-β-CD was found. However, inhibition of uptake of TMC and PTMC polyplexes by chlorpromazine was less pronounced in favor of inhibition by wortmannin. Uptake inhibition was found with nystatin for all polyplexes, but filipin showed no strong inhibitory effect. At this point, it should also be noted that caveolin expression in A549 cells was shown to be very low and no visual evidence for the presence of caveolae was found in this cell line (*53-56*). Therefore, it is unlikely that

uptake by caveolae significantly contributes to polyplex internalization in A549 cells. In contrast, significant caveolin expression was found in L929 cells and caveolae may contribute to endocytosis (*57, 58*). Based on these results, we conclude that clathrin-mediated endocytosis is the main route of uptake in L929 cells, which to a smaller extent might be accompanied by uptake via caveolae, especially in the case of TMC and PTMC polyplexes. In A549 cells, besides clathrin-mediated endocytosis, macropinocytosis potentially contributes to uptake of TMC and PTMC polyplexes. The contribution of macropinocytosis to polyplex uptake of TMC and PTMC polyplexes may serve as an explanation for differences found in internalization kinetics. Route of uptake of free chitosan polymer and nanoparticles prepared with chitosan in A549 cells was studied by Huang et al. (*29*). Similar to our findings, the authors report that clathrin-mediated endocytosis significantly contributes to nanoparticle uptake in these cells while inhibition of caveolae-mediated uptake by filipin had no effect. In a later study, the authors reaffirmed these findings using chitosan/pDNA polyplexes (*59*). It was found that polyplexes at least in part colocalized with transferrin, a marker for clathrin-mediated endocytosis and with lysotracker green, a lysosomal marker. Unfortunately, macropinocytosis as a possible uptake route was not taken into consideration in these studies. However, the finding of contribution of macropinocytosis to cellular uptake in A549 cells is not completely unexpected. Reports from Slevogt et al. and Garcia-Perez et al. showed that Moraxella catarrhalis and Mycobacterium tuberculosis are internalized by macropinocytosis in these cells (*60, 61*). Furthermore, Foster et al. showed that A549 cells internalize microspheres as large as 3 μm (*62*).

6.4.4 Effect of inhibitors on gene expression

The effect of inhibitors used in uptake studies was evaluated at the level of gene expression under conditions comparable to uptake experiments (Figure 5). Two additional drugs, chloroquine and nocodazole, were added in these experiments to study the effect of endosome acidification and microtubule depolymerization on transfection efficiency, respectively.

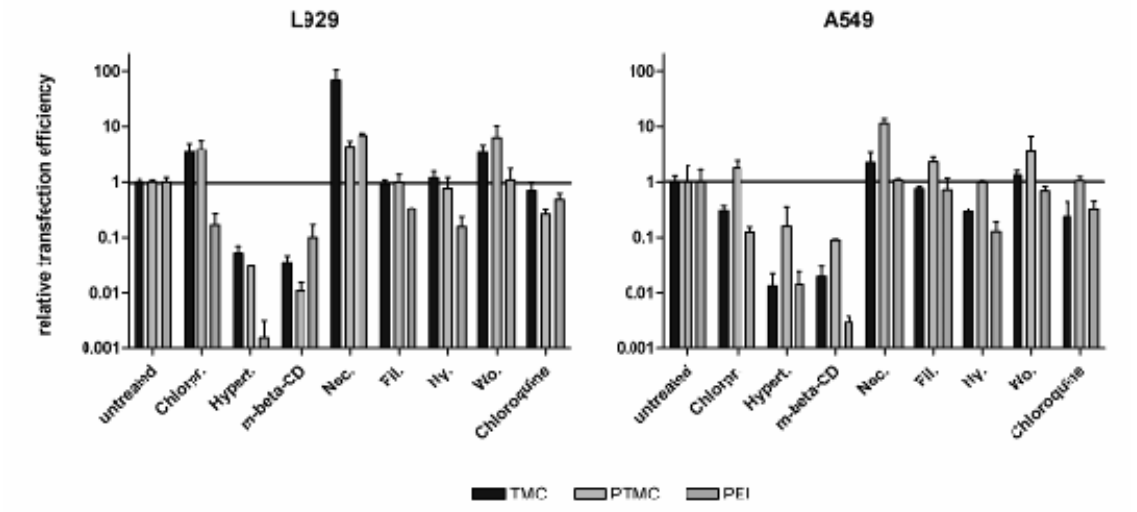

Figure 5: Transfection efficiency of polyplexes in L929 and A549 cells after coincubation with inhibitors of different uptake pathways. Inhibitors were incubated with the cells for 30 min in DMEM without FCS before polyplexes were added. After 3 hours incubation with polyplexes and inhibitors, fresh media was added and cells were incubated for an additional 45 hours.. Results given as mean ± standard deviation of 3 measurements.

In L929 cells, gene expression of PEI polyplexes was inhibited by chlorpromazine, hypertonic treatment, methyl-β-CD, fillipin and nystatine. Furthermore, gene expression was increased after microtubule depolymerization by nocodazole but was not influenced by chloroquine. Compared to PEI, inhibition of transfection of TMC and PTMC was slightly more pronounced with methyl-β-CD and less effective with hypertonic treatment. An increase in transfection efficiency was seen with chlorpromazine, wortmannin and nocodazol. Again, no increased transfection efficiency was seen with chloroquine.

In A549 cells, transfection using PEI polyplexes was inhibited by chlorpromazine, hypertonic treatment, methyl-β-CD and nystatin. Microtubule depolymerization and chloroquine coincubation had no effect on transfection efficiency of PEI polyplexes in this cell line. TMC and PTMC transfection was inhibited by methyl-β-CD and hypertonic treatment. These effects were stronger in the case of TMC polyplexes, which in addition showed inhibition of transfection with chlorpromazine. Transfection efficiency of TMC and PTMC polyplexes was increased with nocodazole but no strong effect was seen with chloroquine.

Due to the relative strong effect of methyl-β-CD and hypertonic treatment on transfection efficiency of all polyplexes in both cell lines, we assume that clathrin-mediated endocytosis significantly contributes to transfection. This conclusion is supported by our finding that nocodazole, a microtubule depolymerizing agent interacting with transport from early endosomes to lysosomes enhanced transfection efficiency in all cases except for PEI polyplexes in A549 cells. Furthermore, inhibition of transfection with nystatin, filipin and methyl-β-CD was seen in the case of PEI polyplexes in L929 cells pointing to a certain contribution of caveolae mediated endocytosis as described by Reijman et al. and van der Aa et al. (*24, 25*). Wortmannin, which showed reduction of uptake of TMC and PTMC polyplexes in A549 cells failed to inhibit transfection. Therefore, a significant contribution of macropinocytosis to transfection is less likely.

Interestingly, chlorpromazine failed to inhibit or even augmented transfection using TMC and PTMC in L929 and PTMC in A549 cells. A possible explanation for this observation was suggested by Manunta et al. and Reijman et al. who found that inhibition of one cellular uptake pathway might trigger uptake via another route (*28, 41*). However, concerning uptake experiments which showed that chlorpromazine strongly inhibited uptake of polyplexes, this seems less likely. Recently, Neukamm et al. described enhanced transfection of both yeast and HepG2 cells after coincubation of DEAE-dextran polyplexes with different phenothiazines and tricyclic antidepressants including chlorpromazine (*63*). The authors suspected that these drugs might affect polyplex integrity by interaction with DNA or may destabilize the endocytic vesicle membrane facilitating endosomal release. Indeed, chlorpromazine is a highly lysosomotropic drug and partitioning of the protonated form into the lipid membrane as well as alkalinization of lysosomes was reported (*64, 65*). Chloroquine was also shown to increase lysosomal pH and to interact with DNA (*66, 67*). Due to the fact that chloroquine in our study failed to increase transfection efficiency in the case of TMC and PTMC the contribution of alkalinization of lysosomes or displacement of polycations seems to be of lower importance. Therefore we conclude that increased transfection efficiency of TMC and PTMC despite their lower uptake after chlorpromazine coincubation might be due to an increased release from endosomes or lysosomes.

Strongly increased transfection efficiencies were also observed when polyplexes were coincubated with nocodazole. A similar effect was observed by Hashimoto et al. for

chitosan/pDNA complexes in HepG2 and COS7 cells and by Lindberg et al. for DOTIM/DOPE lipopplexes in CV-1 cells (*30, 68*). The authors concluded that microtubule depolymerization augments release from early endosomes, decreases degradation in lysosomes and by that enhances transfection efficiency. Furthermore, transfection with PEI/pDNA polyplexes in CHO cells was improved by nocodazole treatment (*69*). This effect was explained by G2/M blockage by nocodazole and increased transfer of polyplexes or pDNA into the nucleus. In contrast, decreased transfection efficiency of PEI polyplexes was found in cystic fibrosis airway epithelial cells and COS7 after nocodazole treatment by Grosse et al. and van der Aa et al. (*25, 38*). Transfection of both cell lines was shown to strongly depend on uptake of polyplexes via caveolae. Caveolar uptake was reported to evade degradation in lysosomes, therefore, microtubule disruption in this case might inversely affect transfection efficiency (*15*).

In conclusion our study shows that clathrin mediated- and potentially caveolar uptake are important routes of polyplex entry in L929 cells. In A549 cells we showed that clathrin mediated uptake as well as macropinocytosis contribute to polyplex uptake. In terms of transfection efficiency, the situation was less clear. However, a significant contribution of clathrin-mediated endocytosis is very likely in both cell lines.

Uptake studies performed with the different chitosan derivatives showed that efficient cellular uptake necessarily precedes efficient transfection. Interestingly, we found improved cellular uptake of chitosan derivatives compared to PEI polyplexes in L929 cells. However, this did not translate in increased transfection efficiency. Similarly, uptake of TMC and PTMC in A549 cells was equally efficient as PEI polyplex uptake but transfection efficiency was significantly lower. The observed differences in polyplex uptake pathways can not sufficiently explain the differences in transfection efficiency. As mentioned above, gene delivery using non-viral vectors is a multistep process. In this study we focused on polyplex entry and its effect on transfection efficiency. Based on our findings, the main bottleneck of chitosan based gene transfer in the case of TMC and PTMC polyplexes is downstream cellular uptake. Surprisingly, not only nocodazole but also chlorpromazine increased transfection efficiency of TMC and PTMC polyplexes in L929 cells. Therefore, we hypothesize that endosomal/lysosomal release of TMC and PTMC polyplexes is lower than that of PEI polyplexes and hampers efficient transfection. Destabilization of endolysosomal membrane by chlorpromazine or de-

creased transport of endosomes towards lysosomes therefore may result in increased transfection efficiency. Another interesting finding in this direction was that chloroquine did not enhance transfection efficiency neither of PEI nor of chitosan derivative polyplexes. In contrast, transfection efficiency of chitosan polyplexes in L929 cells was increased after coincubation with chloroquine (data not shown). Recently it was shown that chloroquine improves transfection efficiency by different mechanisms: it buffers the acidic pH of the lysosome, displaces DNA from certain polycations and by intracellular binding to DNA facilitates gene transfer (*70*). The fact that chloroquine does not improve transfection efficiency of TMC or PTMC can therefore be explained in several ways: Chitosan derivatives might have sufficient intrinsic buffering capacity and therefore do not benefit from chloroquine, chloroquine might not be able to displace DNA from TMC and PTMC polyplexes or release from polyplexes occurs upstream of lysosomes. Effects seen with nocodazole may point to the latter as an reasonable explanation. However, little is known about the intracellular processing and cellular entry of these vectors and the results obtained here merit further investigations in this specific direction. Studying the underlying mechanisms of these steps might help to completely understand differences between chitosan and PEI mediated transfection and will facilitate development of more efficient chitosan derivatives.

6.5 Acknowledgments

We are grateful to Eva Mohr for excellent support in cell culture experiments and to Cornelia Brendel (Flow Cytometry Core Facility, Department of Hematology, Oncology and Immunology, University Hospital Marburg) for generous use of equipment and facilities.

6.6 References

(1) Merdan, T., Kopecek, J., and Kissel, T. (2002) Prospects for cationic polymers in gene and oligonucleotide therapy against cancer. *Adv Drug Deliv Rev 54*, 715-58.

(2) Borchard, G. (2001) Chitosans for gene delivery. *Adv Drug Deliv Rev 52*, 145-50.

(3) Richardson, S. C., Kolbe, H. V., and Duncan, R. (1999) Potential of low molecular mass chitosan as a DNA delivery system: biocompatibility, body distribution and ability to complex and protect DNA. *Int J Pharm 178*, 231-43.

(4) Mao, H. Q., Roy, K., Troung-Le, V. L., Janes, K. A., Lin, K. Y., Wang, Y., August, J. T., and Leong, K. W. (2001) Chitosan-DNA nanoparticles as gene carriers: synthesis, characterization and transfection efficiency. *J Control Release 70*, 399-421.

(5) Rao, S. B., and Sharma, C. P. (1997) Use of chitosan as a biomaterial: studies on its safety and hemostatic potential. *J Biomed Mater Res 34*, 21-8.

(6) Aspden, T. J., Mason, J. D., Jones, N. S., Lowe, J., Skaugrud, O., and Illum, L. (1997) Chitosan as a nasal delivery system: the effect of chitosan solutions on in vitro and in vivo mucociliary transport rates in human turbinates and volunteers. *J Pharm Sci 86*, 509-13.

(7) Kim, T. H., Kim, S. I., Akaike, T., and Cho, C. S. (2005) Synergistic effect of poly(ethylenimine) on the transfection efficiency of galactosylated chitosan/DNA complexes. *J Control Release 105*, 354-66.

(8) Jiang, H. L., Kim, Y. K., Arote, R., Nah, J. W., Cho, M. H., Choi, Y. J., Akaike, T., and Cho, C. S. (2007) Chitosan-graft-polyethylenimine as a gene carrier. *J Control Release 117*, 273-80.

(9) Kim, T. H., Ihm, J. E., Choi, Y. J., Nah, J. W., and Cho, C. S. (2003) Efficient gene delivery by urocanic acid-modified chitosan. *J Control Release 93*, 389-402.

(10) Thanou, M., Florea, B. I., Geldof, M., Junginger, H. E., and Borchard, G. (2002) Quaternized chitosan oligomers as novel gene delivery vectors in epithelial cell lines. *Biomaterials 23*, 153-9.

(11) Mao, S., Shuai, X., Unger, F., Wittmar, M., Xie, X., and Kissel, T. (2005) Synthesis, characterization and cytotoxicity of poly(ethylene glycol)-graft-trimethyl chitosan block copolymers. *Biomaterials 26*, 6343-56.

(12) Germershaus, O., Mao, S., Sitterberg, J., Bakowsky, U., and Kissel, T. (2007) Gene delivery using chitosan, trimethyl chitosan or polyethylenglycol-graft-

trimethyl chitosan block copolymers: Establishment of structure-activity relationships in vitro. *J Control Release 125*, 145-154.

(13) Bally, M. B., Harvie, P., Wong, F. M., Kong, S., Wasan, E. K., and Reimer, D. L. (1999) Biological barriers to cellular delivery of lipid-based DNA carriers. *Adv Drug Deliv Rev 38*, 291-315.

(14) Pelkmans, L., and Helenius, A. (2003) Insider information: what viruses tell us about endocytosis. *Curr Opin Cell Biol 15*, 414-22.

(15) Medina-Kauwe, L. K., Xie, J., and Hamm-Alvarez, S. (2005) Intracellular trafficking of nonviral vectors. *Gene Ther 12*, 1734-51.

(16) Khalil, I. A., Kogure, K., Akita, H., and Harashima, H. (2006) Uptake pathways and subsequent intracellular trafficking in nonviral gene delivery. *Pharmacol Rev 58*, 32-45.

(17) Parton, R. G., and Richards, A. A. (2003) Lipid rafts and caveolae as portals for endocytosis: new insights and common mechanisms. *Traffic 4*, 724-38.

(18) Johannes, L., and Lamaze, C. (2002) Clathrin-dependent or not: is it still the question? *Traffic 3*, 443-51.

(19) Kirkham, M., and Parton, R. G. (2005) Clathrin-independent endocytosis: new insights into caveolae and non-caveolar lipid raft carriers. *Biochim Biophys Acta 1745*, 273-86.

(20) Wadia, J. S., Stan, R. V., and Dowdy, S. F. (2004) Transducible TAT-HA fusogenic peptide enhances escape of TAT-fusion proteins after lipid raft macropinocytosis. *Nat Med 10*, 310-5.

(21) Boussif, O., Lezoualc'h, F., Zanta, M. A., Mergny, M. D., Scherman, D., Demeneix, B., and Behr, J. P. (1995) A versatile vector for gene and oligonucleotide transfer into cells in culture and in vivo: polyethylenimine. *Proc Natl Acad Sci U S A 92*, 7297-301.

(22) Merdan, T., Kunath, K., Fischer, D., Kopecek, J., and Kissel, T. (2002) Intracellular processing of poly(ethylene imine)/ribozyme complexes can be observed in living cells by using confocal laser scanning microscopy and inhibitor experiments. *Pharm Res 19*, 140-6.

(23) Huth, S., Lausier, J., Gersting, S. W., Rudolph, C., Plank, C., Welsch, U., and Rosenecker, J. (2004) Insights into the mechanism of magnetofection using PEI-based magnetofectins for gene transfer. *Journal of Gene Medicine 6*, 923-936.

(24) Rejman, J., Bragonzi, A., and Conese, M. (2005) Role of clathrin- and caveolae-mediated endocytosis in gene transfer mediated by lipo- and polyplexes. *Mol Ther 12*, 468-74.

(25) van der Aa, M. A., Huth, U. S., Hafele, S. Y., Schubert, R., Oosting, R. S., Mastrobattista, E., Hennink, W. E., Peschka-Suss, R., Koning, G. A., and Crommelin, D. J. (2007) Cellular Uptake of Cationic Polymer-DNA Complexes Via Caveolae Plays a Pivotal Role in Gene Transfection in COS-7 Cells. *Pharm Res 24*, 1590-8.

(26) von Gersdorff, K., Sanders, N. N., Vandenbroucke, R., De Smedt, S. C., Wagner, E., and Ogris, M. (2006) The Internalization Route Resulting in Successful Gene Expression Depends on both Cell Line and Polyethylenimine Polyplex Type. *Mol Ther 14*, 745-753.

(27) Grosse, S., Aron, Y., Thevenot, G., Francois, D., Monsigny, M., and Fajac, I. (2005) Potocytosis and cellular exit of complexes as cellular pathways for gene delivery by polycations. *J Gene Med 7*, 1275-86.

(28) Rejman, J., Oberle, V., Zuhorn, I. S., and Hoekstra, D. (2004) Size-dependent internalization of particles via the pathways of clathrin- and caveolae-mediated endocytosis. *Biochem J 377*, 159-69.

(29) Huang, M., Ma, Z., Khor, E., and Lim, L. Y. (2002) Uptake of FITC-chitosan nanoparticles by A549 cells. *Pharm Res 19*, 1488-94.

(30) Hashimoto, M., Morimoto, M., Saimoto, H., Shigemasa, Y., and Sato, T. (2006) Lactosylated Chitosan for DNA Delivery into Hepatocytes: The Effect of Lactosylation on the Physicochemical Properties and Intracellular Trafficking of pDNA/Chitosan Complexes. *Bioconjugate Chem. 17*, 309-316.

(31) Ogris, M., Steinlein, P., Carotta, S., Brunner, S., and Wagner, E. (2001) DNA/polyethylenimine transfection particles: influence of ligands, polymer size, and PEGylation on internalization and gene expression. *AAPS PharmSci 3*, E21.

(32) Wang, Y., Chen, P., and Shen, J. (2007) A facile entrapment approach to construct PEGylated polyplexes for improving stability in physiological condition. *Colloids Surf B Biointerfaces 58*, 188-96.

(33) Sharma, V. K., Thomas, M., and Klibanov, A. M. (2005) Mechanistic studies on aggregation of polyethylenimine-DNA complexes and its prevention. *Biotechnol Bioeng 90*, 614-20.

(34) Zuhorn, I. S., Visser, W. H., Bakowsky, U., Engberts, J. B., and Hoekstra, D. (2002) Interference of serum with lipoplex-cell interaction: modulation of intracellular processing. *Biochim Biophys Acta 1560*, 25-36.

(35) Issa, M. M., Koping-Hoggard, M., Tommeraas, K., Varum, K. M., Christensen, B. E., Strand, S. P., and Artursson, P. (2006) Targeted gene delivery with trisaccharide-substituted chitosan oligomers in vitro and after lung administration in vivo. *J Control Release 115*, 103-12.

(36) MacLaughlin, F. C., Mumper, R. J., Wang, J., Tagliaferri, J. M., Gill, I., Hinchcliffe, M., and Rolland, A. P. (1998) Chitosan and depolymerized chitosan oligomers as condensing carriers for in vivo plasmid delivery. *J Control Release 56*, 259-72.

(37) Rejman, J., Conese, M., and Hoekstra, D. (2006) Gene transfer by means of lipo- and polyplexes: role of clathrin and caveolae-mediated endocytosis. *J Liposome Res 16*, 237-47.

(38) Grosse, S., Aron, Y., Thevenot, G., Monsigny, M., and Fajac, I. (2007) Cytoskeletal involvement in the cellular trafficking of plasmid/PEI derivative complexes. *J Control Release 122*, 111-7.

(39) Mennesson, E., Erbacher, P., Piller, V., Kieda, C., Midoux, P., and Pichon, C. (2005) Transfection efficiency and uptake process of polyplexes in human lung endothelial cells: a comparative study in non-polarized and polarized cells. *J Gene Med 7*, 729-38.

(40) Goncalves, C., Mennesson, E., Fuchs, R., Gorvel, J. P., Midoux, P., and Pichon, C. (2004) Macropinocytosis of polyplexes and recycling of plasmid via the clathrin-dependent pathway impair the transfection efficiency of human hepatocarcinoma cells. *Mol Ther 10*, 373-85.

(41) Manunta, M., Nichols, B. J., Hong Tan, P., Sagoo, P., Harper, J., and George, A. J. (2006) Gene delivery by dendrimers operates via different pathways in different cells, but is enhanced by the presence of caveolin. *J Immunol Methods 314*, 134-46.

(42) Wang, L. H., Rothberg, K. G., and Anderson, R. G. (1993) Mis-assembly of clathrin lattices on endosomes reveals a regulatory switch for coated pit formation. *J Cell Biol 123*, 1107-17.

(43) Heuser, J. E., and Anderson, R. G. (1989) Hypertonic media inhibit receptor-mediated endocytosis by blocking clathrin-coated pit formation. *J Cell Biol 108*, 389-400.

(44) Bolard, J. (1986) How do the polyene macrolide antibiotics affect the cellular membrane properties? *Biochim Biophys Acta 864*, 257-304.

(45) Schnitzer, J. E., Oh, P., Pinney, E., and Allard, J. (1994) Filipin-sensitive caveolae-mediated transport in endothelium: reduced transcytosis, scavenger endocytosis, and capillary permeability of select macromolecules. *J Cell Biol 127*, 1217-32.

(46) Sato, S. B., Taguchi, T., Yamashina, S., and Toyama, S. (1996) Wortmannin and Li+ specifically inhibit clathrin-independent endocytic internalization of bulk fluid. *J Biochem 119*, 887-97.

(47) Araki, N., Johnson, M. T., and Swanson, J. A. (1996) A role for phosphoinositide 3-kinase in the completion of macropinocytosis and phagocytosis by macrophages. *J Cell Biol 135*, 1249-60.

(48) Shpetner, H., Joly, M., Hartley, D., and Corvera, S. (1996) Potential sites of PI-3 kinase function in the endocytic pathway revealed by the PI-3 kinase inhibitor, wortmannin. *J Cell Biol 132*, 595-605.

(49) Ohtani, Y., Irie, T., Uekama, K., Fukunaga, K., and Pitha, J. (1989) Differential effects of alpha-, beta- and gamma-cyclodextrins on human erythrocytes. *Eur J Biochem 186*, 17-22.

(50) Kilsdonk, E. P., Yancey, P. G., Stoudt, G. W., Bangerter, F. W., Johnson, W. J., Phillips, M. C., and Rothblat, G. H. (1995) Cellular cholesterol efflux mediated by cyclodextrins. *J Biol Chem 270*, 17250-6.

(51) Rodal, S. K., Skretting, G., Garred, O., Vilhardt, F., van Deurs, B., and Sandvig, K. (1999) Extraction of cholesterol with methyl-beta-cyclodextrin perturbs formation of clathrin-coated endocytic vesicles. *Mol Biol Cell 10*, 961-74.

(52) Subtil, A., Gaidarov, I., Kobylarz, K., Lampson, M. A., Keen, J. H., and McGraw, T. E. (1999) Acute cholesterol depletion inhibits clathrin-coated pit budding. *Proc Natl Acad Sci U S A 96*, 6775-80.

(53) Yang, C.-P. H., Galbiati, F., Volonte, D., Horwitz, S. B., and Lisanti, M. P. (1998) Upregulation of caveolin-1 and caveolae organelles in Taxol-resistant A549 cells. *FEBS Letters 439*, 368-372.

(54) Belanger, M. M., Gaudreau, M., Roussel, E., and Couet, J. (2004) Role of caveolin-1 in etoposide resistance development in A549 lung cancer cells. *Cancer Biol Ther 3*, 954-9.

(55) Roussel, E., Belanger, M. M., and Couet, J. (2004) G2/M blockade by paclitaxel induces caveolin-1 expression in A549 lung cancer cells: caveolin-1 as a marker of cytotoxicity. *Anticancer Drugs 15*, 961-7.

(56) Barar, J., Campbell, L., Hollins, A. J., Thomas, N. P., Smith, M. W., Morris, C. J., and Gumbleton, M. (2007) Cell selective glucocorticoid induction of caveolin-1 and caveolae in differentiating pulmonary alveolar epithelial cell cultures. *Biochem Biophys Res Commun 359*, 360-6.

(57) Ono, K., Iwanaga, Y., Hirayama, M., Kawamura, T., Sowa, N., and Hasegawa, K. (2004) Contribution of caveolin-1 alpha and Akt to TNF-alpha-induced cell death. *Am J Physiol Lung Cell Mol Physiol 287*, L201-9.

(58) Yamauchi, Y., Abe-Dohmae, S., and Yokoyama, S. (2002) Differential regulation of apolipoprotein A-I/ATP binding cassette transporter A1-mediated cholesterol and phospholipid release. *Biochim Biophys Acta 1585*, 1-10.

(59) Huang, M., Fong, C. W., Khor, E., and Lim, L. Y. (2005) Transfection efficiency of chitosan vectors: Effect of polymer molecular weight and degree of deacetylation. *J Control Release 106*, 391-406.

(60) Slevogt, H., Seybold, J., Tiwari, K. N., Hocke, A. C., Jonatat, C., Dietel, S., Hippenstiel, S., Singer, B. B., Bachmann, S., Suttorp, N., et al. (2007) Moraxella catarrhalis is internalized in respiratory epithelial cells by a trigger-like mechanism and initiates a TLR2- and partly NOD1-dependent inflammatory immune response. *Cell Microbiol 9*, 694-707.

(61) Garcia-Perez, B. E., Mondragon-Flores, R., and Luna-Herrera, J. (2003) Internalization of Mycobacterium tuberculosis by macropinocytosis in non-phagocytic cells. *Microb Pathog 35*, 49-55.

(62) Foster, K. A., Yazdanian, M., and Audus, K. L. (2001) Microparticulate uptake mechanisms of in-vitro cell culture models of the respiratory epithelium. *J Pharm Pharmacol 53*, 57-66.

(63) Neukamm, B., Weimann, A., Wu, S., Danevad, M., Lang, C., and Gessner, R. (2006) Novel two-stage screening procedure leads to the identification of a new class of transfection enhancers. *J Gene Med 8*, 745-53.

(64) Lemieux, B., Percival, M. D., and Falgueyret, J. P. (2004) Quantitation of the lysosomotropic character of cationic amphiphilic drugs using the fluorescent basic amine Red DND-99. *Anal Biochem 327*, 247-51.

(65) Ishizaki, J., Yokogawa, K., Hirano, M., Nakashima, E., Sai, Y., Ohkuma, S., Ohshima, T., and Ichimura, F. (1996) Contribution of lysosomes to the subcellular distribution of basic drugs in the rat liver. *Pharm Res 13*, 902-6.

(66) Jones, R. L., Lanier, A. C., Keel, R. A., and Wilson, W. D. (1980) The effect of ionic strength on DNA-ligand unwinding angles for acridine and quinoline derivatives. *Nucleic Acids Res 8*, 1613-24.

(67) Ciftci, K., and Levy, R. J. (2001) Enhanced plasmid DNA transfection with lysosomotropic agents in cultured fibroblasts. *Int J Pharm 218*, 81-92.

(68) Lindberg, J., Fernandez, M. A., Ropp, J. D., and Hamm-Alvarez, S. F. (2001) Nocodazole treatment of CV-1 cells enhances nuclear/perinuclear accumulation of lipid-DNA complexes and increases gene expression. *Pharm Res 18*, 246-9.

(69) Tait, A. S., Brown, C. J., Galbraith, D. J., Hines, M. J., Hoare, M., Birch, J. R., and James, D. C. (2004) Transient production of recombinant proteins by Chinese hamster ovary cells using polyethyleneimine/DNA complexes in combination with microtubule disrupting anti-mitotic agents. *Biotechnol Bioeng 88*, 707-21.

(70) Cheng, J., Zeidan, R., Mishra, S., Liu, A., Pun, S. H., Kulkarni, R. P., Jensen, G. S., Bellocq, N. C., and Davis, M. E. (2006) Structure-function correlation of

chloroquine and analogues as transgene expression enhancers in nonviral gene delivery. *J Med Chem 49*, 6522-31.

7 Summary and Perspectives

7.1 Summary

In this thesis new non-viral gene delivery systems were synthesized and characterized. In the first part different questions in in vitro and in vivo gene delivery using HER2-targeted PEGylated PEI polyplexes are addressed. The second part deals with in vitro gene delivery using chitosan and its trimethyl- and PEG-trimethyl-derivatives.

Chapter 1 gives a short general introduction into the aims and pitfalls of gene delivery. PEI as a non-viral vector is introduced and major advantages and disadvantages of this system are highlighted. The evolution of PEI based vectors from simple electrostatic complexes to multifunctional targeted copolymers is shown. PEI vectors modified with cell-binding ligands are specially emphasized and relevant studies are summarized.

Secondly, we give a short summary on general properties and areas of application of chitosan. The key benefits as well as drawbacks of chitosan as a non-viral vector are discussed. Furthermore, techniques to improve the transfection efficiency of chitosan with a special focus on quaternized derivatives are discussed.

Chapter 2 describes the synthesis and characterization of a novel targeted gene delivery vector consisting of PEI as DNA condensing agent, PEG for surface shielding and the HER2 directed monoclonal antibody Trastuzumab for cell specific targeting. The resulting PEG-PEI-Trastuzumab conjugate was characterized concerning DNA condensation efficiency, hydrodynamic diameters and zetapotentials of polyplexes with DNA. It was shown that conjugation of Trastuzumab did not affect interaction with DNA. With 130-180 nm size of conjugate complexes was well below the threshold for endocytosis The surface of complexes was uncharged, decreasing non-specific binding to the cell membrane. Flow cytometry and confocal laser scanning microscopy were used to study cell binding and –internalization. It was found that conjugate complexes specifically bound to and were taken up into cells overexpressing HER2 while binding and uptake into HER2 negative cells was negligible. Finally, it was shown that these conjugates mediated efficient transfection in HER2 overexpressing cells. Specificity of transfection was demonstrated by competitive inhibition with free antibody. This study served as a proof of concept and stimulated further research in this direction.

Chapter 3 deals with optimization of the above mentioned vector and its in vivo applicability. In this study, PEG grafting density and chain length of PEG-PEI copolymer used for synthesis, the linker used to covalently couple Trastuzumab to PEI, and the degree of substitution with Trastuzumab was varied. It was found that all conjugates formed small polyplexes with DNA. Due to antibody modification, surface charge of all conjugate polyplexes was virtually neutral at all N/P ratios tested. The stability of polyplexes against DNA displacement by polyanion was tested using heparin. Conjugation of Trastuzumab slightly decreased DNA displacement by heparin. Blood compatibility was tested by incubation with erythrocytes determining the degree of hemolysis and erythrocyte morphology and aggregation. PEI polyplexes induced significant hemolysis and erythrocyte aggregation, both beeing strongly reduced with PEG-PEI copolymers. Conjugate polyplexes showed very low levels of hemolysis and erythrocyte morphology was virtually unchanged. A significant influence of conjugate composition on transfection efficiency and specificity was noted in cell culture. The best results were obtained when Trastuzumab was coupled to PEI via a heterobifunctional PEG linker. Conjugate and PEI complexes with radioactively labeled pDNA as well as free radiolabeled plasmid DNA were injected into the tail vein of BALB/c mice. Pharmacokinetics of conjugates revealed significant improvements over free plasmid DNA and PEI polyplexes. Area under the plasma level-time curve of conjugates was increased up to 48% or 114% compared to PEI or DNA, respectively. Furthermore, significantly decreased disposition of polyplexes in spleen and lung was observed in the case of conjugates. These findings demonstrated that conjugate composition plays a major role in efficiency and specificity of targeted polyplexes. Furthermore, antibody modification significantly improved the in vivo properties of polyplexes.

Chapter 4 aimed at studying the targeted conjugates characterized in chapter 3 in an in vivo tumor model. To establish a suitable in vivo tumor model, different HER2 overexpressing cell lines were tested for their ability to spontaneously form subcutaneous tumors in SCID mice. It was found that after subcutaneous injection of SK-OV-3 cells, mice developed tumors within 10 to 14 days. The tumors were characterized with respect to macroscopic and microscopic appearance, vascularization and HER2 expression level. For comparison, a well established subcutaneous tumor, Neuro2A, showing no HER2 overexpression was used. Compared to Neuro2A tumors, the tissue of SK-

OV-3 tumors appeared to be denser. SK-OV-3 tumors were surrounded by large blood vessels, while Neuro2A tumors macroscopically showed a better vascularization of the tumor tissue. Histological evaluation of hematoxylin and eosin stained sections of paraffin embedded tumors revealed lower vascularization with SK-OV-3 compared to Neuro2A tumors. Using anti-CD31 immunofluorescence, these results were verified. Immunofluorescence using Trastuzumab and a FITC-labeled secondary antibody showed that HER2 was only overexpressed in SK-OV-3 tumors. Trastuzumab-PEG-PEI/pDNA polyplexes were injected into the tail vein and transfection efficiency in main organs and tumor was compared to non-targeted PEI. Unfortunately, targeted polyplexes failed to selectively transfect SK-OV-3 tumors. In a second approach, targeted versus non-targeted polyplexes were administered by intratumoral injection. In this case, targeted polyplexes showed very slightly, but not significantly increased efficiency compared to PEI polyplexes. Further optimization of the tumor model and/or the polyplexes seems to be indispensable to achieve HER2-targeted in vivo gene transfer.

In *Chapter 5,* chitosan, trimethyl chitosan or polyethylenglycol-graft-trimethyl chitosan/DNA polyplexes were characterized concerning physicochemical properties such as hydrodynamic diameter, condensation efficiency and DNA release. The cytotoxicity of the polymers was evaluated during different incubation times in cell culture. Furthermore, uptake- and transfection efficiency of polyplexes were evaluated in vitro. While showing sufficient condensation efficiency under acidic, low ionic strength conditions, chitosan was found to form large aggregates of about 1000 nm accompanied by decreased DNA condensation ability under cell culture conditions. These characteristics resulted in only 7% cellular uptake in NIH/3T3 cells and low transfection efficiencies in 4 different cell lines. Quaternization of chitosan improved the solubility, DNA condensation ability, and complex formation at physiological pH. Accordingly, cellular uptake was increased 8.5-fold compared to chitosan polyplexes resulting in up to 678-fold increased transfection efficiency in NIH/3T3 cells. PEGylation of trimethyl chitosan not only decreased the cytotoxicity as shown by MTT assay and further increased the solubility but also improved colloidal stability of polyplexes. These improvements resulted in a significant, up to 10-fold increase of transfection efficiency in NIH/3T3, L929 and MeWo cells compared to trimethyl chitosan. The study highlights the importance of

colloidal stability of non-viral vector formulations, especially under physiological conditions and correlates these characteristics to a biological readout.

Chapter 6 describes further studies on cellular uptake pathways and intracellular processing of chitosan, trimethyl chitosan and polyethylenglycol-graft-trimethyl chitosan/DNA polyplexes. Specific inhibitors of different uptake- or intracellular processing pathways were employed to study uptake and transfection efficiency of polyplexes in A549 and L929 cells. In this respect, uptake kinetics and the colloidal stability of polyplexes was studied as well. As shown in chapter 5 severe aggregation of chitosan polyplexes was observed in physiological media and cellular uptake was low. With PEI polyplexes aggregation was also observed, but to a lesser extent and with lesser effect on cellular uptake efficiency. TMC and PTMC showed virtually no aggregation. Cellular uptake was strongly increased compared to PEI polyplexes in L929 and was as high as PEI uptake in A549. In L929 cells uptake kinetics were similar for all polyplexes, while PEI polyplexes were faster internalized than TMC or PTMC polyplexes in A549 cells. The main uptake pathway in L929 cells was clathrin-mediated endocytosis accompanied by uptake via caveolae in the case of TMC and PTMC polyplexes. Transfection efficiency was strongly influenced by clathrin-mediated endocytosis. In A549 cells, uptake mainly occurred by clathrin-mediated endocytosis which was accompanied by macropinocytosis but transfection mainly depended on the former. In this study certain differences in polyplex uptake and its effect on transfection were found. However, these could not fully explain the difference in transfection efficiency of PEI versus chitosan vectors. We therefore conclude that besides the uptake pathway other steps and barriers in the transfection process are at least of equal importance for efficient transfection with chitosan based vector systems. Some results pointed to inefficient intracellular release or incomplete vector unpacking as main barriers downstream polyplex uptake.

7.2 Perspectives

As outlined in the introduction, the ultimate goal of non-viral gene delivery is to develop a safe and efficient vector system with a satisfactory toxicity profile which can be administered intravenously. Furthermore, this vector should be able to target a specific cell type or tissue without affecting non-targeted cells. However, even if significant

steps towards this goal are made, the system fulfilling all these points is not yet developed.

The synthesis of targeted copolymers as described in this work is clearly advantageous in terms of characterization, robustness and repeatability of results. However, variations have to be introduced by synthesis of new conjugates, making it difficult to optimize or tailor theses systems in short time. To improve this situation, a "construction set" approach would be beneficial. Polyplexes could be prepared by the mixing of different components, making it easy to vary its properties. Similarly, the polycation could be modified with anchor molecules where shielding or targeting moieties could easily be attached. Furthermore, shielded polyplexes suffer from lower transfection efficiency compared to unshielded PEI possibly which is potentially due to lower endosomal release. Copolymers which change their characteristics in response to their environment could combine shielding and efficient endosomal release. During processing of early endosomes towards lysosomes, the pH gradually decreases. If polymers could respond to changes in pH, e.g. by disassembly of the PEG shell and targeting moieties, transfection efficiency might be improved.

Besides intracellular delivery, a major obstacle in in vivo gene delivery is the stability of the vector system in systemic circulation. It was shown in this work that coupling of antibodies might further improve circulation times of non-viral vectors. This could be a good starting point for further development, e.g. by shielding the polyplex surface with Fc fragments or albumin. Crosslinking of the surface is another possibility to increase circulation times which is under extensive investigation. However, after cellular uptake, unpacking of the crosslinked vector and DNA release is a major problem. More research and knowledge on distinct changes from extracellular to intracellular environment is needed to further optimize such systems.

It was shown in this work that in vivo gene delivery using targeted PEG-PEI did not result in efficient transfection of tumors. We hypothesize that the root cause for this outcome was insufficient vascularization of SK-OV-3 tumors. Therefore, new tumor models are needed to study in vivo targeting of HER2 targeted polyplexes. Several cell lines were reported to form subcutaneous tumors after injection into mice. However, most of these models depend on implantation of estrogen pellets, which was not possible in our

setup. A study on specificity and efficiency of HER2 targeted vectors using different HER2 overexpressing tumor models might verify the results found in vitro.

Chitosan based gene transfer in this work was shown to benefit from quaternization and PEGylation. However, transfection efficiencies still are several orders of magnitude lower than efficiency of PEI polyplexes and large amounts of polymer are needed to produce significant transfection. As described in the introduction, the combination of PEI and chitosan was found to improve transfection efficiency of both vectors. Future research could evaluate if the combination of PEI and trimethyl chitosan or PEG-trimethyl chitosan shows similar synergistic effects. Due to the increased stability of chitosan/DNA polyplexes compared to PEI and its prolonged release of DNA, this combination might be especially beneficial for in vivo application.

Little is known about the obstacles chitosan polyplexes face downstream cellular uptake. Studies on endosomal release and intracellular processing of chitosan and chitosan derivatives might help to optimize gene transfer and might trigger rationale synthesis of new chitosan derivatives.

7.3 Zusammenfassung

In der vorliegenden Arbeit wurden neue nicht-virale Vektoren zum Gentransfer synthetisiert und sowohl in vitro wie auch in vivo charakterisiert. Der erste Teil beschäftigt sich in erster Linie mit Studien zum zielgerichteten Gentransfer mittels Antikörper-modifizerter, PEGylierter Polyethylenimine. Im zweiten Teil der Arbeit werden neue Chitosan-Derivate wie Trimethyl-Chitosan und PEGyliertes Trimethyl-Chitosan hinsichtlich ihrer Eignung zur Transfektion von Zellen in vitro untersucht.

Kapitel 1 gibt eine kurze Übersicht über die Ziele und Hauptprobleme bei der Entwicklung von Genvektoren. Im Weiteren wird auf die wesentlichen Vor- und Nachteile von PEI eingegangen. Die Entwicklung nicht-viraler Vektorsysteme von einfachen elektrostatischen Komplexen hin zu multifunktionellen, zielgerichteten Kopolymeren wird am Beispiel von PEI illustriert. Besonderer Wert wird auf Zielzell-spezifisch modifizierte PEIs gelegt und die wesentlichen Studien in diesem Gebiet werden zusammengefasst.

Der zweite Teil der Einleitung beschäftigt sich mit den Eigenschaften und Hauptanwendungsgebieten von Chitosan. In Hinsicht auf die Anwendung in der nicht-viralen Gentherapie werden die Hauptvor- und -nachteile dieses Biopolymers geschildert. Weiterhin werden Techniken und Modifikation vorgestellt, die die Effizienz von Chitosan erhöhen können.

In *Kapitel 2* wird die Synthese und Charakterisierung eines neuen zielgerichteten Genvektors beschrieben. Dieser multifunktionelle Vektor besteht aus PEI, das zur Komplexierung der Plasmid-DNA dient, PEG zur Abschirmung der Komplexoberfläche und Trastuzumab, einen gegen HER2 gerichteten monoklonalen Antikörper, der für die zielgerichtete Transfektion bestimmter Zellen sorgen soll. Die synthetisierten Konjugate wurden physikochemisch hinsichtlich ihrer DNA-Komplexierungsfähigkeit, ihrer Größe sowie ihres Zetapotentials charakterisiert. Wir konnten zeigen, dass die Komplexierungseffizienz durch die Kopplung von Trastuzumab nicht negativ beeinflusst wurde. Es bildeten sich 130 bis 180 nm große, neutrale Komplexe. Die erzielte Größe erschien für die endozytotische Zellaufnahme geeignet. Eine neutrale Komplexoberfläche vermindert die unspezifische Anheftung an die Zellmembran über

elektrostatische Wechselwirkungen und ist somit in der Lage eine zielgerichtete Transfektion zu unterstützen. Die Zellbindung und –aufnahme der Polyplexe wurde mit konfokaler Mikroskopie und Durchflusszytometrie untersucht. Mit Hilfe dieser Techniken konnte nachgewiesen werden, dass die hergestellten Komplexe spezifisch an HER2 überexprimierende Zellen binden und von diesen aufgenommen werden. Die Bindung und Aufnahme in HER2-negative Zellen war hingegen gering. Die spezifische Bindung und Aufnahme resultierte in einer spezifischen Expression des verwendeten Reportergens in HER2-positiven Zellen, während die Transfektion HER2-negativer Zellen wesentlich weniger effizient war. Mittels kompetitiver Hemmung mit freiem Antikörper konnte nachgewiesen werden, dass die Reportergenexpression durch die Bindung der Polyplexe an HER2 Rezeptoren vermittelt wird. Damit diente diese Studie als „proof-of-concept“, die weitere Aktivitäten in dieser Richtung stimulierte.

Kapitel 3 behandelt die Optimierung des in Kapitel 2 charakterisierten Vektors und erste Studien zur Anwendbarkeit in vivo. Zunächst wurden verschiedene PEG-PEI-Trastuzumab Derivate synthetisiert, wobei die Anzahl der PEG-Ketten pro PEI Molekül, das Molekulargewicht des verwendeten PEGs sowie die Linkerchemie variiert wurden. Die Komplexe dieser Konjugate mit Plasmid DNA wurden physikochemisch charakterisiert. Mit allen Konjugaten bildeten sich kompakte Polyplexe. Durch die Kopplung von Trastuzumab und die hierdurch vermittelte zusätzliche Abschirmung zeigten alle Komplexe ein neutrales Zetapotential bei allen getesteten N/P-Verhältnissen. Die Stabilität der Polyplexe gegen DNA-Verdrängung durch Polyanionen wurde mit Hilfe von Heparin untersucht. Die Kopplung von Trastuzumab vermittelte eine leicht erhöhte Stabilität gegen DNA-Verdrängung durch Heparin. Indem die prozentuale Hämolyse und die Aggregation von Erythrozyten untersucht wurde, konnten Aussagen über die Blutkompatibilität der Komplexe gemacht werden. PEI Polyplexe verursachten sowohl eine relativ ausgeprägte Hämolyse wie auch eine verstärkte Erythrozytenaggregation. Durch PEGylierung konnten Hämolyse und Erythrozytenaggregation stark vermindert werden. Wurden Trastuzumab-PEI-PEG Komplexe mit Erythrozyten inkubiert, wurden hingegen nur sehr geringe Hämolyse und keine morphologischen Veränderungen beobachtet. In der Zellkultur wurden deutliche Unterschiede zwischen den Konjugaten hinsichtlich Effizienz und Spezifität festgestellt. Im Fall der Kopplung von Trastuzumab an PEI über einen heterobifuntionalen PEG-

Linker wurden die besten Ergebnisse erzielt. Die Pharmakokinetik und Biodistribution der Konjugate wurde nach intravenöser Applikation in BALB/c Mäusen untersucht. Dabei zeigten sich deutliche Verbesserungen gegenüber freier DNA und PEI Polyplexen. Einerseits war die AUC der Konjugat-Komplexe um bis zu 48% gegenüber PEI und um bis zu 114% gegenüber freier DNA erhöht. Andererseits konnte eine signifikant verminderte Deposition der Trastuzumab-modifizierten PEG-PEI Polyplexe sowohl in der Milz wie auch in der Lunge nachgewiesen werden. Diese Resultate zeigen, dass die Zusammensetzung zielgerichteter PEG-PEI Kopolymere wesentlich die Effizienz und Spezifität in vitro beeinflusst. Zudem wurden durch Antikörperkopplung sowohl die Zirkulationeigenschaften verbessert wie auch die unspezifische Deposition in Lunge und Milz vermindert.

Das Ziel der in *Kapitel 4* beschriebenen Experimente war die Untersuchung der Zielführungs- und Transfektionseigenschaften der in Kapitel 3 beschriebenen Konjugate. Zunächst musste ein HER2 überexprimierendes Tumormodell etabliert und charakterisiert werden. Hierzu wurden verschiedene Tumorzellinien subkutan in SCID-Mäuse injiziert und das Tumorwachstum untersucht. Einzig mit SK-OV-3 Zellen konnten subkutane Tumoren initiiert werden, die innerhalb von 10-14 Tagen deutliches Tumorwachstum zeigten. Diese Tumoren wurden makroskopisch und mikroskopisch auf Vaskularisierung und HER2-Expression untersucht. Als Vergleich wurden Neuro2A Tumoren, ein etabliertes und HER2 negatives Tumormodell verwendet. Im Vergleich zu Neuro2A erschien das Tumorgewebe der SK-OV-3 Tumoren dichter, zudem waren die letzteren von großen Blutgefässen umgeben, während die ersten von einem feinen Adergeflecht durchzogen waren. Die histologische Beurteilung der mit Hematoxylin und Eosin gefärbten Paraffin-Schnitte ergab eine geringere Vaskularisierung des Tumorgewebes bei SK-OV-3 Tumoren im Vergleich zu Neuro2A Tumoren. Immunfluoreszenuntersuchungen auf CD31 bestätigten dieses Ergebnis. Die HER2 Expression im Tumorgewebe wurde ebenfalls mittels Immunfluoreszenz untersucht. SK-OV-3 Tumoren zeigten eine deutliche Überexpression von HER2, während Neuro2A negativ getestet wurden. Trastuzumab-PEG-PEI/pDNA sowie PEI/pDNA Komplexe wurden intravenös über die Schwanzvene verabreicht. Leider konnte in diesen Experimenten keine selektive Transfektion HER2 exprimierender Tumoren nachgewiesen werden. Ein zweiter Ansatz bestand aus der intratumoralen Injektion der

Polyplexe. In diesem Fall schienen Trastuzumab-modifizierte Komplexen eine leicht verbesserte Transfektioneffizienz zu zeigen, jedoch konnte kein signifikanter Unterschied nachgewiesen werden. Diese Studie zeigte, dass eine weitere Optimierung sowohl des Tumormodells wie auch der zielgerichteten Polyplexe unumgänglich ist, um einen spezifischen und effizienten Gentransfer in vivo zu erreichen.

Kapitel 5 beschäftigt sich mit Untersuchungen zur Eignung von Chitosan, Trimethyl-Chitosan und PEGyliertem Trimethyl-Chitosan zum nicht-viralen Gentransfer. Polyplexe dieser Polymere mit pDNA wurden auf ihre Größe, die DNA-Komplexierungseffizienz und die DNA-Freisetzung untersucht. Die Toxizität der Polymere wurde während verschiedener Inkubationszeiten in der Zellkultur gemessen. Weiterhin wurde die Aufnahme und Transfektionseffizienz in vitro untersucht. Während Chitosan in aziden Medien mit niedriger Ionenstärke eine zufrieden stellende Affinität zu DNA zeigte, war diese in physiologischen Medien mit neutralem pH stark vermindert. In diesen Medien bildeten sich bis 1000 nm große Aggregate. Die zelluläre Aufnahme dieser Polyplexe in NIH/3T3 Zellen war mit 7% positiv angefärbter Zellen relativ ineffizient. Dies resultierte in sehr niedrigen Transfektionseffizienzen in 4 verschiednen Zelllinien. Durch Quarternisierung kann die Löslichkeit sowie die DNA Komplexierungsfähigkeit und damit die Komplexbildung bei physiologischen pH wesentlich gesteigert werden. Die zelluläre Aufnahme in NIH/3T3 war dementsprechend gegenüber Chitosan um das 8,5-fache, die Transfektionseffizienz um das 678-fache erhöht. Die PEGylierung von Trimethyl-Chitosan bewirkte nicht nur eine Verringerung der Zytotoxizität, wie mittels MTT-Methode nachgewiesen wurde, sondern verbesserte auch zusätzlich die Löslichkeit der Polymere und die Kolloidstabilität der Komplexe. Diese verbesserten Eigenschaften resultierten in einer signifikanten, bis zu 10-fachen Erhöhung der Transfektionseffizienz in NIH/3T3, L929 und MeWo Zellen gegenüber unmodifizierten Trimethyl-Chitosan. Diese Studie hebt die Bedeutung der Kolloidstabilität für die Formulierung nicht-viraler Vektoren hervor und korreliert diese mit der biologischen Effizienz.

Weitere Studien, die zelluläre Aufnahme und –Prozessierung der auf Chitosan basierenden Vektoren betreffend, stellt *Kapitel 6* vor. Die Aufnahme- und Transfektionseffizienz von Chitosan, Trimethyl-Chitosan und PEG-Trimethyl-Chitosan wurde nach Inhibition bestimmter Aufnahmerouten in A549 und L929 Zellen studiert.

In dieser Hinsicht wurde auch die Aufnahmekinetik und die Kolloidstabilität im Detail untersucht. Wie bereits in Kapitel 5 beschrieben, bildeten Chitosan Polyplexe in physiologischen Medien Aggregate, was zu einer geringen zellulären Aufnahme führte. Eine Aggregation der Polyplexe wurde auch im Fall von PEI beobachtet, diese war aber weniger ausgeprägt als bei Chitosan und hatte einen geringeren Einfluss auf die zelluläre Aufnahme. TMC und PTMC hingegen zeigten nahezu keine Aggregation. Die zelluläre Aufnahme war ebenso effizient wie die von PEI Polyplexen in A549 und war deutlich verbessert gegenüber PEI in L929 Zellen. Die Aufnahmekinetik war in L929 Zellen für alle untersuchten Polyplexe mit Ausnahme von Chitosan sehr ähnlich, in A549 Zellen wurde PEI wesentlich schneller aufgenommen als TMC oder PTMC. Der Hauptaufnahmeweg aller untersuchten Polyplexe war in L929 Zellen Clathrin-vermittelte Endozytose. Im Fall von TMC und PTMC wurde eine Beteiligung von Caveolae bei der Aufnahme festgestellt. Die Transfektionseffizienz war in diesen Zellen stark von Clathrin-vermittelter Endozytose beeinflusst. Auch in A549 Zellen war Clathrin-vermittelte Endozytose der Hauptaufnahmeweg für alle untersuchten Polyplexe, welche zum Teil von Macropinozytose begleitet wurde. Auch hier wurde die Transfektionseffizienz am stärksten durch Inhibitoren der Clathrin-vermittelten Endozytose beeinflusst. Wir konnten gewisse Unterschiede im Aufnahmemechanismus und ihren Effekt auf die Transfektionseffizienz feststellen. Dennoch reichen die gefunden Unterschiede in der Aufnahme nicht für eine vollständige Erklärung der Unterschiede in den Transfektionseffizienzen aus. Wir vermuten deshalb, dass neben der zellulären Aufnahme andere Schritte und Barrieren mindestens einen ebenso starken Einfluss auf die Tarnsfektionseffizienz haben. Einige Ergebnisse der hier vorgestellten Studie deuten in Richtung einer ineffektiven intrazellulären Freisetzung oder einer unvollständigen DNA Freisetzung als weitere wesentliche Hindernisse auf dem Weg zu einer effizienten Transfektion.

7.4 Ausblick

Wie bereits in der Einleitung umrissen, ist die Entwicklung sowohl effizienter wie auch sicherer Vektorsysteme eines das Hauptziele der Forschung zum nicht-viralen Gentransfer. Diese Vektoren sollten ein zufrieden stellendes Toxizitätsprofil aufweisen, intravenös applizierbar sein und spezifisch bestimmte Zielgewebe transfizieren. Trotz

der Tatsache, dass einige dieser Punkte bereits mit Erfolg bearbeitet wurden, konnte bisher ein Vektorsystem welches alle Punkte vereint noch nicht entwickelt werden.

Hinsichtlich der Charakterisierung der Konjugate, der Robustheit des Systems und der Reproduzierbarkeit der Ergebnisse ist die chemische Synthese von Liganden-modifizierten Kopolymeren wie in dieser Arbeit vorgestellt äußerst vorteilhaft. Nachteilig wirkt sich allerdings aus, dass jegliche Veränderung eine Neusynthese bedingt, was die Optimierung des Systems und die Anpassung an besondere Bedürfnisse stark verlangsamt. Eine Möglichkeit, dieses Problem zu lösen, könnte die Verwendung von „Bausteinen“ sein, aus denen gezielt Vektoren bestimmter Eigenschaften zusammengesetzt werden können. Falls man das verwendete Polykation mit Ankermolekülen versehen könnte, wäre auch ein einfaches Anhängen abschirmender oder zielführender Moleküle denkbar. Ein Problem PEG-modifizierter PEIs besteht in der relativ geringen Transfektionseffizienz dieser Copolymere selbst nach effektiver Aufnahme in die Zelle. Dies wurde auf eine möglicherweise verminderte endosomale Freisetzung zurückgeführt. Ein Ansatzpunkt wäre hier die Synthese „intelligenter“ Polymere, die Veränderungen wie den sinkenden pH-Wert während der Prozessierung vom frühen Endosom zum Lysosom wahrnehmen und ihre Eigenschaften entsprechend ändern. Beispielsweise wären Polymere denkbar, die bei niedrigem Umgebungs-pH-Werten sowohl PEG als auch Targeting-Moleküle verlieren und so die endosomale Freisetzung verbessern.

Neben Optimierungsmöglichkeiten die sich nach der zellulären Aufnahme bieten, ist auch die Verbesserung der Stabilität des Vektorsystmes auf seinem Weg zum Zielgewebe von großer Bedeutung für die Effizienz in vivo. In dieser Arbeit konnte gezeigt werden, dass die Kopplung von Antikörpern möglicherweise auch der Vebesserung der Zirkulationseigenschaften dienen kann. Dies könnte einen interessanten Ansatzpunkt für zukünftige Entwicklungen darstellen. Beispielsweise könnten Fc Fragmente oder Albumin an PEI gekoppelt werden und zu einer Abschirmung der Oberfläche und zu verminderter Opsonisierung beitragen. Auch die Quervernetzung der Polyplex-Oberfläche ist eine interessante Möglichkeit der Komplexstabilisierung, welche bereits intensiv untersucht wird. Hier stellt sich jedoch vor allem das Problem der DNA-Freisetzung nach zellulärer Aufnahme. Auch an dieser

Stelle wären detailliertere Kenntnisse der Veränderungen der Umgebungsbedingungen nach zellulärer Aufnahme hilfreich, um diesen Prozess weiter zu optimieren.

Eine wesentliche Erkenntnis dieser Arbeit besteht darin, dass die intravenöse oder intratumorale Applikation der zielgerichteten PEG-PEI Komplexe keine effiziente Reportergenexpression in HER2 exprimierenden Tumoren vermitteln konnte. Wir vermuten, dass dies auf die geringe Vaskularisierung der verwendeten SK-OV-3 Tumoren zurückzuführen war. Um die in vivo Effizienz Trastuzumab-modifizierter PEG-PEIs besser studieren zu können, sind Tumormodelle mit günstigeren Eigenschaften unabdingbar. Die Bildung subkutaner Tumoren wurde bereits für verschiedene HER2 exprimierende Zelllinien beschrieben. Bei vielen dieser Modelle ist jedoch die gleichzeitige Implantierung Östrogen-freisetzender Pellets nötig. Leider war dies bei den von uns durchgeführten Tierversuchen keine Option. Deshalb könnte die Etablierung eines geeigneteren Tumormodells die Untersuchung HER2-zielgerichteter nicht-viraler Vektoren wesentlich erleichtern.

In dieser Arbeit wurde gezeigt, dass die Quarternisierung und PEGylierung von Chitosan dessen Transfektionseffizienz deutlich verbessert. Dennoch waren relative große Polymermengen für die Transfektion nötig und die erreichte Effizienz lag deutlich unter der von PEI. Wie in der Einleitung beschrieben zeigt die Kombination von PEI und Chitosan synergistische Effekte hinsichtlich der Transfektionseffizienz, die unter Umständen auch im Fall trimethylierter Chitosane oder deren PEG-Derivate genutzt werden könnten. Durch die höhere Stabilität von Chitosan/DNA Komplexen könnte sich dies insbesondere auch günstig auf die Anwendung in vivo auswirken.

Bisher ist wenig zur intrazellulären Prozessierung von Chitosan/DNA Komplexen bekannt. Wie in dieser Arbeit gezeigt wurde, stellt die zelluläre Aufnahme offenbar nicht unbedingt die wesentliche Barriere für eine effiziente Transfektion mit Chitosan-Derivaten dar. Studien zu wichtigen intrazellulären Schritten wie endosomaler Freisetzung, Freisetzung der DNA und Translokation in den Nukleus könnten sich für die Entwicklung effizienterer Chitosan-Derivate als hilfreich erweisen.

8 Appendices

8.1 Abbreviations

AFM	Atomic force microscopy
AUC	Area under the curve
CLSM	Confocal laser scanning microscopy
DAPI	4',6-diamidino-2-phenylindole, dihydrochloride
EtBr	Ethidium bromide
FACS	Fluorescence assisted cell sorting
HBG	HEPES buffered glucose
HBS	HEPES buffered saline
HEPES	2-[4-(2-Hydroxyethyl)-1-piperazinyl]ethanesulfonic acid
HER2	Human epithelial growth factor receptor 2
Mw	Molecular weight
N/P	Nitrogen to phosphate ratio
PBS	Phosphate buffered saline
pDNA	Plasmid DNA
PEG	Polyethylenglycol
PEI	Polyethylenimine
PTMC	Polyethylenglycol-modified trimethyl chitosan
RES	Reticuloendothelial System
RGD	Arginine-glycine-aspartic acid
SCID	Severe combined immunodeficiency syndrome
SPDP	N-succinimidyl 3-(2-pyridyldithio)propionate
TMC	Trimethyl chitosan

8.2 List of Publications

8.2.1 Articles

S. Mao, O. Germershaus, D. Fischer, T. Linn, R. Schnepf, T. Kissel, Uptake and transport of PEG-graft-trimethyl-chitosan copolymer-insulin nanocomplexes by epithelial cells. Pharm Res 22(12) (2005) 2058-2068.

O. Germershaus, T. Merdan, U. Bakowsky, M. Behe, T. Kissel, Trastuzumab-polyethylenimine-polyethylene glycol conjugates for targeting Her2-expressing tumors. Bioconjug Chem 17(5) (2006) 1190-1199.

S. Mao, M. Neu, O. Germershaus, O. Merkel, J. Sitterberg, U. Bakowsky, T. Kissel, Influence of polyethylene glycol chain length on the physicochemical and biological properties of poly(ethylene imine)-graft-poly(ethylene glycol) block copolymer/SiRNA polyplexes. Bioconjug Chem 17(5) (2006) 1209-1218.

O. Germershaus, M. Neu, M. Behe, T. Kissel, HER2 Targeted Polyplexes: The Effect of Polyplex Composition and Conjugation Chemistry on in Vitro and in Vivo Characteristics. Bioconjug Chem (2007).

O. Germershaus, S. Mao, J. Sitterberg, U. Bakowsky, T. Kissel, Gene delivery using chitosan, trimethyl chitosan or polyethylenglycol-graft-trimethyl chitosan block copolymers: Establishment of structure-activity relationships in vitro. J Control Release 125 (2007) 145-154.

S. Mao, J. Xu, C. Cai, O. Germershaus, A. Schaper, T. Kissel, Effect of WOW process parameters on morphology and burst release of FITC-dextran loaded PLGA microspheres. Int J Pharm 334(1-2) (2007) 137-148.

M. Neu, O. Germershaus, S. Mao, K.H. Voigt, M. Behe, T. Kissel, Crosslinked nanocarriers based upon poly(ethylene imine) for systemic plasmid delivery: In vitro characterization and in vivo studies in mice. J Control Release 118(3) (2007) 370-380.

M. Neu, O. Germershaus, M. Behe, T. Kissel, Bioreversibly crosslinked polyplexes of PEI and high molecular weight PEG show extended circulation times in vivo. J Control Release 124(1-2) (2007) 69-80.

O. Germershaus, S. Mao, T. Kissel, Kinetics and Mechanism of Uptake of Chitosan, Trimethyl Chitosan and PEG-Trimethyl Chitosan Polyplexes in L929 mouse fibroblasts and A549 human alveolar epithelial cells. In preparation for J Gene Medicine

8.2.2 Poster Presentations

O. Germershaus, T. Kissel, Specific gene delivery to HER2-expressing cell lines using Trastuzumab-Polyethylenimine-Polyethylenglycol conjugates. CRS German Chapter Annual Meeting, Heidelberg, Germany, 2004.

O. Germershaus, S. Mao, A. Jintapattanakit, T. Kissel, Pegylated quarternized chitosan as novel gene delivery vector. Proceed. Int. Symp. Control. Rel. Bioact. Mater. 32, Vol. 32, Miami, Florida, USA, 2005.

O. Germershaus, S. Mao, A. Jintapattanakit, T. Kissel, Pegylated quarternized chitosan as novel gene delivery vector. CRS German Chapter Annual Meeting, Marburg, Germany, 2005.

O. Germershaus, S. Mao, J. Nguyen, T. Kissel, Comparative Studies on Complex Size and Route and Efficiency of Cellular Entry of Chitosan Derivatives in a Cell Line of Pulmonary Epithelium A549. 33rd Annual Symposium Controlled Release Society, Vienna, Austria, 2006.

O. Germershaus, M. Neu, M. Behe, T. Kissel, PEI-PEG-Trastuzumab Conjugates for Targeted Tumor Therapy: Does Pegylation and Antibody Modification Improve in vivo Pharmacokinetics and Biodistribution? , Gordon Research Conference, Big Sky, Montana, USA, 2006.

O. Germershaus, S. Mao, T. Kissel, Comparative Studies of Kinetics and Cellular Uptake Mechanism of Chitosan, Trimethyl Chitosan and Pegylated Trimethyl Chistosan - pDNA Polyplexes in a Cell Line of Pulmonary Epithelium A549. CRS German Chapter Meeting, Jena, Germany, 2006.

S. Mao, J. Xu, C. Cuifang, O. Germershaus, A. Schaper, T. Kissel, Influence of process parameters on the internal porosity and burst release of FITC-dextran loaded PLGS microspheres. 33rd Annual Symposium Controlled Release Society, Vienna, Austria, 2006.

S. Mao, O. Germershaus, M. Neu, O. Merkel, T. Kissel, Physicochemical characterization of polyethyleneimine-graft-poly(ethylene glycol) block copolymers as carrieres of siRNA: Influence of polyethylene glycol chain length. 33rd Annual Symposium Controlled Release Society, Vienna, Austria, 2006.

S. Mao, J. Xu, C. Cuifang, O. Germershaus, A. Schaper, T. Kissel, Influence of process parameters on the internal porosity and burst release of FITC-dextran loaded PLGS microspheres. Materialforschungstag, Rauischholzhausen, Germany, 2006.

O. Merkel, S. Mao, O. Germershaus, M. Neu, T. Kissel, Physicochemical characterization of polyethyleneimine-graft-poly(ethylene glycol) block copolymers as carrieres of siRNA: Influence of polyethylene glycol chain length. Materialforschungstag, Rauischholzhausen, Germany, 2006.

O. Merkel, M. Neu, O. Germershaus, T. Kissel, PEGylated PEI for siNRA delivery: Structure-function relationships of poly (ethylene imine)-graft-poly (ethylene glycol) block copolymer/ siRNA polyplexes. Gordon Research Conference, Big Sky, Montana, USA, 2006.

J. Nguyen, M. Neu, O. Germershaus, T. Schmehl, T. Gessler, W. Seeger, T. Kissel, Correlation of uptake mechanism and complex size for low-toxicity bioconjugates based on TAT-derived peptides covalently coupled to PEG-PEI. 33rd Annual Symposium Controlled Release Society, Vienna, Austria, 2006.

C. Cai, O. Germershaus, S. Mao, A. Schaper, T. Kissel, Influence of porosity and PLGA polymer type on the release behavior of FITC-dextran loaded PLGA microspheres. CRS German Chapter Annual Meeting, Freiburg, Germany, 2007.

8.2.3 Lectures

O.Germershaus, Development of a non-viral gene delivery system for targeting of HER2 expressing tumor xenografts in mice. Novartis Pharma AG, Basle, Switzerland, 2007

O. Germershaus, Gene delivery using HER2 targeted PEG-PEI polyplexes and modified chitosan, Pharmazeutisches Kolloquium, Marburg, Germany, 2008

8.3 Curriculum Vitae

Personalien:

Germershaus, Oliver
geb. am 19.08.1977 in Erfurt

Ausbildung und Berufspraxis:

Juni 1997	Abitur, Modellschule Obersberg, Bad Hersfeld
Juli 1997 - Juli 1998	Zivildienst, Kreiskrankenhaus Bad Hersfeld
Okt. 1998 - Sept. 2002	Studium der Pharmazie, Philipps-Universität Marburg
Nov. 2002 - April 2003	1. prakt. Halbjahr: Institut für pharmazeutische Technologie und Biopharmazie, Philipps-Universität Marburg Anfertigung einer Diplomarbeit
Mai 2003 - Okt 2003	2. prakt. Halbjahr: Altstadt-Apotheke Nürnberg
Dezember 2003	Approbation zum Apotheker
Feb. 2004 - Okt. 2007	wiss. Mitarbeiter, Institut für pharmazeutische Technologie und Biopharmazie, Philipps-Universität Marburg Anfertigung der vorliegenden Dissertation
Seit Nov. 2007	Pharmaceutical Research and Development, Novartis Pharma AG, Basel, Schweiz

8.4 Danksagung

Mein besonderer Dank gilt meinem Doktorvater Herrn Prof. Dr. Thomas Kissel, der mir bei der Anfertigung dieser Arbeit mit vielen interessanten Diskussionen und Ideen zur Seite stand und mir vetrauensvoll ebenso viele Freiheiten ließ. Sein großer Erfahrungsschatz und seine Aufgeschlossenheit gegenüber neuen Ansätzen haben maßgeblich zum Gelingen dieser Arbeit beigetragen.

Herrn Prof. Dr. Udo Bakowsky möchte ich einerseits für die Erstellung des Zweitgutachtens, andererseits aber auch für die vielen anregenden wissenschaftlichen und nichtwissenschaftlichen Diskussionen danken. Sein Können und seine weitreichendes Wissen auf dem Gebiet der Rasterkraftmikroskopie haben die Charakterisierungsmöglichkieten der untersuchten Polyplexe wesentlich erweitert. An dieser Stelle möchte ich auch Herrn Johannes Sitterberg meinen Dank aussprechen, der seine wertvolle Zeit und seine Erfahrung in die rasterkraftmikroskopische Analyse meiner zum Teil nicht ganz unproblematischen Polyplexe investiert hat.

Herzlich danken möchte ich Herrn Prof. Dr. Ernst Wagner, Herrn Dr. Manfred Ogris, Herrn PD Dr. Carsten Culmsee, Frau Nicole Tietze, Herrn Markus Kovac sowie dem gesamten Arbeitskreis von Herrn Prof. Wagner am Insitut für pharmazeutische Biologie-Biotechnologie an der LMU München für die freundliche Aufnahme im Arbeitskreis und für die lehrreiche und interessante Zusammenarbeit. Ohne die weitreichenden Erfahrungen mit in vivo Tumormodellen und die vielen etablierten Untersuchungsmethoden, auf die ich zurückgreifen durfte, wäre die Durchführung der Experimente zum in vivo Targeting nicht möglich gewesen.

Herrn Dr. Martin Behe vom Institut für Nuklearmedizin danke ich herzlich für die Möglichkeit zur unkomplizierten Verwirklichung der in vivo Pharmakokinetik- und Biodistributionsversuche. Die Arbeit in der Nuklearmedizin war immer sehr angenehm und äußerst produktiv. Ebenso möchte ich mich für die vielen Diskussionen mit Herrn Dr. Behe bedanken, die mir oftmals wertvolle neue Perspektiven eröffnet haben.

Frau Dr. Cornelia Brendel, Frau Andrea Grün und Frau Barbara Lickfers vom Institut für Hämatologie, Onkologie und Immunologie sei herzlich für Ihre Offenheit und Ihr Entgenenkommen sowie für die Möglichkeit gedankt, flowzytometrische Messungen zu nahezu jeder Tages- und Nachtzeit durchführen zu können.

Allen Mitgliedern des Instituts für pharmazeutische Technologie und Biopharmazie bin ich zu größtem Dank verpflichtet.

Besonders hervorheben möchte ich die Mitglieder der „PEI-Gruppe“. Ich danke Herrn Dr. Thomas Merdan für die intensive Einführung in die wissenschaftliche Forschung im Allgemeinen und die Besonderheiten nicht-viraler Systeme zum Gentransfer im Besonderen. Herrn Dr. Michael Neu und Frau Dr. Shirui Mao möchte ich für die interessante und fruchtbare Zusammenarbeit danken. Durch Sie konnte ich tiefere Einblicke in die Polymerchemie von PEI und Chitosan gewinnen. Frau Juliane Nguyen und Frau Olivia Merkel danke ich für die freundliche Aufnahme in der „Aussenstelle Behringvilla“, für die vielen interessanten Diskussionen und für die schönen Stunden in der Zellkultur.

Mein außerordentlicher Dank gilt meiner langjährigen Laborkollegin Frau Dr. Claudia Packhäuser. Es war mir immer eine große Freude, mit Dir zusammenarbeiten zu dürfen. Deine freundliche und aufgeschlossene Art wie auch Dein großes Organisationsgeschick werden mir immer in bester Errinerung bleiben.

Ich danke Frau Eva Mohr und Frau Nicole Bamberger für ihre ausgezeichnete Arbeit in der Zellkultur, Herrn Lothar Kempf für die Unterstützung in allen technischen Belangen und die Anfertigung vieler Apparaturen und Herrn Klaus Keim für die Organisiation der Bestellungen und für die stete Unterstützung in allen grafischen Fragen.

Weiterhin möchte ich meinen Kollegen und Freunden Nadja Bege, Markus Benfer, Dr. Cuifang Cai, Dr. Lea-Ann Dailey, Eyas Dayyoub, Nico Harbach, Dr. Peter Hölig, Anchalee Jintapattanakit, Dr. Elke Kleemann, Dr. Dorothee Kriha, Tobias Lebhardt, Dr. Martina Lehmann, Sascha Maretschek, Frank Morell, Aybike Özcetin, Solen Pichereau, Regina Reul, Jens Schäfer, Dr. Julia Schnieders, Christoph Schweiger, Nina Seidel, Anett Sommerwerk, Dr. Terry Steele, Dr. Florian Unger und Nan Zhao für die vielen schönen Stunden in der Uni und in der Freizeit ganz herzlich danken. Die Zeit mit Euch war einfach toll!

Von tiefstem Herzen möchte ich mich bei meiner Familie und bei meiner Freundin Nicole Tietze für die ununterbrochene Unterstützung bedanken, ohne die diese Arbeit nicht möglich gewesen wäre.